



University of Natural Resources
and Applied Life Sciences, Vienna

Institute of Silviculture

Diploma thesis

**Assessing the productivity and water regime in the
Schmittenbach catchment area**

Author:

Bakk. Biol. Elisabeth Pötzelsberger

Supervisor: Univ. Prof. Dipl.-Ing. Dr. Hubert Hasenauer

Co-supervisor: Dr. Mag. Stephan Pietsch

External-supervisor: doc. Ing. Róbert Marušák, Ph.D.

Vienna, in June 2008

Abstract

This study was initiated by a project that aims at assessing the protection function of forests (against flood events etc.) in alpine areas. Flux dynamics (water, carbon, nutrients) within a watershed, which may depend on vegetation patterns in the area and the forest management practices, are analysed by using the mechanistic ecosystem model BIOME-BGC. The Schmittenbach catchment area was selected for the study because of its very good historical data on both vegetation dynamics and hydrology. Procedure: (1) field campaign and consistency test between the point sampling results and data from the current forest management plan of the local forest company and (2) application of the BIOME-BGC model for the analysis of flux dynamics within the simulation points. The analysis showed a significant correlation between field data and data from the management plan for the stand age, but in the case of site productivity, it was found underestimated by the management plan. Simulations with the BIOME-BGC model exhibited no bias between observed and predicted volume data. Various dependencies on stand and site characteristics like Leaf Area Index (LAI), standing volume, age, aspect and elevation were revealed. Net Primary Production (NPP) and LAI correlated strongly but in young development phases and in old growth stands NPP differed significantly despite same LAI values. Water use efficiency was found the highest for juvenile stands, and it differed similarly between juvenile and old growth stands. Annual evapotranspiration (ET) strongly correlated with the LAI and the NPP, whereas for a growing stock of $>100 \text{ m}^3 \cdot \text{ha}^{-1}$ no trend of annual ET was noticed. Highest annual outflow values were found for a growing stock of $<100 \text{ m}^3 \cdot \text{ha}^{-1}$ and for $>200 \text{ m}^3 \cdot \text{ha}^{-1}$ no correlation between annual outflow and growing stock was evident.

Keywords: Productivity, vegetation dynamics, water regime, catchment area, biogeochemical modelling

Abstrakt

Mit dieser Studie wird das Verständnis von Stoffkreisläufen (Energie, Wasser, Nährstoffe, Kohlenstoff) in Waldökosystemen ausgeweitet und eine Beurteilung der Schutzfunktionen des Waldes in alpinem Gelände anhand von Messungen vor Ort in Kombination mit einem mechanistischen Ökosystemmodell (BIOME-BGC Modell) vorbereitet. Dabei müssen in gebirgigen Landschaften aufgrund von Austrags- und Eintragsprozessen Nachbarschaftsverhältnisse einzelner Landschaftselemente wie Wald, Wiese etc. und folglich auch die Bestandesstruktur (und damit die Art der forstlichen Nutzung) berücksichtigt werden. Bisweilen sind diese Interaktionen für die Simulationseinheiten im BIOME-BGC Modell nicht realisiert, jedoch wird mit dieser Studie an der Modellerweiterung gearbeitet. Im umfassend hydrologisch und vegetationsdynamisch untersuchten Einzugsgebiet des Schmittenbaches wurden Bestandesaufnahmen durchgeführt und die Ergebnisse mit dem örtlichen Waldwirtschaftsplan auf Konsistenz überprüft. Dies diente der Evaluierung, ob vorhandene Operatsdaten bei der Beurteilung der Schutzfunktionen des Waldes herangezogen werden können. Das im Operat angegebene Alter stimmt im Mittel mit unseren Messungen überein, jedoch wird die Produktivität massiv unterschätzt. Die Untersuchung des Höhenwachstums von Bäumen zeigte, dass das in der empfohlene Ertragstafel 'Fichte Hochgebirge' beschriebene Wachstum durch das tatsächliche zunehmend übertroffen wird. Weiters wurden die Stoffflüsse innerhalb der Simulationseinheiten analysiert. Abhängigkeiten zwischen Produktivität, Transpiration und Wasserabfluss einerseits und Blattflächenindex, Alter und Holzvorrat, sowie Seehöhe, Exposition und Bodentiefe andererseits konnten festgestellt werden.

Schlagwörter: Produktivität, Vegetationsdynamik, Wasserhaushalt, Einzugsgebiet, biogeochemische Modellierung

Acknowledgements

I would like to express my sincere gratitude to my supervisor Univ. Prof. Dipl. Ing. Dr. Hubert Hasenauer for his proper guidance and constructive suggestions during my thesis work. My deep appreciation goes to my co-supervisor Dr. Mag. Stephan A. Pietsch for all his expertise and extensive support during the whole working process. I am much obliged to my colleagues Dipl. Ing. Mario Klopff and Dipl.-Ing. Friedrich Putzhuber for their involvement in the field campaign and all the inspiring discussions. For the introduction to the BGC model and the processing of the meteorological data I am very thankful to Dipl.-Ing. Dr. Richard Petritsch. For the technical support from the Institute of Silviculture my acknowledgements go to Ing. Monika Lex and Eva-Maria Fuker.

With deep appreciation I want to thank Dipl.-Ing. Wolfgang Hartwagner of the 'Forsttechnischer Dienst der Wildbach und Lawinenverbauung, Gebietsbauleitung Pinzgau' for his expertise and Dipl.-Ing. Josef Kirchberg and Mr. Peter Wanker from the forest management in Zell am See for their readily copious support before and during the field campaign.

Further gratitude goes to my external supervisor doc. Ing. Róbert Marušák, Ph.D. from the Faculty of Forestry and Wood Sciences of the Czech University of Life Sciences, Prague for his encouraging comments. Deep thanks go to Mgr. Marie Kafková of the International Relations Office at Czech University of Life Sciences for the perfect organisation of my documents.

Beneficial review comments were generously provided by Ms. Emily Procter and my dear colleagues Eric Jaeschke and Sishir Gautam.

I will be ever grateful to my parents who enabled my studies and always caringly supported me, and to my friends who were always there for me.

Table of contents

1	Introduction	1
1.1	Forest functions and vegetation dynamics within a catchment area	1
1.2	The Schmittenbach watershed	2
1.2.1	Topography and morphology	2
1.2.2	Geology.....	2
1.2.3	Hydrology, precipitation and flood events	3
1.2.4	Vegetation and land use	3
1.2.4.1	Current vegetation cover.....	4
1.2.4.2	Changes in the vegetation cover	5
1.2.4.2.1	The big afforestation efforts	5
1.2.4.2.2	Interventions of the skiing industry in the vegetation cover	9
2	Methods	14
2.1	Field campaign in the Schmittenbach watershed	14
2.1.1	Current vegetation distribution	14
2.1.2	Stem analysis	14
2.1.3	Stand parameters	16
2.1.3.1	Stand age	17
2.1.3.2	Dominant height.....	17
2.1.3.3	Volume.....	18
2.1.3.4	Site index	18
2.1.3.5	Stand Density Index (SDI)	19
2.1.4	Soil parameters	19
2.1.4.1	Soil sampling	19
2.1.4.2	Soil carbon and nitrogen content determination in the lab	19
2.2	Mechanistic biogeochemical ecosystem modelling	20
2.2.1	The BGC model.....	20
2.2.2	Input data	20
2.2.2.1	Weather data and other atmospheric characteristics	21
2.2.2.2	Site constants.....	22
2.2.2.3	Eco-physiological parameters - Species specific parameterization	22

2.2.3	The simulation	23
2.2.3.1	Spin-up	23
2.2.3.2	Historic land use	23
2.2.3.3	Thinning	23
2.2.3.4	The BGC model output	24
2.2.3.4.1	Volume	24
2.2.3.4.2	Soil.....	24
3	Results and discussion	25
3.1	Field campaign outcome	25
3.1.1	Current vegetation distribution	25
3.1.2	Stem analysis	25
3.1.3	Stand parameters	28
3.1.3.1	Stand age	28
3.1.3.2	Dominant height	28
3.1.3.3	Total volume per hectare	29
3.1.3.4	Site index	30
3.1.4	Soil parameters	30
3.2	BGC model simulation results	31
3.2.1	Volume	31
3.2.1.1	Regression analysis between observations and model predictions	32
3.2.2	Productivity	36
3.2.3	Water use efficiency.....	40
3.2.4	Water regime	44
3.2.4.1	Precipitation	45
3.2.4.2	Transpiration & evapotranspiration	46
3.2.4.3	Outflow	51
3.2.5	Soil analysis	57
4	Summary and conclusion.....	61
5	References	65
6	Appendix	67

List of figures

Figure 1. Map of the Schmittenbach watershed, demarcated with the red line, the red spot marks the location of the main runoff gauge at the river Schmittenbach ('Abflussmesswehr').....	2
Figure 2. The Schmittenbach watershed seen from the East side of the lake Zellersee in 2001.....	3
Figure 3. Vegetation at the timber line with dwarf-shrub vegetation, alpine grassland and afforestation between avalanche barriers.....	4
Figure 4. Different forest covers in the Schmittenbach watershed from 1887 to 1986	8
Figure 5. Ski slopes 'Künstlerhang' and 'Jedermann' in the area of the Auermaiß in the North and the 'Standartabfahrt' in the South of the Schmittenbach watershed.	10
Figure 6. Map of ski slopes, ski lifts and cable cars in the Schmittenbach watershed.....	11
Figure 7. West part of the Schmittenbach watershed above the main runoff gauge (approximately 7.3 km ²)..	13
Figure 8. Forest map of the Schmittenbach watershed from 2003	17
Figure 9. Orthophoto of the Schmittenbach watershed (from 2003) with the current vegetation distribution..	25
Figure 10. Stem analysis: Comparison of dominant tree height functions of Mitscherlich/Richard for the yield table 'Fichte Hochgebirge' with growth functions of trees in the Schmittenbach watershed.....	26
Figure 11. Stem analysis: Comparison of dominant tree height functions of Mitscherlich/Richard for the yield table 'Fichte Bayern' with growth functions of trees in the Schmittenbach watershed	27
Figure 12. Comparison of the stand age between the management plan 2003 of the local forest company and the age for 2003 derived from measurements 2007	28
Figure 13. Comparison of the dominant tree height in the single stands between dominant tree height derived from data of the management plan 2003 of the local forest company, using the dominant height growth functions of Mitscherlich/Richard (1919), and the dominant height measurements 2007	29
Figure 14. Comparison of the total volume per hectare of the single stands between the management plan 2003 of the local forest company and the measurements 2007.	29
Figure 15. Comparison of the site index of the single stands between the management plan 2003 of the local foest company and the measurements 2007 (value of the single stands as average among the plots).	30
Figure 16. Predicted vs. observed volume per hectare for the single plots (A) and predicted vs. observed volume per hectare on stand level (average of the plots per stand) (B) in 2005.	32
Figure 17, Part 1. Trend analysis of standardisde volume residuals (i.e. predicted minus observed volume divided by the standard deviation of the observations) for all plots and for the stand means vs. stand age (A, B), dominant height (measured in the field; C, D), basal area (tree number per plot multiplied with the basal area factor 4; E, F) and Stand density index (G, H) in 2005.....	34
Figure 18, Part 2. Trend analysis of standardisde volume residuals (i.e. predicted minus observed volume divided by the standard deviation of the observations) for all plots and for the stand means vs. site index (A, B), elevation (measured in the field; C, D), slope (E, F) and aspect (G, H) in 2005.....	35
Figure 19. Net Primary Production vs. Leaf Area Index for all plots showing all data of the years 1960-2005. ...	36

Figure 20. Net Primary Production vs. Leaf Area Index for two different plots showing all data of the years 1960-2005.	37
Figure 21. Net Primary Production (NPP) ($\text{kg C.m}^{-2}.\text{yr}^{-1}$) vs. site and stand parameters, i.e. Leaf Area Index (A), stand age (B), predicted volume (C), site index (D), aspect (E), elevation (F) and Stand Density Index (G) for all plots and the stand means (only for SDI) (H) in 2005.	39
Figure 22. Water use efficiency ($\text{g C m}^{-2}.\text{yr}^{-1}.\text{mm}^{-1}$) vs. Leaf Area Index (A), aspect (B), Net Primary Production (C), elevation (D), predicted volume (E) and stand age (F) for all plots in 2005.	40
Figure 23. Water use efficiency ($\text{g C m}^{-2}.\text{yr}^{-1}.\text{mm}^{-1}$), the ratio of annual NPP and transpiration, vs. Leaf Area Index (A) and vs. Net Primary Production (B), for all 78 plots in the years 1960-2005.	42
Figure 24. Water use efficiency ($\text{g C m}^{-2}.\text{yr}^{-1}.\text{mm}^{-1}$) vs. Leaf Area Index (A) and vs. Net Primary Production (B), for a young stand (Plot 15_1) and an old stand (Plot 16_3) in the years 1960-2005.	42
Figure 25. Water use efficiency ($\text{g C.m}^{-2}.\text{yr}^{-1}.\text{mm}^{-1}$) vs. predicted volume for all plots in the years 1960-2005. .	43
Figure 26. Annual water balance: Precipitation, evapotranspiration and outflow vs. elevation shown for all 78 plots in the year 2005.	45
Figure 27. Annual precipitation and annual outflow at two separate plots in the years 1960-2005.	46
Figure 28. Annual transpiration (A) and annual evapotranspiration (ET) (B) over Leaf Area Index (A, B), Net Primary Production ($\text{kg C.m}^{-2}.\text{yr}^{-1}$) (C, D), elevation (E, F) and aspect (G, H) for all plots in 2005.....	47
Figure 29. Annual transpiration (A) and annual evapotranspiration (B) vs. Leaf Area Index (A, B) and vs. Net Primary Production ($\text{kg C.m}^{-2}.\text{yr}^{-1}$) (C, D) for all plots in the years 1960-2005.	49
Figure 30. Annual transpiration (A) and annual evapotranspiration (B) vs. predicted volume for all plots in the years 1960-2005.....	50
Figure 31. Annual outflow vs. various stand and site characteristics, i.e. predicted volume (A), basal area (B), Stand Density Index (C), stand age (D), slope (E), soil depth (as interpolated from the Austrian Federal Soil Survey; F), Leaf Area Index (G) and Net Primary Production ($\text{kg C.m}^{-2}.\text{yr}^{-1}$) (H) for all plots in the year 2005.....	52
Figure 32. Annual outflow vs. Leaf Area Index (A) and vs. Net Primary Production (B) for all plots in the years 1960-2005.	54
Figure 33. Ratio of annual outflow and annual precipitation vs. Leaf Area Index (A) and vs. Net Primary Production (B) for all plots in the years 1960-2005.	54
Figure 34. Development of the Leaf Area Index (A) and the annual outflow/precipitation share (B) in the years 1960 to 2005 for the two exemplary plots 15_1 and 16_3.....	55
Figure 35. Relation between the annual outflow/precipitation share and the Leaf Area Index for the plots 15_1 and 16_3 for the years 1960 – 2005.	56
Figure 36. Annual outflow vs. predicted volume (A) and the ratio of annual outflow and annual precipitation vs. predicted volume (B) for all plots in the years 1960-2005.....	56
Figure 37. Predicted vs. observed soil carbon (A) and soil nitrogen (B) for all plots in 2005.....	57
Figure 38. Trend analysis of standardised soil carbon residuals and soil nitrogen residuals (i.e. predicted minus observed soil carbon or nitrogen divided by the standard deviation of the observations) vs. stand age (A, B), soil depth from field measurements (C, D), aspect (E, F) and elevation (G, H) for all plots in 2005.	59

List of tables

Table 1.	The main ski slopes in the Schmittenbach watershed	11
Table 2.	Loss of area for skiing purposes in the Schmittenbach watershed until 1981.....	12
Table 3.	Share of the different land use types in the Schmittenbach watershed from 1884 to 1987.....	12
Table 4.	Parameters for the dominant height growth functions of Mitscherlich/Richard (1919) for 'Fichte Bayern' (FiBay) and for 'Fichte Hochgebirge' (FiHgb).....	15
Table 5.	Input parameter for the BGC model simulations, which are identical for all plots in the Schmittenbach-watershed.....	21
Table 6.	Meteorological data from the DAYMET climate model for the simulated plots in the Schmittenbach region	22
Table 7.	Tree and wood parameters needed for the conversion of the BGC model output stem carbon into the target parameter volume per hectare ($\text{m}^3 \cdot \text{ha}^{-1}$).....	24
Table 8.	Results of the error analysis for the volume per hectare.....	31
Table 9.	Minimum, maximum and mean volume residuals for all plots (78) and for the stand-mean volume residuals (20) in 2005.....	32
Table 10.	Statistical parameters for volume residuals analysis on different stand and site parameters	33
Table 11.	Minimum, maximum, mean and median of the Net Primary Production and the Leaf Area Index for all 78 plots in the years 1960-2005.	37
Table 12.	Minimum, maximum, mean and median of the water use efficiency for all 78 plots in the years 1960-2005.	41
Table 13.	Important water regime parameters for all plots in the years 1960 – 2005 (the time of full weather data from the DAYMET climate model).....	44
Table 14.	Result of the error analysis for soil carbon and soil nitrogen for all plots in the year 2005.	57
Table 15.	Minimum, maximum and mean soil carbon and soil nitrogen - residuals for all plots (78) and for the stand-means soil carbon and soil nitrogen - residuals (20) in the year 2005.....	58
Table 16.	Mean, minimum and maximum soil carbon/nitrogen ratio for all plots of the soil sampling in the Schmittenbach watershed in 2007 and of the model predictions for all plots in 2005.....	58
Table 17.	Part 1. Site characteristics measured and calculated for all plots during the field campaign in the Schmittenbach watershed 2007.....	67
Table 18.	Part 2. Site characteristics measured and calculated for all plots during the field campaign in the Schmittenbach watershed 2007.....	68
Table 19.	Thickness of soil layers at the different stands in the Schmittenbach watershed in 2007.....	69
Table 20.	Mean and standard deviation (SD) of soil carbon ($\text{t} \cdot \text{ha}^{-1}$) and nitrate ($\text{t} \cdot \text{ha}^{-1}$) and the C/N ratio for each stand in the Schmittenbach watershed in 2007. The analyse values include humus and topsoil.	70
Table 21.	Part 1. Stand characteristics measured and calculated for all plots in the Schmittenbach watershed 2007.....	71

Table 22.	Part 2. Stand characteristics measured and calculated for all plots in the Schmittenbach watershed 2007.	72
Table 23.	Comparison of stand characteristics between the management plan 2003 of the local forest company 'Zeller Waldgemeinschaft' with the results from the field campaign 2007. For the point sampling data the mean and the median of all (4) plots per stand are calculated.	73
Table 24.	Plausibility check: comparison of the data from the field campaign 2007 with suitable data from the local yield table 'Fichte Hochgebirge'. For the point sampling data the mean and the median of all (4) plots per stand are calculated.	74
Table 25.	Mean and median of aspect, slope, elevation and coordinates for all stands.	75

List of abbreviations

a	Regression coefficient
ba	Basal area ($\text{m}^2 \cdot \text{ha}^{-1}$)
baf	Basal area factor, parameter of the Relascope
CI	Confidence interval
$\overline{D_i}$	Mean difference between predictions and observations
dbh	Diameter at breast height (cm)
ET	Evapotranspiration (mm)
f	Form factor, according to Pollanschütz (1974)
h	Tree height (m)
LAI	Leaf Area Index (area of leaves per area of ground)
NPP	Net Primary Production ($\text{kg C} \cdot \text{m}^{-2} \cdot \text{yr}^{-1}$)
N_{rep}	Represented tree number
\overline{obs}	Mean of the observations
OH	Dominant height
OH100	Dominant height at the age of 100
PI	Prediction interval
r	Correlation coefficient
r^2	Coefficient of determination
SD	Standard deviation
SDI	Stand Density Index, according to Reinecke (1933)
V	Volume ($\text{m}^3 \cdot \text{ha}^{-1}$)
WUE	Water Use Efficiency ($\text{g C m}^{-2} \cdot \text{yr}^{-1} \cdot \text{mm}^{-1}$)

1 Introduction

1.1 Forest functions and vegetation dynamics within a catchment area

Forest has always played a key role in human existence. Throughout many decades forests were primarily considered as the source of construction and fuel wood (besides domestic usage mainly for the salt pans and iron smelters in the Alpine region), but also as a source of litter for agricultural purposes (spread in the stable or used as a fodder for the livestock) and as a place for grazing of the livestock, etc. Human pressure on the forest resulted in massive and widespread forest degradation and eventually local and regional deforestation in central Europe (Küster, 2002). Undoubtedly, valuable forest functions go far beyond the extraction of materials for human usage. Besides the 'production function', forests have a significant 'protection function'. Forests stabilise the soil, keep the nutrients on the site and retard the water from rainfall or snowmelt. In mountainous areas, the significance of this site stabilising function can easily surpass the value of forests as a source of matter for human use. Humans have to painfully realised this mostly, when the forest was already degraded heavily or even already missing due to human exploitation. Soil erosion, landslides, rock falls, floods and avalanches were the unambiguous results of bad forest conditions especially in Alpine regions. In the second half of the 19th century the people of Zell am See, Salzburg were among the first to realise that a comprehensive reforestation and melioration project in the heavily degraded catchment area of the mountain brook Schmittenbach could possibly stop the centuries of flood and landslide catastrophes endangering the life and human existence in the Schmittenbach watershed (Hinterstoisser, 1985).

Today, the task is to assess the protection function of forests by investigating the flux dynamics (of water, nutrients, carbon) within a watershed. For example, the transport of water and nutrients along topographic gradients can decrease the productivity of the upper slope, whereas matter input in lower areas can significantly increase the production capacity. A deeper understanding of how energy and matter cycles within a stand and the landscape depend on the forest structure (and therefore on the management practices) and on the vegetation pattern within a catchment (neighbouring forests, pastures, bare soil etc.) will help in assessing the protection and production function of forests in mountainous terrain. This shall be achieved by conducting field measurements and linking them with model theories (mechanistic ecosystem model or BGC model) where photosynthetic production, allocation of assimilates, growth, respiration, transpiration, evaporation etc. in dependency of the site, stand and daily changing climatic conditions can be simulated. The important hydrological interactions among the vegetation units within mountainous terrain and connected nutrients and carbon transport are not yet realised in the model. This is considered as a drawback of the model for assessing the protection function of forests in Alpine regions. Thus, interactions among the simulation points should be implemented. The catchment area of the Schmittenbach, situated in the Northern Central Alps in the province of Salzburg, Austria, is considered as a suitable research area and test case for a model revision due to its long history of flood catastrophes caused by forest degradation and the comprehensive historical and recent data about vegetation dynamics and hydrology in the catchment area. This study shall serve as the preparatory analysis work for the necessary model revision.

The main objectives of this study are: (i) consistency analysis between stand data from the management plan of the local forest company 'Zeller Waldgemeinschaft' and field observations in the Schmittenbach watershed and (ii) simulation of the point sampling plots with the mechanistic ecosystem model BIOME-BGC and analysis of flux dynamics within the simulation points.

1.2 The Schmittenbach watershed

1.2.1 Topography and morphology

The area of the Schmittenbach watershed comprises 1040 ha. The area is moderately steep but several deep, V-shaped ditches / torrents with partly very steep ravines can be found spread across the watershed. The highest point of the watershed is the Schmittenhöhe located in the West, with a height of 1964 m above sea level. In the North of the valley, the Glocknerwand (1516 m), the Wandkrautkopf (1762 m) and the Schrambachkopf / Sonnkogel (1856 m) are situated from East to West, in the North-West is the Salersbachköpfl (1934 m), in the West the already mentioned Schmittenhöhe (1964 m), in the South-West there are the Breiteneck (1769 m) and the Dürnbergeck (1711 m), and in the South the long mountain ridge with the Glocknerhaus (1583 m), the Hirschkogel (1585 m), the restaurant Mittelstation (1362 m), and the Plettsaukopf (1301 m) with its steep slope towards the Zeller See is located. The longest extension of the watershed reaches 4.8 km into West-East direction from the Schmittenhöhe to the huge alluvial cone of the river Schmittenbach where the small town of Zell am See is situated. Average width is 2.1 km (Hagen, 2003). An overview of the area is shown in the following map (Figure 1).



Figure 1. Map of the Schmittenbach watershed, demarcated with the red line, the red spot marks the location of the main runoff gauge at the river Schmittenbach (germ. 'Abflussmesswehr') (Hagen, 2003).

1.2.2 Geology

The Schmittenbach watershed is located in the Greywacke Zone and mostly consists of Wildschönauer Shale, also called 'Pinzgauer Phyllit'. Shale predominates with interstratified thin layered, fine-grained sandstone and clay, with a low proportion of Quartz. Easy weathering causes large quantities of fine debris. As a consequence, the evolving soil is quite compact with a low infiltration rate. Water runs off quickly at the steep slopes resulting in sometimes massive erosion at the partly very steep ravines of the watershed's brooks. Due to its high debris-flow potential, the Schmittenbach is considered to be a very dangerous torrent (Hagen, 2003).

1.2.3 Hydrology, precipitation and flood events

Main side creeks of river Schmittenbach are the Breitenbach, Gießbach I, II, III and the Finsterbach. The Schmittenbach begins just where the Finsterbach discharges into the Gießbach at an altitude of 960 m. Farcheneckgraben, Köhlergraben and Pfaffenbach are additional side watersheds. The average grade of the Schmittenbach is 8%. At an altitude of 757m, the Schmittenbach discharges into the lake Zeller See (Hagen, 2003).

A time series of weather records in the years 1981 to 1998 show an average annual precipitation of about 1400 mm. The highest precipitation quantity was registered in 1981 with 1777 mm. The average annual course of precipitation reaches its maximum in summer, although absolute peak values are also possible in December and January. Results of the calculation and extrapolation of the 100 year daily precipitation events, using the Gumbel analysis, showed 113 mm at Sonnalm and 129 mm at the Schmittenhöhe (Hagen, 2003).

Heavy rainfall events have repeatedly lead to devastating floods, debris floods and land slides during the last centuries. Huge catastrophes were recorded in the years 1737, 1854, 1857, 1866, 1875, twice in 1884 and in 1966. The repeated catastrophes in the second half of the nineteenth century triggered comprehensive discussions on the state of the land cover and the land use practices in the watershed. They culminated into what is called the first comprehensive melioration effort within Europe (Hinterstoisser, 1985). Technical structures at the Schmittenbach and its tributaries were aimed at stabilising the profile and a big afforestation project was launched (see also chapter 1.2.4.2.1).

1.2.4 Vegetation and land use



Figure 2. The Schmittenbach watershed seen from the East side of the lake Zellersee in 2001 (Hagen, 2003).

1.2.4.1 Current vegetation cover

The Schmittbach watershed belongs to the Austrian growth district “Northern central alps – Fir-Spruce forest region, western part”. 77% of the watershed area is covered with forests (Forsttechnischer Dienst für Wildbach und Lawinenverbauung, Gebietsbauleitung Pinzgau, 1996). Up to approximately 1700 m above sea level, production forests mainly consisting of subalpine Norway Spruce (*Picea abies*) with a little amount of European Larch (*Larix decidua*) and European Silver Fir (*Abies alba*) form the predominant forest stands. In the North and North-West near the Schrambachkopf the forest stand even reaches elevations of 1800 m. Farther west, a broad curved wood area (germ. ‘Kampfwaldbereich’) exists, from about 1700 to 1900 m in the region of the Salersbachkopf and in the West below the Schmittenhöhe from 1700 to 1750 up to 1850 m (see Figure 3).

In areas where avalanches are more frequent Green Alder (*Alnus alnobetula*) can be found, whereas around the ditches Grey Alder (*Alnus incana*), Sycamore Maple (*Acer pseudoplatanus*), Silver Birch (*Betula pendula*), and European Rowan (*Sorbus aucuparia*) are the predominant species. In the highest regions dwarf-shrub vegetation and alpine grassland exist (Forsttechnischer Dienst für Wildbach und Lawinenverbauung, Gebietsbauleitung Pinzgau 1996). At single spots remnants of the high elevation reforestation project with Stone Pine (*Pinus cembra*) can be found (Hagen, 2003).

Uncovered surfaces also exist near some ditches. Those spots of bare soil or rock are areas of former landslides and are called ‘Plaiken’ in the region. An example is the ‘Pützelplaike’ located in the North-West of the ‘Mittelstation’. At the ravines of the Grießbach and the Breitenbach several ‘Plaiken’ with an extension of approximately 2 or 1.5 ha exist (Hinterstoisser, 1985). In 1885 about 30 ha of ‘Plaiken’ could be detected mainly in the alp and pasture area, according to geodetic measurements (Thoma, 1900) (compare Table 3).



Figure 3. Vegetation at the timber line with dwarf-shrub vegetation, alpine grassland and afforestation between avalanche barriers.

1.2.4.2 Changes in the vegetation cover

1.2.4.2.1 The big afforestation efforts

In former times, the forest has probably reached the top of the ridge of the Schmittenhöhe at an altitude of 1880 to 1960 m (Gayl, 1958). In 1885, when the first big reforestation project of its type was launched, it was reported that only 600 ha of the total 1040 ha watershed were still covered with forests; however, at least ten percent of that area was barely stocked. 300 ha were alps and pastures and the rest were areas of different agricultural utilisation. The non-forest area at this time was exclusively private property. The livestock of the residents grazed on the mountain pastures, which were also located below the timberline. The number of cattle rights was 110 (Thoma, 1900). Today field names still indicate the extent of the pastureland: 'Auermaiß', 'Brunner Maiß', 'maiß' meaning deforested area. Especially near the watershed's centre and above 1400 m above sea level much forest had been converted into mountain pastures. Unfortunately, the condition of those pastures was mostly poor. Many of them were covered with *Rhododendron* sp. and *Vaccinium myrtillus*, *V. vitis-idea*, *V. uliginosum*. Only the larger 'Alpsmäder' had a sound grass cover and could be considered free of trees and bushes (Haiden, 1935).

The reforestation from 1888 to 1922 was considered the first big afforestation project in the Pinzgau (Haiden, 1935). Together with the technical facilities established at the Schmittenbach torrent and its tributaries the whole project was regarded as the first considerable comprehensive melioration effort within Europe (Hinterstoisser, 1985).

At the more or less steep slopes with east to southeast exposure at an altitude from 1400 to 1880 m above sea level, and thus 200 m above the timber line, reforestation with Norway Spruce, European Larch, Scots Pine, Green Alder and a little bit of Mountain Pine was attempted. Five alps with a total area of 142.37 ha were purchased to be converted into forests (Hinterstoisser, 1985). Until the end of the 1890s, the Breiteckalpe, 14.7 ha, Fillalpe und Wimmelalpe, 48 ha and from 1900 to 1910 the Hinterfalleckhochalpe, approximately 26 ha, were reforested. A reforestation plan for the 53.67 ha of the Hinerfalleckgrundalpe and the Beilalpe for the years from 1913 to 1922 was approved. However, due to increasing inflation and the resultant reduction of money the reforestation activity from 1916 onwards were substantially reduced and thus only 28 of the 53.67 ha in those two alps had been successfully reforested by the end of 1922 (Haiden, 1935). Thus, the total area where reforestation activities within this project had been conducted can be estimated as 117 ha. According to a different source of information about 158 ha had been reforested in the course of the project. Reforestations of barely stocked forestland are included in that calculation. (Forsttechnischer Dienst für Wildbach und Lawinenverbauung, Gebietsbauleitung Pinzgau, 2002). Over the course of that project, slopes with wet areas and a tendency of landslides were planted with small bushes of Green Alder. Those plantations matured to dense impenetrable vegetation cover and soil erosion was substantially reduced.

At the Breiteckalpe, reforestation with Norway Spruce was successful due to the fact that this alp is situated below the timber line on a slope with north-east exposure and thus, it offers quite favourable conditions for the plants.

The other alp and pasture land was divided into three reforestation zones:

- From the valley-bottom up to an elevation of 1730 m the Spruce – Larch – Zone was defined. 4,500 young trees per hectare were planted, 80% Norway Spruce and 20% European Larch.
- From 1730 to 1780 m the Larch – Spruce – Zone was defined. 4,500 plants per hectare were planted, 50% Larch and 50% Spruce.
- From 1780 to 1880 m the Scots Pine – Zone was defined. 2,250 plants per hectare were planted in small groups, depressions with long snow cover completely barren spots were exempt.

In the Fillriedel and the Wimmriedel plants grew well during the first 20 years. Trees in the highest zone grew well during the first 20 years and had reached a height of 0.8 – 1 m, however, from 1913, with first appearances of red needles, to 1920 almost all the Scots Pine trees in the Fillriedel and the Wimmriedel in elevations higher than 1.700 m died. Frost drought was considered as the main trigger on those steep slopes with south-east exposure and infection with *Lophodermiumi seditiosum* was also discussed.

European Larch and Norway Spruce trees started to suffer also once they had grown higher than the winter's snow cover. Reasons were hail and high forces from sliding snow as well as drying in the case of the Norway Spruce.

Below 1,650 m altitude, where the relicts of the former forest line could be found, trees flourished despite the partly rather steep terrain. Together with the dense vegetation of the planted Green Alder on the former landslide spots, the reforestation project was a success. The objective of improving the runoff pattern in the Schmittenbach watershed was to be met by improvements in the vegetation cover of these lower but partly steeper regions. It was discussed that the reforestation of those steep slopes might be more important for retarding rainfall runoff compared to elevating the timber line into a region where the terrain is actually not that steep and a dense vegetation cover of *Rhododendron* sp. and *Vaccinium myrtillus*, *V. vitis-idea*, *V. uliginosum*, etc. exists.

The financial resources for the years 1925 to 1934 were allocated to reforestation projects below 1700 metres elevation and for reforesting missing spots on the Beilalpe.

In 1958, high-elevation reforestation (1650 – 1850 m a.s.l.) was launched between Schmittenhöhe and Salersbachkopf. It was finished in 1970 with some necessary additional reforestation work later on. Norway Spruce and European Larch together with Mountain Ash as pioneer crop and Scots Pine between Hochzeller-Alm and Salersbachkopf Scots were planted. Unfortunately, a large part of the Spruce and Larch trees died soon thereafter. Below the Hochzeller-Alm, Spruce was planted again in 'Bermen' but the snow pressure loosened the plants and they died. Pure Spruce and Larch forests were re-established in the following years below the mountain ridge.

Given the fact that these species composition is more suitable for lower elevations, the mentioned Spruce and Larch forests are regarded as a suboptimal solution. This is consistent with findings of the vegetation mapping of Gayl in 1958 and the work by Aultizky (1963) on wind-snow-ecograms.

The Norway Spruce plants in the larger reforestation areas were reduced by a snow blight-infection (*Phacidium infestans*). The European Larch trees mainly died when they exceeded the height of one meter. The situation was better for the Scots Pine for sometime until the plants faced stress by summer and winter tourists either by tearing off parts from the plants or scratching them with their skis. In addition, a large part of the remaining Pine trees died suddenly during the winter 1979/80, presumably by an infection with dieback (*Brunchorstia pinea*) (Hinterstoisser, 1985). Additionally a snow blight infection from the year 1970 onwards was reported (Forsttechnischer Dienst für Wildbach und Lawinenverbauung, Gebietsbauleitung Pinzgau, 2002).

In 1992, the 'Flächenwirtschaftliches Projekt Schmittenhöhe' (reforestation plan) was launched. It aimed at the continuation and maintenance of high elevation reforestation. Avalanche control systems below the 'Hochzelleralm' were established and Norway Spruce and European Larch were planted in between (Forsttechnischer Dienst für Wildbach und Lawinenverbauung, Gebietsbauleitung Pinzgau, 2002).

With the launch of the first big reforestation project at the end of the nineteenth century, a more than 100 years long history of considerate forest management and big afforestation efforts began. On the other hand, interventions of a completely opposite direction – the establishment of a skiing area – started sometime earlier.

Changing land cover from the late nineteenth century to the 1980s is clear in the following three pictures taken of the Schmittenbach valley (Figure 4). Highest point is the Schmittenhöhe, where the mountain station of the Schmittenhöhe cable car (built in 1927) can be seen in the latter two pictures.

Deep and very productive soils were evident up to 1700 m above sea level. In higher elevations stones, rubbles, and a dense vegetation of *Rhododendron* sp. and *Vaccinium* sp. together with single small groups of bush-like Norway Spruce could be found.



Figure 4. Different forest covers in the Schmittenbach watershed from 1887 to 1986 (Hagen, 2003). In the picture of 1976 and 1986 the skiing slope 'Trassabfahrt' can be seen in the left half of the pictures. The cable car crossing the skiing slope and going up to the Schmittenhöhe, the highest top, can be distinguished as well.

1.2.4.2.2 Interventions of the skiing industry in the vegetation cover

Technical skiing industry in the area had a long history. Building of lifts and ski runs which initiated changes in the plant cover began more than 80 years prior. Important activities connected with the development of the skiing industry and eventually with changes/reductions in plant cover in the Schmittenbach watershed are summarised in the following list (Hinterstoisser, 1981 and Internet: Schmittenhöhebahn-AG, 2007):

1. In 1927 the Schmittenhöhen-cable car was built.
2. The first ski slope was the '**Nordabfahrt**' going from the restaurant Mittelstation (formerly Schweitzerhütte) down to close the city. That ski slope initially was far narrower than it is today. At that time people were very cautious about cutting the trees necessary for making a width of even 4-10 m! In 1932 an area of 2800 m² was cut illegally and afterwards the slope was lengthened through the Wimmwald to Zell am See.
3. At the end of 1933 the '**Südabfahrt**' ski slope in the area of Hochfalleck was approved.
4. In 1934 the construction of the Köhlergrabensprungsschanze (ski jump) was built despite opposition by foresters.
5. In 1935 the enlargement of the Nordabfahrt (northern slope) from the Breiteckalm to the Fillbank and to the Knappenmais was discussed. In the upper part near the timber line its width was 40m, whereas more slopes were in the forested area with a width of 6 m. As a compensation for the clear cut of 4.7 ha the alp-parcel 376 KG Schmitten (Waxegg) with an area of 3.4 ha had to be reforested.
6. In 1946 the Ebenberglift (the first ski lift) was built.
7. A plan for a 'slalom slope' today's '**Trassabfahrt**', was not approved by the land owner nor the 'Forest commission'. This ski slope was planned to run from the Schmittenhöhe to the Breiteckalpe with a continuation to the base station of the Schmittenbahn. After the establishment of the National Socialist regime the land Salzburg and the 'Gauleiter' (head of local district Zell/see) licensed the project. In 1948 it was decided to enlarge the 10 to 20 m wide Trassabfahrt resulting in a 2 km long and on average 30 m wide downhill race track.
8. The first ski lift at the top of the Schmittenhöhe, the Breitecklift, was put into place and is in use since 1948.
9. In 1956 the Sonnenalmbahn and in 1958 the Sonnberglift were built. It is interesting to note that this was a different company but the Schmittenhöhen AG took over the Sonnbergbahn in 1968.
10. The Kettinglift was opened in 1958.
11. The Fallegglift was built in 1961.
12. From 1966 to 1968 the Nordabfahrt was enlarged.
13. The Trassabfahrt was further enlarged in 1967 and 1970 with an extent of 2.5 ha.
14. In 1969/1970 the enlargement of the Sonnkogel skiing area was conducted by building the Hochmaislift, creating the '**Hochmais-**' and '**Osthangabfahrt**' and by the construction of the Osthanglift in 1969/1970.
15. In 1969 the enlargement of the Nordabfahrt was approved, whereas the planned cuttings at the Trassabfahrt lead to big controversies. The city council forest-officials believed that the objective of the reforestation project – the pacification of the Schmittenbach – was endangered, given that great quantities of trees, also from stocks planted during the big reforestation project at the end of the 19th/ beginning of the 20th century, had already been cut. Nonetheless, the cutting was approved after further discussions. The prerequisite was the reforestation of spots in the region of the old 'Köhlergrabenschanze' and a short and recently abandoned bypass of the Trassabfahrt, the total area comprising approximately 3 ha.
16. (A second way up to the Schmittenhöhe was created by the erection of the Areitbahn coming from Schüttdorf in 1970 but this area does not belong to the Schmittenbach watershed.)
17. In 1971 the ski slope '**Standardabfahrt**' between the Mittelstation (of the Areitbahn) and the base station of the Schmittenhöhebahn was established. About 8 ha of forest had to be cut. As

they lacked areas to be reforested as compensation in the watershed the company had to pay for the reforestation of clear cutting area and paid for the recultivation

18. In 1971/72 the Hirschkogellift and the ski slope 'Hirschkogel' as well as the Bruckberglift were built.
 19. The Trassabfahrt was enlarged in 1971 as well as the Standardabfahrt in 1972.
 20. In 1973/74 the Breiteckbahn was established.
 21. The next step towards a further enlargement of the skiing area was the construction of the so-called Zeller Bergbahn, a cable car lift directly from the city centre. In 1977 the Sonnenalmbahn was rebuilt and substantially improved.
 22. The modification of the Sonnkogellift in 1984 resulted in the cutting of 0.5 ha.
 23. In 1981 the Sonnengratlift was built.
 24. In 1988 a big artificial snow system was built for the skiing slopes Standardabfahrt, Trassabfahrt, the Slalomhang and the skiing path Schmittental, which covers an area of 17 ha.
 25. After the enlargement of the artificial snow system for the Nord-, Standard- and Trassabfahrt in 1989/90, 38 ha could now be covered with artificial snow.
 26. Recultivation and sanitation of the Höhenpromenade between Schmittenhöhe and Sonnkogel was achieved in 1995.
 27. The Schmittenweg between Schmittenhöhe and Panorama-Pfiff was recultivated in 2002.
 28. The Zeller Bergbahn was reconstructed as the CityXpress in 2003.
 29. Construction work on the plateau at the mountain top was finished in 2003.
 30. In the area of Sonnenalm / Sonnkogel a new chair lift and a ski slope were opened.
- Until 1965 about 50 ha had been cleared for lifts and ski slopes.
 - Until 1971 already 55.8 ha had been cut again. Only about 20 ha had been reforested as compensation at other spots belonging to the WGZ.
 - Until 1981 about 94.7 ha had been cleared for lifts and ski slopes in the Schmittenbach watershed (see Table 2).
 - The reforestations at the Sonnkogel, as a compensation for other clear cuts, as well as the reforestation attempts in high altitudes between Schmittenhöhe and Salersbachkopf from 1958 to 1970 have not yet been well established.

An impression of the interventions in land cover by the skiing industry in the Schmittenbach watershed is illustrated below (Figure 5).

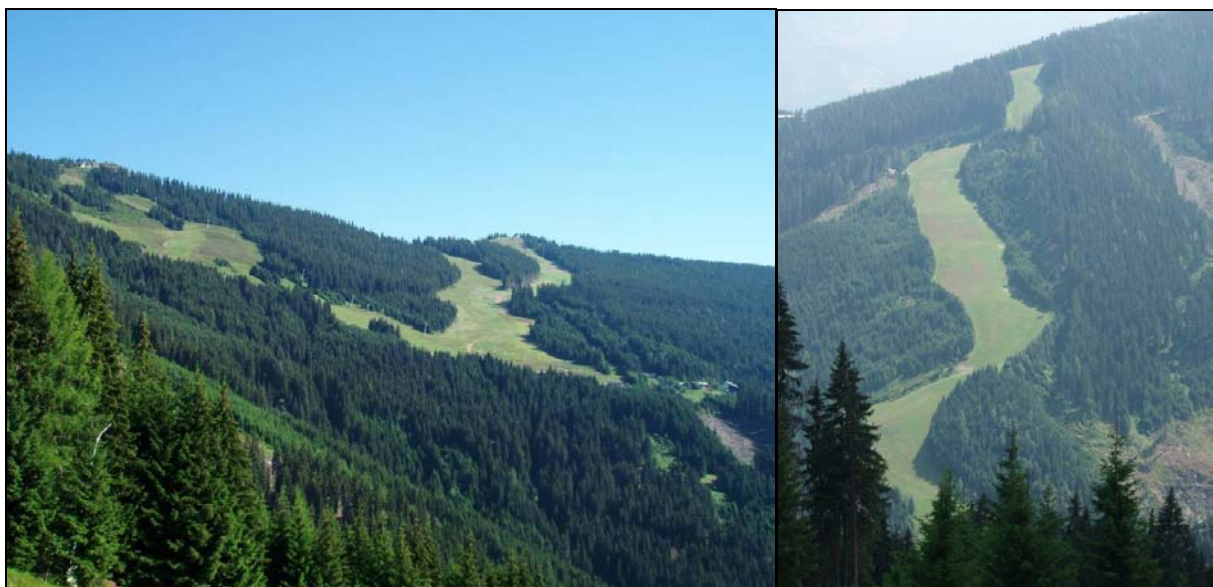


















Figure 5. Ski slopes 'Künstlerhang' and 'Jedermann' in the area of the Auermaiß in the North (left picture) and the 'Standardabfahrt' in the South (right picture) of the Schmittenbach watershed in July 2007.

Table 1. The main ski slopes in the Schmittenbach watershed (the colours blue, red and black indicate the degree of difficulty) (Internet: Schmittenhöhebahn-AG, 2007)

Ski slope sign	Name of the ski slope	Ski slope sign	Name of the ski slope	Ski slope sign	Name of the ski slope
 1	Panorama	 12	Skiweg Nord	  17	Slalomhang
  2	Hirschkogel	 13	Standardabfahrt	 20	Sonnengalerie
 4	Sonnengrat	 14	Trassabfahrt	 21	Künstler-Hang
 5	Westwechsel	 15	Südabfahrt	 22	Sonnenschein
 11	Nordabfahrt	 16	Zeller Skiweg	 23	Jedermann

Currently, more than a dozen skiing slopes are situated within the Schmittenbach watershed (Table 1). The skiing map below shows all the skiing slopes and lifts in the region (Figure 6). It visualises that the density of skiing premises is already high.



Figure 6. Map of ski slopes, ski lifts and cable cars in the Schmittenbach watershed (Internet: Schmittenhöhebahn-AG, 2007)

Table 2. Loss of area for skiing purposes in the Schmittenbach watershed until 1981 (Hinterstoisser, 1985).

Ski slope	Vegetation type	Area (ha)	Sum (ha)
Trassabfahrt	forest	9.4954	9.4954
Hirschkogel (Breiteck to Standardabfahrt)	alp	0.1219	18.9621
	forest	16.4584	
	alp	2.3818	
Standardabfahrt	forest	10.3041	10.3041
Umfahrung Mittelstation (Standard-Nord)	forest	1.2394	1.3381
	alp	0.0987	
Nordabfahrt (Ebenbergalm)	forest	8.7240	8.8500
	alp	0.1260	
Sonnkogel	forest	27.7939	27.7939
Hochmaishang - Osthang	alp	6.2618	7.9919
	forest	1.7301	
Südabfahrt	forest	0.8325	0.8325
Sonnengratbahn + Abfahrt	forest	2.2690	2.2690
	High elevation afforestation		
Zeller Schiweg	forest	1.4220	1.4220
lift-routs not on ski slopes	forest	5.4364	5.4364
Whole area for skiing purposes (ha)			94.6954

The skiing industry occupied much space in the Schmittenbach watershed. By the middle of the 1980s, an area of 95 hectares had been handed over to skiing purposes. Mostly forests in low to mid high elevations, but even high elevation forests (see Table 2), and alps in mid to high elevations have been transformed into land mainly serving for skiing purposes. On the other hand, due to the high afforestation efforts, the total forest cover was actually increased from the late 19th century onwards when the first afforestation projects were initiated (compare Table 3 and Figure 4). The area of bare soil, so called 'Plaiken', was reduced substantially from almost 3% of the total area to less than 1% already by the mid of the 20th century.

Table 3. Share of the different land use types in the Schmittenbach watershed from 1884 to 1987 (Forsttechnischer Dienst für Wildbach und Lawinenverbauung, Gebietsbauleitung Pinzgau, 1996).

Land use type	1884		1954		1975		1987	
	Area (ha)	(%)	Area (ha)	(%)	Area (ha)	(%)	Area (ha)	(%)
Forest	600 ^a	57,7%	784	75,4%	781	75,1%	801	77,0%
Alps	300	28,8%	141	13,6%	114	11,0%	20	1,9%
Bare soil	30	2,9%	4	0,4%	5	0,5%	5	0,5%
Ski slopes and lifts	0	0,0%	19	1,8%	48	4,6%	95	9,1%
Other agricultural area, houses, etc.	110	10,6%	92	8,8%	92	8,8%	120	11,5%
Total	1040	100,0%	1040	100,0%	1040	100,0%	1040	100,0%

a ...at least 10% of the 600 ha forest area were barely stocked (Thoma, 1900)

For the years 1963 to 1995, a visual description of the state and changes in the land cover had been done for the West part of the Schmittenbach watershed, i.e. for the sub-watershed of the main outflow gauge at the river Schmittenbach (Figure 7, compare Figure 1). The sub-watershed includes the highest mountain, the Schmittenhöhe, in the West and makes up 70% of the total Schmittenbach watershed. Of the approximately 7.3 km² of this area, 57% was forest and 24% was grassland and pastures. Reforestation, primarily high elevation reforestation, amounted to roughly 88 hectares or 12% of this sub-watershed, whereas in the same time, 51 hectares or 7% had been deforested mainly for skiing purposes. Most problematic was the enlargement of the ski slope 'Trassabfahrt' in the sensible zone of the left branch of the brook 'Breitenbach' in the Southwest of the watershed. The deforestation associated with the new ski slope 'Standardabfahrt' in the South is easily visible (Hagen, 2003).

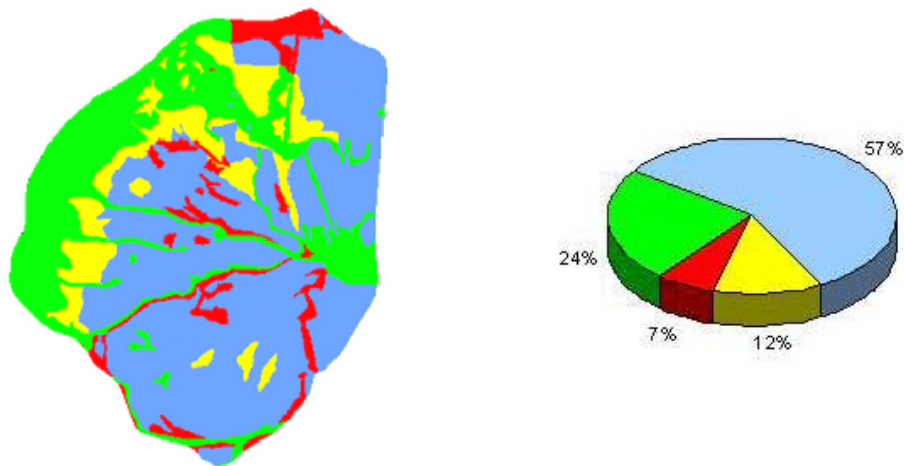


Figure 7. West part of the Schmittenbach watershed above the main runoff gauge (approximately 7.3 km²): Vegetation and vegetation changes during 1963 – 1995 are shown: green: alps and grassland, yellow: afforested area, blue: forest, red: deforested area. The pie chart gives the percentages of vegetation and vegetation changes (Hagen, 2003).

2 Methods

2.1 Field campaign in the Schmittenbach watershed

The field campaign in the Schmittenbach watershed was carried out during two weeks in July 2007. A basic and crucial part of the field campaign was stem analysis in the Schmittenbach watershed. As the main part of the field work, forest stand and soil data were collected in the forest of the local forest company 'Zeller Waldgemeinschaft'. Additionally, the current vegetation distribution in the Schmittenbach watershed was assessed during that time. These data serve eventually as the basis for the in-depth studies using a mechanistic ecosystem model to assess the protection function of the forests in the watershed.

2.1.1 Current vegetation distribution

The vegetation cover in the Schmittenbach watershed was categorised into the following vegetation types: forest, good pastures, planed pastures, and dwarf shrub/curved wood area with alpine pastures. The purpose was to get an idea of the current distribution of the seven biome types (evergreen needle, deciduous needle, deciduous broadleaf and evergreen broadleaf forest, shrub land, C3 grass and C4 grass land), which can be simulated with the BIOME-BGC model (Pietsch and Hasenauer, 2002).

2.1.2 Stem analysis

One important incentive of the stem analysis was to build future analyses on existing data provided by the management plan of the local forest company. Production of forests is a key issue in assessing the protection function, so the question was if the regional suggested site index system as a measure for assessing the production function is comparable with data from field measurements.

One option to study such comparisons was stem analyses (drawing tree growth curves) and to then compare the field data with the dominant tree height development of the regional suggested yield table. If they are consistent, then the yield table mimics the production potential properly, and if not, then an under or overestimation is evident. For this purpose we selected the sites and cut the trees in such a way that we got a wide range of different age classes in combination with a broad spectrum of different site qualities.

At each of those sites, mostly three dominant trees were felled and measured to reconstruct the height development. Special emphasis was given to old trees growing on the best and on the poorest sites to ensure that the extreme growing conditions are covered in the data. According to previous experiences, the applied yield table suites best for trees growing in areas of average site quality.

Three dominant trees were felled per site and the stems were cut into sections of a length of approximately 4 meter. Since the tree top is just of low economic value it can be cut into smaller sections in order to increase the accuracy of the measurements. The year rings were counted for each cut and the distance of the cut to the next whorl above the cut had to be also measured. This could only be done if the location of the next whorl could be determined. This was hardly possible at the branchless parts of the stem.

To calculate the total age of the tree the year rings of the stump were counted and then the estimated age to the stump height was added. Our assumption was that it took the trees three years to achieve the stump height of approximately 30 cm. To get the tree age at the heights of the other cuts the counted year ring number at a certain cut had to be subtracted from the total tree age. Finally, it had to be taken into consideration that that age was not exactly true for the height in which it has been counted but in the height of the next whorl! Therefore, the distance of the whorl from the cut had to be added to the height of the cut.

The tree growth functions resulting from these data were compared with 'dominant height growth functions' from the literature for different yield tables. In this case the 'dominant height growth functions' of Mitscherlich/Richard (1919) for 'Fichte Bayern' and 'Fichte Hochgebirge' (see Marschall, 1975) were used (equations 1.) (Kindermann and Hasenauer, 2005).

Dominant height growth functions of Mitscherlich/Richard (1919):

$$\begin{aligned}
 OH &= a \times (1 - e^{-b \times t})^c \\
 a &= a_0 + a_1 \times OH_{100} + a_2 \times OH_{100}^2 \\
 b &= b_0 + b_1 \times OH_{100} + b_2 \times OH_{100}^2 \\
 c &= c_0 + c_1 \times OH_{100} + c_2 \times OH_{100}^2
 \end{aligned}
 \tag{1.}$$

OH dominant height

OH100 dominant height at the age of 100 (OH100 and site index are directly correlating)

t age of the tree

a, b, c parameters, different for 'Fichte Bayern' and 'Fichte Hochgebirge' (Table 4)

Table 4. Parameters for the dominant height growth functions of Mitscherlich/Richard (1919) for 'Fichte Bayern' (FiBay) and for 'Fichte Hochgebirge' (FiHgb) (Kindermann and Hasenauer, 2005).

	a_0	a_1	a_2	b_0	b_1	b_2	c_0	c_1	c_2
FiBay	1.05E+01	7.46E-01	3.52E-03	7.72E-03	7.96E-04	-8.77E-06	2.31E+00	-1.55E-02	
FiHgb	6.35E+00	1.32E+00	-9.38E-03	1.24E-02		1.18E-05	2.08E+00	-2.65E-02	8.48E-04

2.1.3 Stand parameters

The objective was to compare the data of the management plan 2003 of the local forest company 'Zeller Waldgemeinschaft' in the town 'Zell am See' with our own measurements. According to this, data were recorded and following parameters were investigated and compared:

- the dominant tree height,
- stand age,
- total volume per hectare and
- site index

20 locations representing different forest stands were chosen across the forest of the 'Zeller Waldgemeinschaft'. Four points were selected for data recording at each location. The aim was to obtain data with a wide spectrum of tree age, site quality, elevation and exposure. For the comparison of the management plan 2003 with our own figures, the average as well as the median of the mostly four plots at a given location/stand were calculated and used.

The stands for the measurements should cover the full range of different age classes and site qualities. Therefore, they were selected according to the following rough principles:

- (1) covering (i) young, (ii) middle aged and (iii) mature forests (age classes 2–7+)
- (2) covering (i) poor, (ii) medium and (iii) very good sites (lowest to highest possible site index)

At each of the 20 forest stands, four plots (with one exemption where only two plots could be chosen due to the small size of the stand) were randomly chosen.

At each of the 78 plots, the following measures were taken:

- dbh (diameter at breast height), tree height, height to the live crown base
- humus and topsoil samples for further analyses of the nitrogen and carbon content at different soil layers in the lab.

The inclination was measured with a 'Relascope'. The slope and aspect were determined with a 'Vertex' and the exact location of the plot was recorded with a GPS-device.

Working with the Relascope and a basal area factor [baf] of 4, the trees of the point sampling were selected and numbered. Then the dbh was measured with a diameter tape and the total height and the height to the live crown was assessed with the Vertex for each of the selected trees. Tree species and broken tree tops had to be noted as well.

78 points were recorded in total covering the main site and stand conditions within the Schmittenbach watershed. An overview of the locations gives the following map (Figure 8).

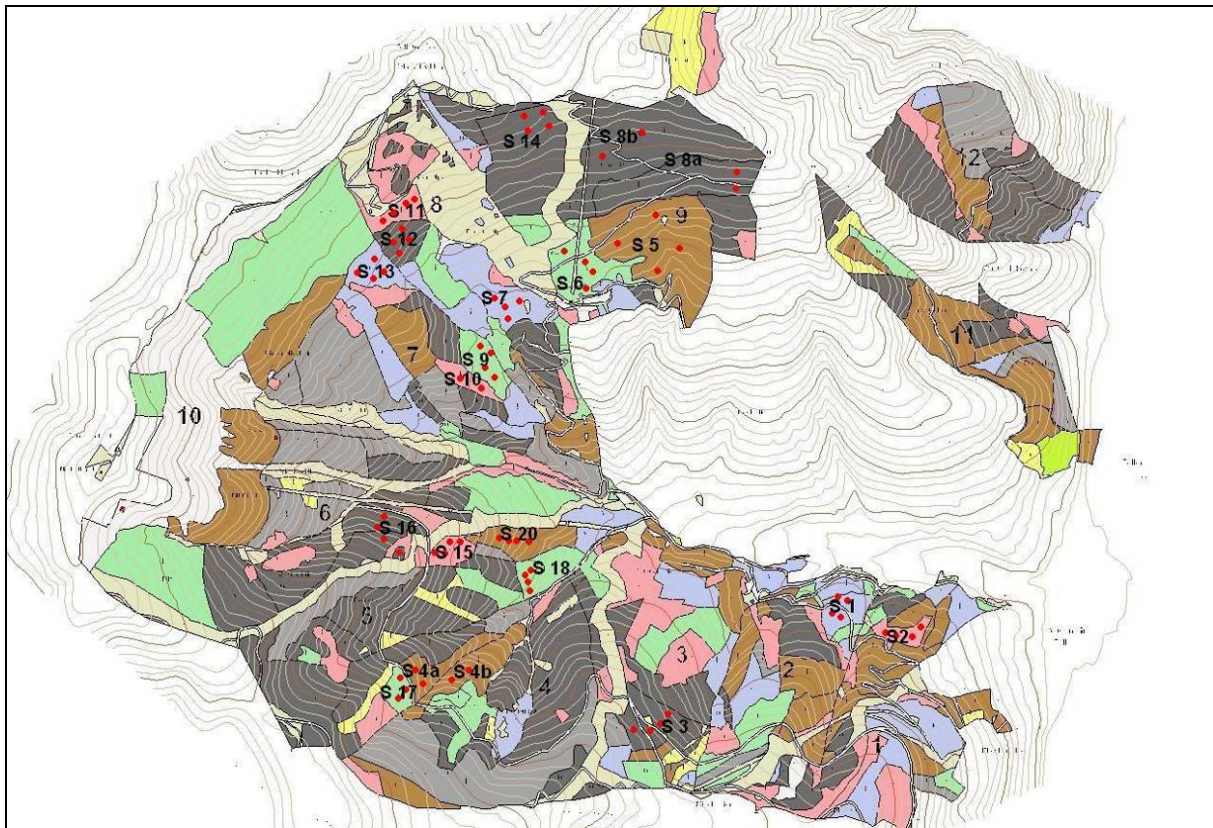


Figure 8. Forest map of the Schmittenbach watershed from the forest management plan 2003 of the local forest community: the colours indicate the different age classes (yellow: 1-20, pink: 21-40, green: 41-60, blue: 61-80, brown: 81-100, light grey: 101-120, dark grey: 121<), the big numbers (1-12) give the number of the forest unit; S # (1-20) gives the number of the point sampling stand from the field campaign in 2007, the red points indicate the location of the single point samplings (78).

2.1.3.1 Stand age

One typical tree (ideally the tree with the median diameter) was cored to get information about the stand age.

2.1.3.2 Dominant height

The dominant tree height per plot can be calculated as the average of the tree heights of the three biggest trees. The average dominant tree height for the four plots at a given location is calculated and compared with the dominant tree heights derived from the local yield table. The idea was to investigate the consistency between dominant tree heights observed in our study versus the dominant tree height of the management plan. Since the dominant tree height at a given stand age is a measure for productivity it gives us some insights how comparable the different numbers are for assessing forest productivity.

The dominant height from the management plan 2003 of the local forest company was not given directly. It was derived from the stand age and the site index using the dominant height growth functions of Mitscherlich/Richard (1919) for 'Fichte Hochgebirge' (see equations 7.) (Kindermann and Hasenauer, 2005).

2.1.3.3 Volume

For calculating the total volume per hectare for one plot ($V \cdot \text{ha}^{-1}$) the diameter breast height [dbh] and tree height [h] as well as the form factor for stem wood [f] of each tree of the point sampling are needed. The form factor function of Pollanschütz (1974) was applied to get the form factor for each tree. For different tree species different parameters for the form factor function are required. In our case the tree species Norway Spruce (*Picea abies*), European Larch (*Larix decidua*), European Silver Fir (*Abies alba*), Sycamore Maple (*Acer pseudoplatanus*), Silver Birch (*Betula pendula*) are relevant and were assessed.

For the Silver Birch and the other broadleaf tree species the form factor function for the European Beech (*Fagus sylvatica*) was applied, as for them no special parameters for the form factor function exist.

- Represented volume per hectare for one tree:

With the dbh the basal area [ba] is calculated. Multiplying the basal area with the form factor [f] one gets the tree volume [v]. To get the represented tree number per hectare [N_{rep}] the basal area factor [baf] (in our case 4) is divided by the basal area of one tree. Now v is multiplied with N_{rep} and the result is the represented volume per hectare [$V \cdot \text{ha}^{-1}$] for one tree (equations 2.-6.).

Form factor function of Pollanschütz (1974):

$$f = b_1 + b_2 \times \ln^2 d + b_3 \times \frac{1}{h} + b_4 \times \frac{1}{d} + b_5 \times \frac{1}{d^2} + b_6 \times \frac{1}{(d \times h)} + b_7 \times \frac{1}{(d^2 \times h)} \quad (2.)$$

$$ba = dbh^2 \times \pi / 4 \quad (\text{m}^2) \quad (3.)$$

$$v = ba \times f \quad (\text{m}^3) \quad (4.)$$

$$N_{\text{rep}} = baf / ba \quad (\text{m}^{-2}) \quad (5.)$$

$$V = v \times N_{\text{rep}} \quad (\text{m}^3 \cdot \text{ha}^{-1}) \quad (6.)$$

f form factor

b1 – b7 parameters, varying among different tree species

d dbh (dm!)

h tree height (dm!)

ba basal area (m^2)

dbh diameter at breast height (m)

v volume of one tree (m^3)

N_{rep} represented tree number (m^{-2})

V represented volume of one tree ($\text{m}^3 \cdot \text{ha}^{-1}$)

- For the total volume per hectare for a single plot the represented volumes per hectare of all trees of one point sampling are summed up.

2.1.3.4 Site index

To determine the site index of each plot the tree age (determined by coring) and the dominant height [h_{dom}] of the trees of the point sampling were needed. With the values from the yield table for 'Fichte Hochgebirge' the site index was interpolated (see Marschall, 1975).

2.1.3.5 Stand Density Index (SDI)

Finally, the Stand Density Index (SDI) according to Reinecke (1933) was calculated. The purpose was not the comparison with the management plan 2003 but for use in the analysis of the BGC model predictions.

The SDI is calculated from the total represented tree number per plot [N_{rep_p}], which is the sum of all represented tree numbers of the trees per plot and the mean dbh per plot [$\overline{dbh_p}$] (equation 7.). The SDI shall be calculated only for even aged stands. One plot (plot 13_3) absolutely did not fulfil this requirement. Since the dbh range was much too high in that stand the SDI calculation resulted in an extremely high value. Therefore the plot was excluded from further analysis of SDI.

$$SDI = N_{rep_p} \times \left(\frac{\overline{dbh_p}}{25} \right)^{1.605} \quad (7.)$$

N_{rep_p} total represented tree number per plot

$\overline{dbh_p}$ mean diameter breast height per plot

2.1.4 Soil parameters

The soil carbon and nitrogen content was determined for each plot. Samples taken in the field were analysed in the lab. The information is required for the later modelling exercise since soil conditions affect not only degradation but also water holding capacities, nutrient status etc.

2.1.4.1 Soil sampling

With a core soil sampler (length: 1 m, inner diameter: 2.5 cm) four soil samples were taken at each plot. The four soil sampling spots were situated up slope, down slope, to the left and to the right of each sampling point centre in a distance of 4 meters. If there was an obstacle at one of the spots the distance to the centre could have been prolonged by 2 metres. The thickness of the humus layer and the topsoil horizon were measured. The four humus samples of one plot were collected in one plastic bag, the four top soil samples were collected likewise. If the centre of the point sampling was too near to the edge of the stand so that one of the spots for soil sampling was already situated outside the stand this very soil sample was skipped. At a swampy plot the differentiation of humus layer and topsoil was not possible so the thickness of the upper soil horizon was measured at once and the samples were put together in just one bag. The bags were labelled and brought to the lab after the field work had been finished. The mean thickness of the humus layer and the mean total thickness of the humus layer and the topsoil were calculated for each plot as well as for each stand.

2.1.4.2 Soil carbon and nitrogen content determination in the lab

The soil samples were dried and afterwards sieved to remove stones. The < 2 mm fraction including litter residues was milled and analysed for its carbon content using LECO SC – 444. The nitrogen content of the samples was determined using the Kjeldahl method. Values received from the lab were in unit weight proportion. We had to multiply them with the soil density (humus: 600 kg.m⁻³ (Fosberg, 1977), topsoil: 1400 kg.m⁻³) and the soil depth (m) to receive our target unit (kg.m⁻²) (= output unit of BGC model for soil carbon and soil nitrogen).

2.2 Mechanistic biogeochemical ecosystem modelling

2.2.1 The BGC model

In this project we use the BIOME-BGC model version 4.1.1. (Thornton et al., 2002) incorporating extensions on hydrology (Pietsch et al., 2003), species specific parameterisation (Pietsch et al., 2005) and self initialisation (Pietsch and Hasenauer, 2006). Cycling of energy, water, carbon and nitrogen are simulated in a daily time resolution. The daily simulations calculate:

- daily canopy interception, evaporation and transpiration
- soil evaporation, outflow, water potential and water content
- Leaf Area Index (LAI) (m^2 leaf area per m^2 ground area)
- stomatal conductance and assimilation of sun-lit and shaded canopy fractions
- Gross Primary Production (GPP) and Net Primary Production (NPP)
- allocation of carbon and nitrogen to the different ecosystem compartments (soil, litter, roots, stem, leaves)
- litter-fall and -decomposition
- mineralisation, denitrification, leaching and volatile nitrogen losses.

Leaf Area Index is obtained from multiplying the carbon allocated to leaves with the specific leaf area (m^2 leaf area per kg leaf carbon) (Pietsch and Hasenauer, 2002). The LAI controls canopy radiation absorption, water interception in the canopy, photosynthesis and litter inputs to the detrital pools.

Photosynthesis – calculated with the Farquhar photosynthesis regime – results in Gross Primary Production (GPP). Net Primary Production (NPP) is the difference between GPP and autotrophic respiration. The latter comprises (i) maintenance respiration – a function of tissue nitrogen concentration – and (ii) growth respiration that depends on the amount of carbon allocated to the various plant compartments (leaf, root and stem). NPP gives the mass of carbon that is fixed and kept by square meter ground per year ($\text{kg C} \cdot \text{m}^{-2} \cdot \text{yr}^{-1}$) and is partitioned into the different plant compartments as a function of a dynamic allocation pattern, which considers eventual limitations due to the availability of and compensation for nitrogen. The total ecosystem carbon storage results from the balance between NPP and heterotrophic respiration, which is regulated by decomposition activity, the seasonal input of vegetation biomass into litter and soil organic matter pools and the annual mortality rate commonly set to 0.5% of vegetation biomass (Pietsch and Hasenauer, 2006).

2.2.2 Input data

The principle ecological processes modelled by the BIOME-BGC model include: daily meteorological data, atmospheric (CO_2 content, Nitrogen deposition) and soil characteristics, geographic location and eco-physiological parameters of the vegetation/tree species. In addition, at the beginning of the simulation process, input data is provided for the starting values of carbon, nitrogen and water in the ecosystem, these are necessary for the self-initialisation procedure. In the table outlined below, the input parameters are combined, which are identical for all plots in the Schmittbach-watershed (Table 5).

Table 5. Input parameter for the BGC model simulations, which are identical for all plots in the Schmittenbach-watershed, i.e. albedo, texture (percent of sand, silt and clay content of the soil), preindustrial and actual Nitrogen deposition (Ndep1 and Ndep2), Nitrogen fixation (Nfix), the CO₂-file (with the necessary information for the automatic regulation of the annual CO₂ concentration in the atmosphere) and the epc-file (for the species specific parameterisation, (Pietsch et al., 2005)).

Albedo	Sand	Silt	Clay	Ndep1	Ndep2	Nfix	CO ₂ -file	epc-file
0.2	21.81	38.82	39.37	0.0004	0.0027	0.0006	IS92a.dat	<i>Picea abies</i> (highland)

2.2.2.1 Weather data and other atmospheric characteristics

The meteorological input parameters comprise daily precipitation, minimum and maximum temperature, incident short wave solar radiation, vapour pressure deficit and day length. As these six characteristics are not directly available for the area they had to be interpolated from surrounding weather stations separately for each plot. For this purpose the point version of DAYMET (Petritsch, 2002), validated for Austria (Hasenauer et al., 2003), was applied. The program needs the geographic position, elevation, slope, aspect and the angle to the horizon in the West as well as the East to calculate the weather for a location.

Daily weather records were available for the years 1960 – 2005 and provided by the Austrian National Weather Centre in Vienna. This 46 years series of daily weather data was used repeatedly throughout the whole simulation process, beginning with the self-initialisation up to present day simulations. Only for 1960, at the beginning of the record of the weather data, was it essential to reset the weather record to the real data for that time. This was to make sure that during the years 1960 to 2005 the exact data measured for that period were used.

For the six meteorological input parameters, the means of all plots for the 46 years of weather records are given in following table (Table 6). In addition, the means can be separately calculated for all 20 stands in these 46 years. The minimum and the maximum values of these 20 means per meteorological parameter are listed as well (Table 6). For the purpose of clarity in the case of precipitation, annual values and not daily means are given.

For the CO₂ content of the atmosphere the preindustrial CO₂ concentration of 280ppm (IPCC WG I, 1996) was used in the model for the spin-up. From 1765 onwards, CO₂ concentration was annually increased to present day levels. This was done automatically by the model. Only a specific CO₂-file with the necessary data (IS92a.dat) must be used for the parameterisation of the model.

For the atmospheric nitrogen deposition, a preindustrial level of 0.0004 kg m⁻² yr⁻¹ was assumed (Ulrich and Williot, 1993) and this value was increased at the same rate as the CO₂ concentration to an actual value of 0.0027 kg m⁻² yr⁻¹.

Table 6. Meteorological data from the DAYMET climate model for the simulated plots in the Schmittenbach region: Mean over all 78 plots for the 46 years of meteorological data from 1960 to 2005; minimum and maximum mean of all 20 means per stands (- the means of the mainly four plots per stand) for the years 1960-2005.

	Mean of all plots	Minimum mean (stand level)	Maximum mean (stand level)
Annual precipitation (mm.yr⁻¹)	1286	1179	1377
Daily minimum temperature (°C)	0.39	-0.62	1.85
Daily maximum temperature (°C)	8.9	6.9	11.6
Vapour pressure deficit (Pa)	6.57	4.86	8.95
Solar radiation (W.m⁻²)	273.8	192.9	313.5
Average day length (h)	12	12	12

2.2.2.2 Site constants

Further site descriptive characteristics are needed as input parameters: geographic latitude, elevation (see Appendix, Table 17 and Table 18), albedo, soil texture (given as the relative share of sand, silt and clay), effective soil depth (depth of soil with water storing capacity, calculated as real soil depth reduced by the volume percentage of soil particles < 2 mm) and the nitrogen fixation (kg N m⁻².yr⁻¹). For nitrogen fixation, the value of 0.0006 kg N m⁻².yr⁻¹ was used. Albedo depends on the land cover type. For coniferous forests, an albedo of 0.2 is commonly used (Pietsch et al., 2005).

Soil texture and effective soil depth were interpolated from values from the Austrian Federal Soil Survey (Petritsch and Hasenauer, 2007). Soil texture did not vary among the plots and was given by 21.81% of sand, 38.82% silt and 39.37% clay. Interpolated effective soil depth at the plots gradually decreased from 74.9 cm to 58.2 cm with increasing elevation.

2.2.2.3 Eco-physiological parameters - Species specific parameterization

A set of eco-physiological characteristics of the prevalent vegetation at the site is another prerequisite for the simulations. The species-specific parameterisation for the main Central-European tree species (Pietsch et al., 2005) was applied. In our case only one tree species, i.e. Norway Spruce (parameterisation for lowland and highland) was potentially relevant, as the experimental area lies in the ecological optimum for Spruce dominated forests. Due to the location of the Schmittenbach watershed in the Northern Central Alps the parameterisation for 'Highland Norway Spruce' was used.

2.2.3 The simulation

2.2.3.1 Spin-up

The self-initialisation of the model or spin-up run serves to reach a dynamic equilibrium of all ecosystem pools. It starts with a minimal amount of carbon in the leaves (0.001 kg.m^{-2}) and a soil water saturation of 50%. It is finished when the running average of the soil carbon content (as the last pool to reach that state) does not change more than $0.0005 \text{ kg C m}^{-2}$ between two successive simulation periods of the length of the weather record (46 years). That tree species has to be selected for the spin-up, which is considered to form the potential natural vegetation in the area, no matter which species are found today under management impact. The time period this process varies between 3000 and 60000 years under different climatic conditions, at different sites and with different vegetation types (Pietsch and Hasenauer, 2006). For the Schmittbach region, we consider Norway Spruce (highland variant) as the dominating tree species before human intervention. The self-initialisation took 4500 – 8250 simulation years, depending on the plot.

2.2.3.2 Historic land use

With the self-initialisation procedure, a state of the ecosystem is reached that represents a situation without any human interference. Obviously, this is not the state in which forest ecosystems normally can be found in Central Europe today. Land use practices such as logging, litter raking, pruning for fodder production and livestock grazing have been disturbing the ecosystem considerably over several centuries. Eventually, it resulted in the degradation of the forest soil: a loss of carbon and nutrients and thereby a reduction of site-productivity has been the result (Pietsch and Hasenauer, 2002). To incorporate these effects in the simulation it is necessary to model a few rotations with the proper tree species. Each rotation begins and ends with a clear-cut/planting intervention. With a clear cut, all the above ground biomass is removed and the below ground biomass is transferred to the coarse woody debris compartment. Planting means that 10 grams of carbon are added to the leaf pool and 25 grams to the stem pool. With a planting intervention, the tree species may be exchanged. Rotation length obviously depends on the tree species, but can also be set by the user. To mimic historic land use in our experimental region, two rotations with Norway Spruce (100 years) were simulated before the establishment of the current stands.

2.2.3.3 Thinning

Current management of the forest needs to be considered, otherwise fully stocked stands are assumed and simulated, a misrepresentation of the managed forest in our case. A recently developed management sub-module for the BIOME-BGC supports the thinning intervention (Petritsch et al., 2007). In this new thinning regime, duration of acceleration of growth following thinning depends on the thinning intensity. In addition, changing distribution patterns of assimilates between above and below ground biomass and between wood and leaf biomass observed after a thinning intervention are addressed by a new dynamic carbon allocation regime. In the new model setup, the user can explicitly define the thinning procedure, i.e. it is possible to fix exactly the amount or percentage of stem carbon removal, leaf carbon removal, stem carbon that is left in the forest and is transferred to the coarse woody debris carbon compartment, root carbon that also contributes to the coarse woody debris carbon pool and leaf and fine root carbon that is added to the carbon litter pool. We assumed a thinning variant where the whole bole is removed but the leaves remain in the forest and are therefore added to the litter pool. Values are given as the percentage of the total pool

size. The same percentage of fine roots as stem carbon removed will therefore be allocated to the litter pool and coarse roots are assigned to the coarse woody debris carbon pool.

If the objective is to obtain similar carbon stocks with the BGC-simulations as have been observed in the field irrespective of the real thinning history of the stands, then thinning has to be conducted in such a way that the results are not biased against the SDI (Stand Density Index, after Reinecke, 1933). Having measured four plots per stand, a restriction for the thinning intervention is that those four plots are treated similarly, since management has to be considered as homogenous at the stand level due to common management planning practice.

In case a much smaller volume had been measured for one of those four plots (resulting from adverse site conditions or a natural disaster), it seems reasonable to add one additional intensive intervention. Otherwise, the average of the plots for the one stand would be distorted.

2.2.3.4 The BGC model output

The model produces over 600 daily output variables. In this study, we selected the following state variables: live stem and dead stem carbon, soil carbon 1-4 (1. Fast microbial recycling pool, 2. Medium microbial recycling pool, 3. Slow microbial recycling pool, 4. Recalcitrant soil organic matter) and soil nitrogen 1-4. For the flux variables we selected Net Primary Production, Leaf Area Index, annual precipitation, outflow, soil evaporation, snow sublimation, canopy evaporation and transpiration.

2.2.3.4.1 Volume

Volume per hectare is no output variable of the current BGC model version. It was derived from live- and dead-stem-carbon as model results. The carbon in the above ground woody biomass (live- plus dead-stem-C) was divided by the carbon fraction of woody dry mass [b] to obtain the dry mass. This value was then divided by the dry matter fraction of the fresh weight [c] in order to find the fresh weight. A division by the timber density [d] gives the whole volume of above ground woody biomass. Since only the merchantable timber volume is measured with common forest inventory techniques, e.g. angle count sampling like in our case, the above ground woody biomass is multiplied with the merchantable timber fraction [a] to receive the timber volume (Table 7) (Pietsch et al., 2005).

Table 7. Tree and wood parameters needed for the conversion of the BGC model output stem carbon into the target parameter volume per hectare ($\text{m}^3 \cdot \text{ha}^{-1}$) (Pietsch et al., 2005).

Merchantable timber fraction [a]	Dry biomass carbon fraction [b]	Fresh weight dry matter fraction [c]	Timber density ($\text{kg} \cdot \text{m}^{-3}$) [d]
0.700	0.503	0.440	800

2.2.3.4.2 Soil

In the BGC model the soil pool is divided into four sub-pools for carbon and nitrogen each. The matter in these four sub-pools can be distinguished by its degradability. Fraction 1 is the very labile soil carbon and nitrogen, fraction 2 and 3 are the less easily microbiologically degradable parts and fraction 4 is the recalcitrant soil carbon and nitrogen, i.e. the humus fraction. The self-initialisation of the BGC model finishes when the soil carbon pool does not change more than $0.0005 \text{ kg C m}^{-2}$ between two successive simulation periods of the length of the weather record (46 years). Simulated management practices (i.e. harvesting and thinning) that are introduced into the model subsequent to spin up reduce the soil carbon and nitrogen pools.

3 Results and discussion

3.1 Field campaign outcome

3.1.1 Current vegetation distribution

The vegetation cover in the Schmittenbach watershed was categorised. The largest area is covered by evergreen needle forest, as one of the seven biome types, which can be simulated with the BIOME-BGC model (Pietsch and Hasenauer, 2002), but also grassland/pastures and (dwarf) shrub land can be found. The vegetation types distinguished in detail were: Spruce forest, good pastures, planed pastures (ski slopes with poor grass cover) and dwarf shrub/curved wood area with alpine pastures (see Figure 9).

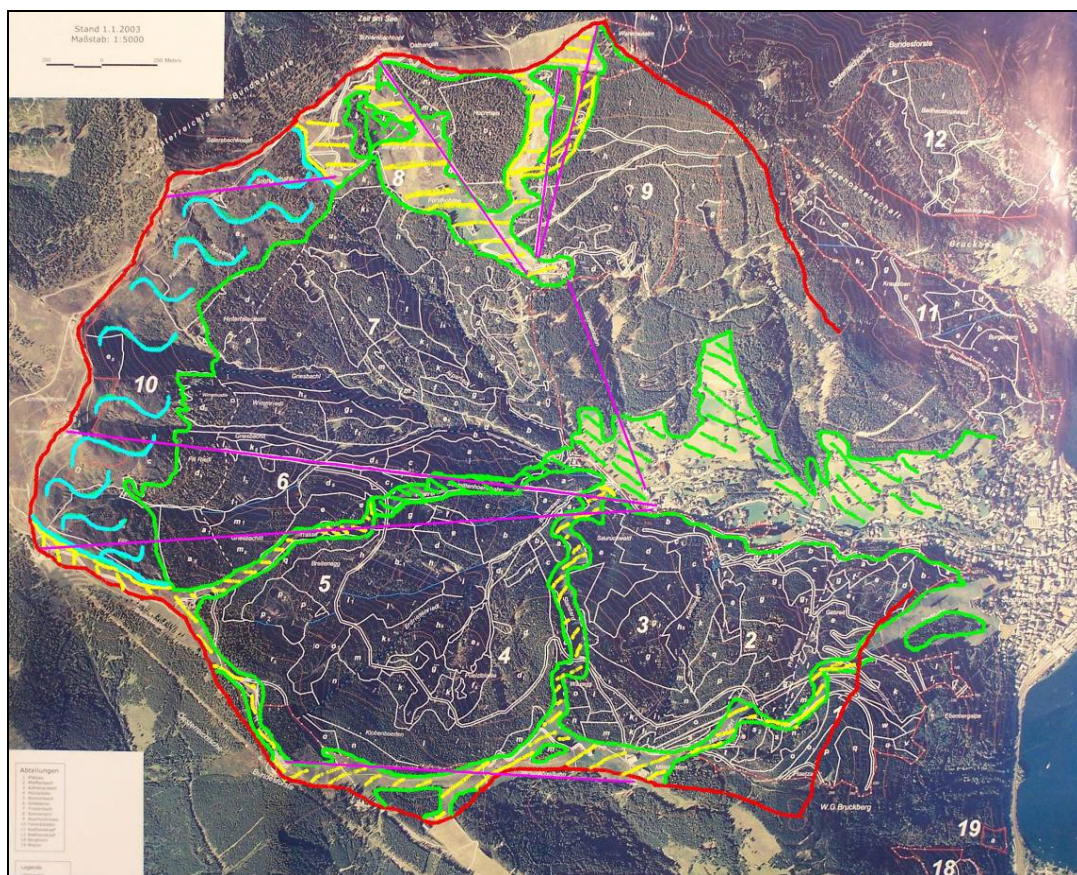


Figure 9. Orthophoto of the Schmittenbach watershed (2003) with the current vegetation distribution: green shaded: pastures, yellow shaded: planed pastures (together: ski slopes), in blue – curled: dwarf shrub/curve wood area and alpine pastures; red line: boundary of the Schmittenbach watershed, pink lines: ski lifts.

3.1.2 Stem analysis

We were interested in whether or not the site index system suggested regionally as a measure for assessing the production function is comparable with field data. For the Schmittenbach watershed the yield table 'Fichte Hochgebirge' is recommended (Marshall, 1975). In fact, tree height functions of the analysed trees in the Schmittenbach watershed fit better to the dominant tree height curves for 'Fichte Hochgebirge' than for 'Fichte Bayer'. However, in both cases the older trees intersect the dominant height growth curves. This can be explained by generally better growing conditions during the last decades due to temperature and atmospheric CO₂ content increase.

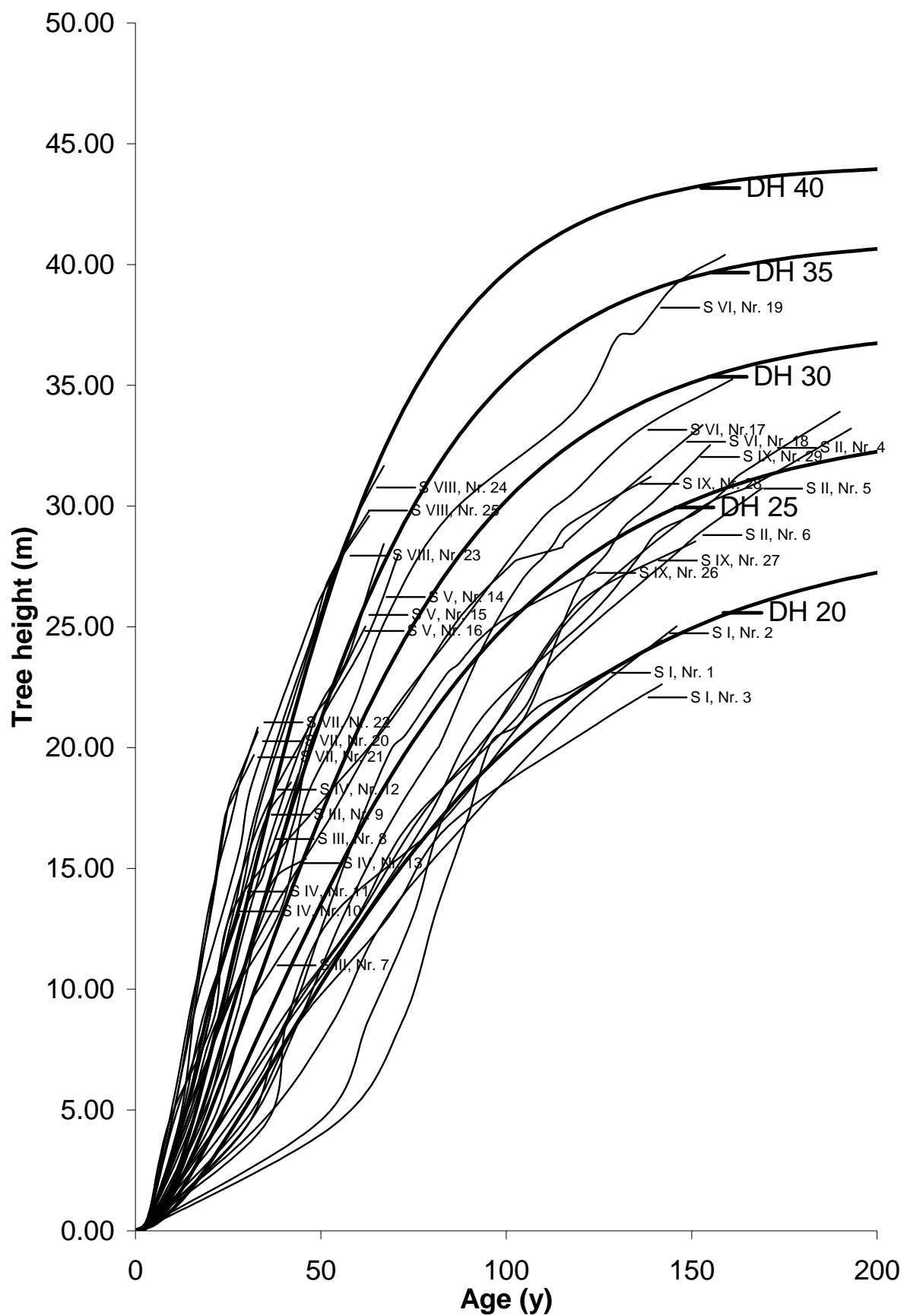


Figure 10. Stem analysis: Comparison of dominant tree height functions of Mitscherlich/Richard (1919) for the yield table 'Fichte Hochgebirge' with growth functions of trees in the Schmittbach watershed. S I – IX are the different stands, Nr. 1 – 29 are the tree numbers. DH 20 – 40 are the dominant height growth curves.

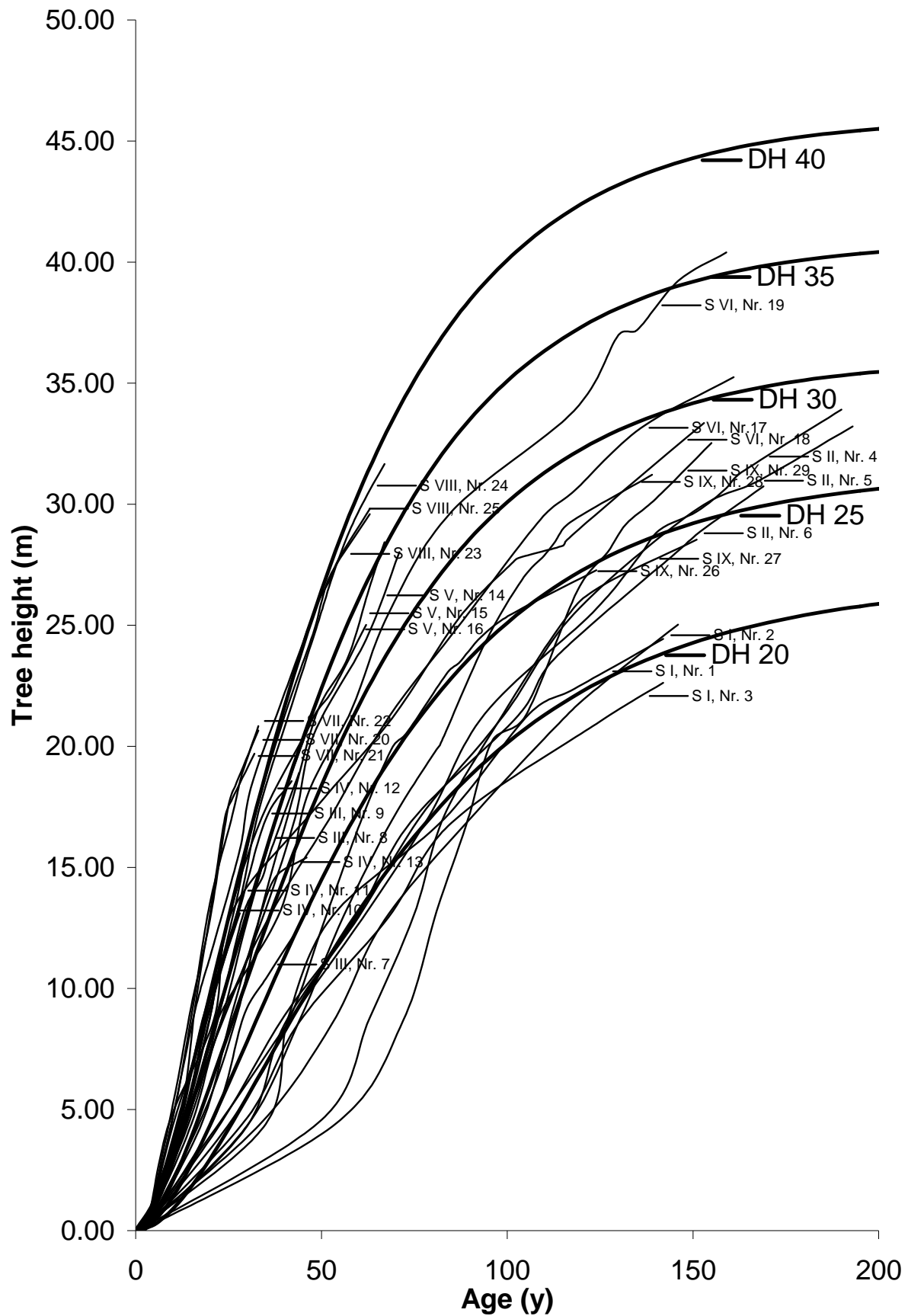


Figure 11. Stem analysis: Comparison of dominant tree height functions of Mitscherlich/Richard (1919) for the yield table 'Fichte Bayern' with growth functions of trees in the Schmittbach watershed. S I – IX are the different stands, Nr. 1 – 29 are the tree numbers. DH 20 – 40 are the dominant height growth curves.

3.1.3 Stand parameters

3.1.3.1 Stand age

Firstly, we analysed the stand age as given in the existing management plan versus our own age measurements using the results of the increment cores. The average age by location is given in the following section. Note that at each location four plots were recorded. The mean of the four plots was reduced by 3 years to get the age for the year 2003. This age was used for comparison with the age given by the management plan 2003 (Figure 12).

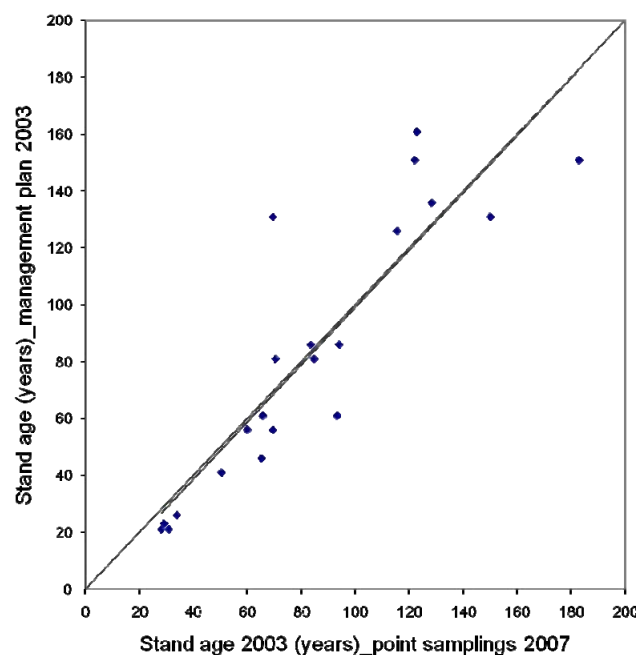


Figure 12. Comparison of the stand age between the management plan 2003 of the local forest company and the age for 2003 derived from measurements 2007 (value of the single stands as average among the plots minus 3 years).

On average, our stand age determination fits very well to the stand age given by the management plan of the local forest company. A slight deviation of the regression line from the 1:1 correlation line can be detected for only the youngest stands. For the youngest stands, the age determined in the field is slightly higher than the age given by the management plan (Figure 12).

3.1.3.2 Dominant height

The dominant tree height per plot at a given location was calculated as the average of the tree heights of the three biggest trees. The dominant tree height [h_{dom}] in combination with the mean stand age can be used as a measure for site quality or site index. Since the dominant tree height at a given stand age is a measure for productivity it gives us some insights how comparable the different numbers are for assessing forest productivity.

The dominant tree height determined in field clearly exceeds values derived from the management plan (necessary data: stand age, site index) using the dominant height growth functions of Mitscherlich/Richard (1919) (Figure 13). Since stand age of the management plan and the determined stand age in the field fit very well, the underestimation of the dominant height can be set in correlation with results for analysis on other stand parameters such as growing stock and site index (see chapter 3.1.3.3 and 3.1.3.4).

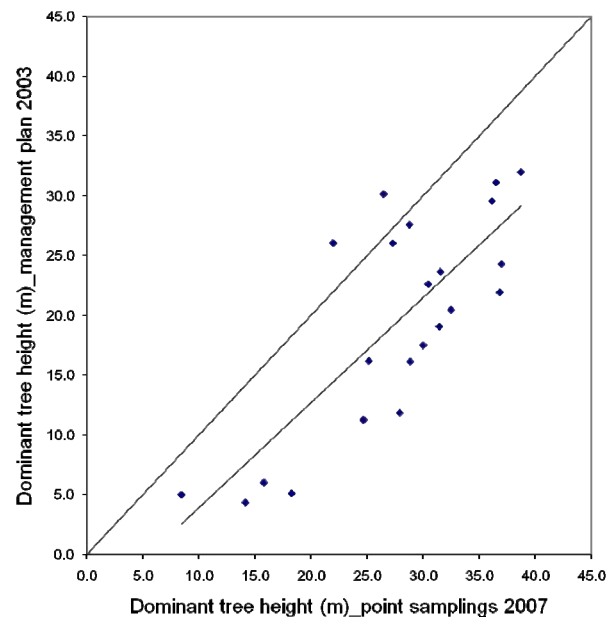


Figure 13. Comparison of the dominant tree height in the single stands between dominant tree height derived from data of the management plan 2003 of the local forest company, using the dominant height growth functions of Mitscherlich/Richard (1919), and the dominant height measurements 2007 (value of the single stands as average among the plots).

3.1.3.3 Total volume per hectare

Volume per hectare given in the management plan is clearly less than volume determined by the point sampling. Not surprisingly, the trend of underestimation of the management plan already observed for the dominant tree height is also evident for the growing stock. Volume underestimation gets higher with increasing measured volume (Figure 14).

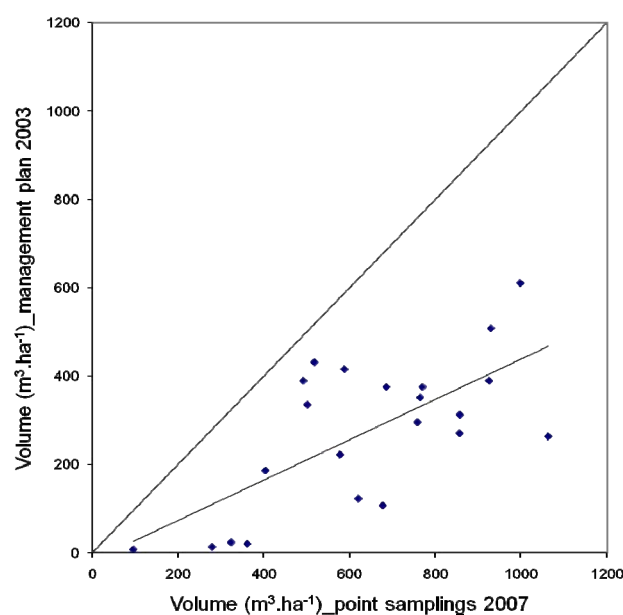


Figure 14. Comparison of the total volume per hectare of the single stands between the management plan 2003 of the local forest company and the measurements 2007 (value of the single stands as average among the plots).

3.1.3.4 Site index

The site index was interpolated from the yield table 'Fichte Hochgebirge' using the stand age and the dominant height of a plot. Problems arose for a few plots younger than 40 years situated at very good sites. The interpolation from the yield table delivered site index values of higher than 20 (i.e. 21-48!). The reason is that the applied procedure is only suitable and therefore used normally for stands older than 30-40 years, especially in mountainous area. Thus, the site index for those five plots was fixed to 20 (compare Appendix, Table 21 and Table 22).

We calculated the average site index for the four plots at a given location and compared it with the site index given in the management plan 2003 (Figure 15).

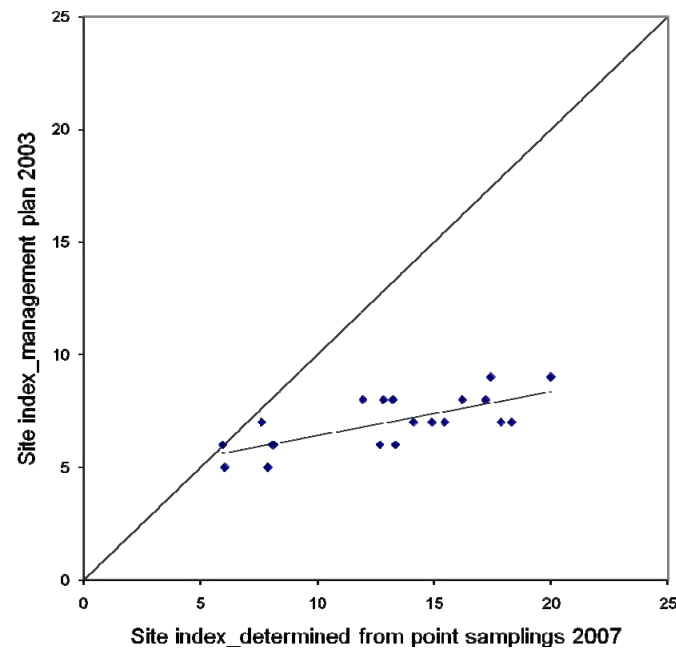


Figure 15. Comparison of the site index of the single stands between the management plan 2003 of the local forest company and our assessment for 2007 (value of the single stands as average among the plots).

The site index is clearly underestimated in the management plan. It does not exceed the value of 9, whereas mean stand site index derived from the field measurements goes up to 20. The relative difference between the site index of the management plan and the observed site strongly increases the higher the observations get. The highest productive sites are the most underestimated stands.

3.1.4 Soil parameters

Depth of the humus layer and the topsoil and the total depth are summarised and given as the stand mean and the median. Mean humus depth was 10 cm and mean topsoil depth was 27 cm (Appendix, Table 19). From these values and the results of the lab analysis of soil carbon and nitrogen content the soil carbon and nitrogen for each plot and each stand was calculated. Mean soil carbon of all plots was 408 t.ha⁻¹ and mean nitrogen of all plots was 18 t.ha⁻¹ (Appendix, Table 20).

3.2 BGC model simulation results

It should be stressed for the reader that in all following sections, the results are describing mainly one of two situations that should not be confused: 1) model outputs that include all 78 plots but only for the final year of simulation (2005), or 2) model outputs that include all 78 plots but for all years for which the weather data was available (1960-2005).

3.2.1 Volume

Volume per hectare was calculated from the model output parameters dead stem and live stem carbon (compare chapter 2.2.3.4). Mean predicted volume per hectare for all 78 sampling plots was $614 \text{ m}^3 \cdot \text{ha}^{-1}$, whereas average observed volume was $640 \text{ m}^3 \cdot \text{ha}^{-1}$ (see Appendix, Table 21 and Table 22). This means a slight underestimation of the observed growing stock by approximately 4%. The simulation period ended with the year 2005, but field observations were done in July 2007. Average volume increment in 2005 was $13 \text{ m}^3 \cdot \text{ha}^{-1}$. As such, it is justifiable to imagine the predicted growing stock to be roughly $15 \text{ m}^3 \cdot \text{ha}^{-1}$ higher one and a half years later. Thus, volume underestimation by the model would be 2% then. This guess was not included in the following modelling evaluations; nonetheless, it is worth indicating this time lag between final year of model simulations and time of data collection.

For determining the limits and range of errors in future predictions the confidence and prediction intervals according to Reynolds (1984, in Pietsch et al., 2005) can be applied. For examining divergences between the expected difference and the estimator \bar{D}_i the confidence interval CI is helpful (equation 8.):

$$CI = \bar{D}_i \pm \frac{SD}{\sqrt{n}} \cdot t_{1-\alpha/2(n-1)} \quad (8.)$$

\bar{D}_i is the mean of differences between predicted and observed volume, SD the standard deviation of the differences \bar{D}_i , n is the sample size and t is the $1-\alpha/2$ quantile of the t-distribution with n-1 degrees of freedom. The range of the differences D_i among prediction versus observations is given by the prediction interval (equation 9.):

$$PI = \bar{D}_i \pm \sqrt{1 + \frac{1}{n}} \cdot SD \cdot t_{1-\alpha/2(n-1)} \quad (9.)$$

Table 8. Results of the error analysis for the volume per hectare. Values are given in $\text{m}^3 \cdot \text{ha}^{-1}$, figures in brackets are percent of the observed volume.

\overline{obs}	\bar{D}_i	SD	t	CI	PI
640	-25	164	1.4627	-68 – 17	-403 – 352
	(-3.98%)	(25.63%)		(-10.61 – 2.66%)	(-62.95 – 54.99%)

Where \overline{obs} is the mean of observations, \bar{D}_i the mean of the differences between predicted and observed values, SD the standard deviation of the differences and t the value from paired t-statistics. CI and PI are the confidence and prediction intervals of the error ($\alpha = 0.05$) (Reynolds, 1984, in Pietsch et al., 2005).

3.2.1.1 Regression analysis between observations and model predictions

The linear regression analysis between predicted and observed volume exhibits consistent results. The regression line does not diverge much from the 1:1 observed vs. predicted volume line (Figure 16). The examined relation between observed and predicted volume was statistically tested for correlation with the coefficient of determination r^2 . Correlation on stand level is higher ($r^2 = 0.91$) (Figure 16, A) than for the single plots ($r^2 = 0.66$) (Figure 16, B).

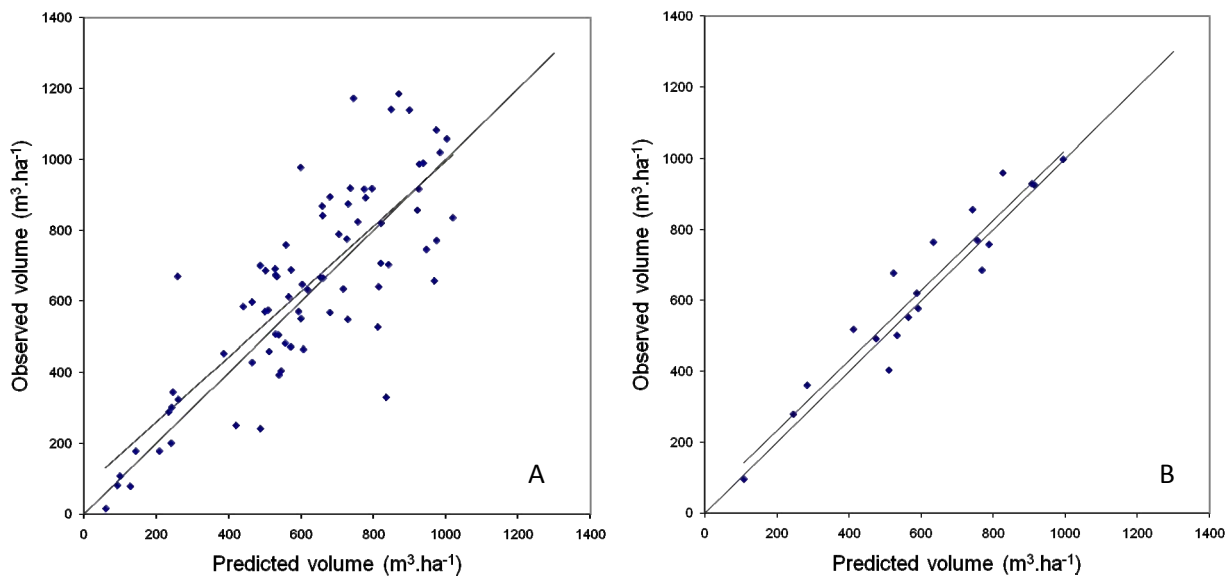


Figure 16. Observed vs. predicted volume per hectare for the single plots (A) and observed vs. predicted volume per hectare on stand level (average of the plots per stand) (B) in 2005.

To test volume results for consistency, standardised residuals are plotted against various stand and site characteristics, i.e. stand age, dominant height, basal area, Stand Density Index (SDI) according to Reinecke (1933), elevation, slope and aspect (see Figure 17 and Figure 18). Standardised volume residuals are calculated as the difference between predicted volume and observed volume, divided by the mean of the observed volume of all plots. The analysis of the residuals plotted over stand and site characteristics should not reveal a trend. Otherwise, we would have to admit that the volume results are biased for that parameter where a trend in the residual analysis has been detected.

The consistency tests for the predict volume reveal that the BGC model is able to describe the current volume state as observed in the Schmittenbach watershed well. Volume residuals vary around zero and their mean is slightly negative (see Table 9). The same is true for the mean volume residuals for the stands (mostly four plots belong to one stand, therefore we can make a volume residuals-mean for each stand).

Table 9. Minimum, maximum and mean volume residuals (– predicted minus observed volume divided by the standard deviation of the observations) for all plots (78) and the stand-mean volume residuals (20) in 2005.

		Minimum	Maximum	Mean
Volume - residuals	all plots	-1.54	1.82	-0.09
	stand means	-0.63	0.44	-0.11

For most of the stand and site parameters, no significant trend of the volume residuals exists (Table 10). Significant trends can only be detected for the stand age, the basal area (tree number per plot multiplied with the basal area factor 4), the Stand Density Index (SDI) and the site index. Considering the stand-mean volume residuals (mean of the volume residuals of the mostly four plots per stand), significant trends only exist for the stand age and the site index. The trend of the volume residuals over the stand age is positive on a 5% significance level on the plot as well as on the stand level. The trend is negative on a 1% significance level for the site index.

For all plots the trend of the volume residuals over the basal area and the SDI is negative on a 0.001 significance level for both, but for the stand-mean volume residuals the trend is not significant any more. The negative trends on plot level can be explained by thinning activities resulting in not fully stocked stands. Thinning interventions in the simulations were only conducted homogenously on stand level (same management at all plots) but in reality in the forest this homogenous management of a stand might not be the case. Therefore, we have to expect volume overestimations at single not fully stocked plots within a stand and consequently a bias on plot level.

Table 10. Statistical parameters for volume residuals analysis on different stand and site parameters (determined during the field work in the Schmittbach watershed in 2007): a...regression coefficient (= slope of the linear trend line), r...correlation coefficient, r^2 ...coefficient of determination and the significance level of the trend.

		a	r	r^2	P	Trend
Stand age	all plots	0.0038	0.2646	0.0700	0.0192	*
	stand mean	0.0033	0.4494	0.2020	0.0468	*
Dominant height	all plots	-0.0014	0.0189	0.0004	0.8694	
	stand mean	6.2891E-005	0.0017	2.8001E-006	0.9944	
Basal area	all plots	-0.0215	0.6157	0.3791	<0.001	***
	stand mean	-0.0105	0.4212	0.1774	0.0644	
SDI	all plots	-0.0004	0.3712	0.1378	0.0009	***
	stand mean	-0.0002	0.2655	0.0705	0.2579	
Site index	all plots	-0.0433	0.3299	0.1088	0.0032	**
	stand mean	-0.0416	0.6161	0.3796	0.0038	**
Elevation	all plots	0.0004	0.1554	0.0242	0.1742	
	stand mean	0.0006	0.4066	0.1654	0.0752	
Slope	all plots	0.0001	0.0017	2.8588E-006	0.9883	
	stand mean	0.0118	0.2165	0.0469	0.3594	
Aspect	all plots	0.0005	0.0581	0.0034	0.6135	
	stand mean	109155E-005	0.0035	1.2479E-005	0.9882	

*significant trend ($0.05 > P \geq 0.01$), **very significant trend ($0.01 > P \geq 0.001$), ***highly significant trend ($0.001 > P$)

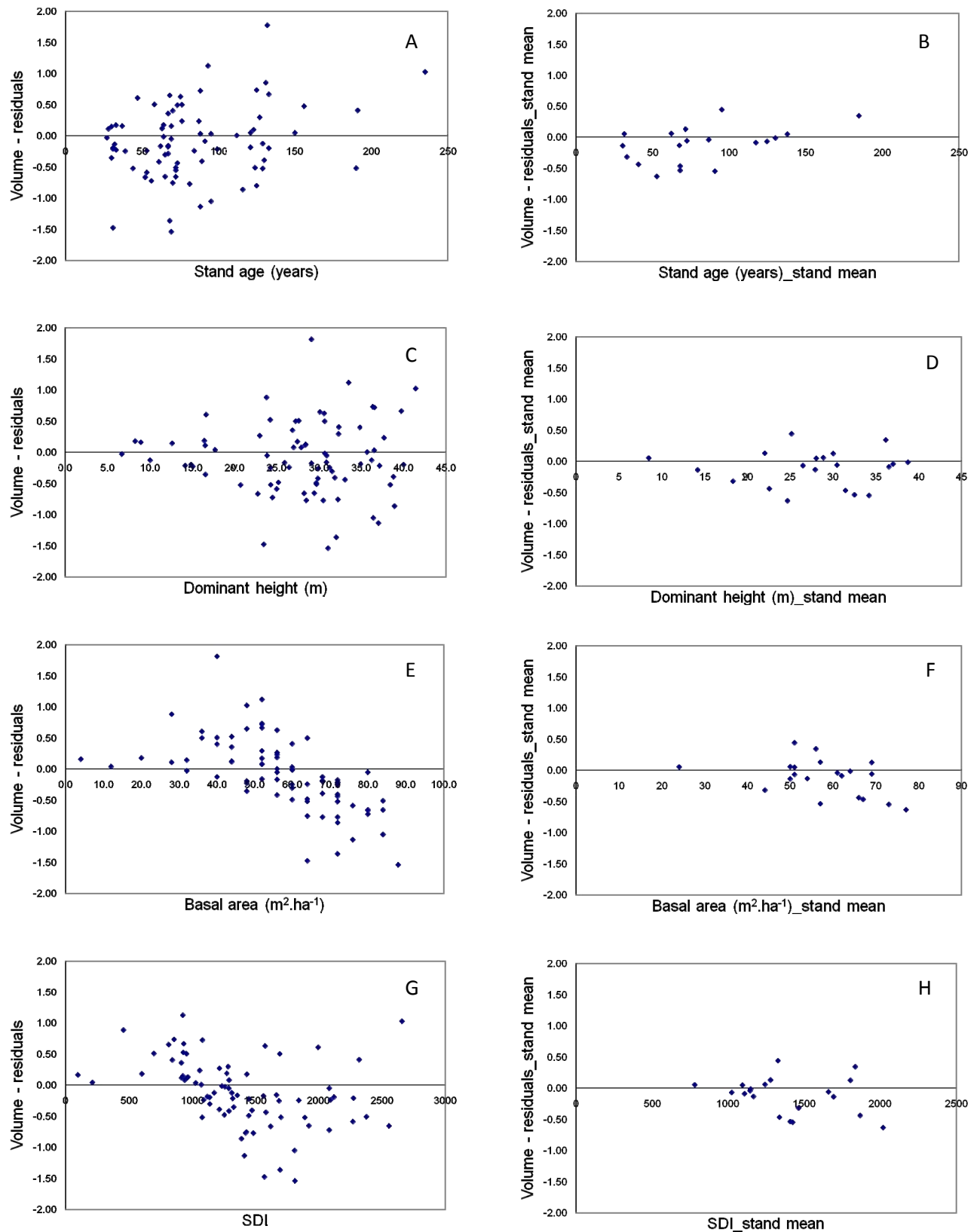


Figure 17. Part 1. Trend analysis of standardised volume residuals (i.e. predicted minus observed volume divided by the standard deviation of the observations) for all plots and for the stand means vs. stand age (A, B), dominant height (measured in the field; C, D), basal area (tree number per plot multiplied with the basal area factor 4; E, F) and Stand density index (G, H) in 2005.

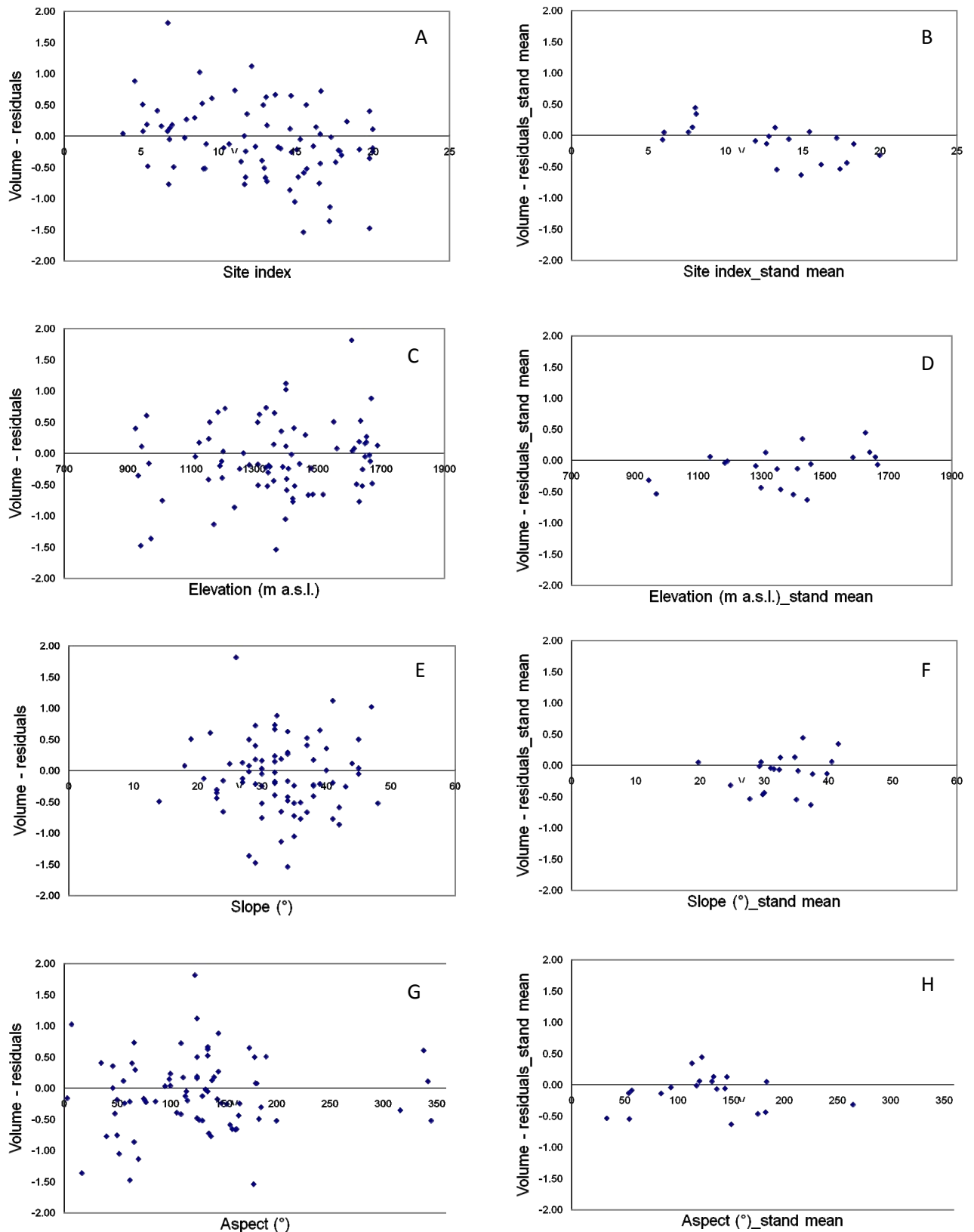


Figure 18. Part 2. Trend analysis of standardised volume residuals (i.e. predicted minus observed volume divided by the standard deviation of the observations) for all plots and for the stand means vs. site index (A, B), elevation (measured in the field; C, D), slope (E, F) and aspect (G, H) in 2005.

3.2.2 Productivity

The productivity of a stand can be expressed as the Net Primary Production (NPP). It gives the mass of carbon that is fixed and kept by square meter ground per year ($\text{kg C.m}^{-2}.\text{yr}^{-1}$). Net Primary Production shall be analysed in relation to stand and site parameters. Since Leaf Area Index controls photosynthesis and thus Gross Primary Production, a strong dependence of NPP on LAI can be anticipated. For the data of the final simulation year 2005, the strong positive linear relation between NPP and LAI holds from an LAI of around 7 up to the maximum value of 9 (Figure 21, A). In this interval, the NPP rises from 0.65 to 0.9 $\text{kg C.m}^{-2}.\text{yr}^{-1}$. Below the LAI of 7, a decreasing LAI down to the minimum value of 4.1 doesn't result in a similarly strong decreasing NPP. This indicates that different LAI is not solely responsible for changes in NPP. The stand age is another factor that has an impact on the NPP. NPP gets lower for older stands (Figure 21, B). The three oldest stands belong to those four stands with the lowest NPP.

We can have an expanded view on the issue when the NPP is plotted over the LAI with the full NPP and LAI data of all 78 plots in the 46 years of the detailed weather record from 1960 - 2005 in a single graph (Figure 19).

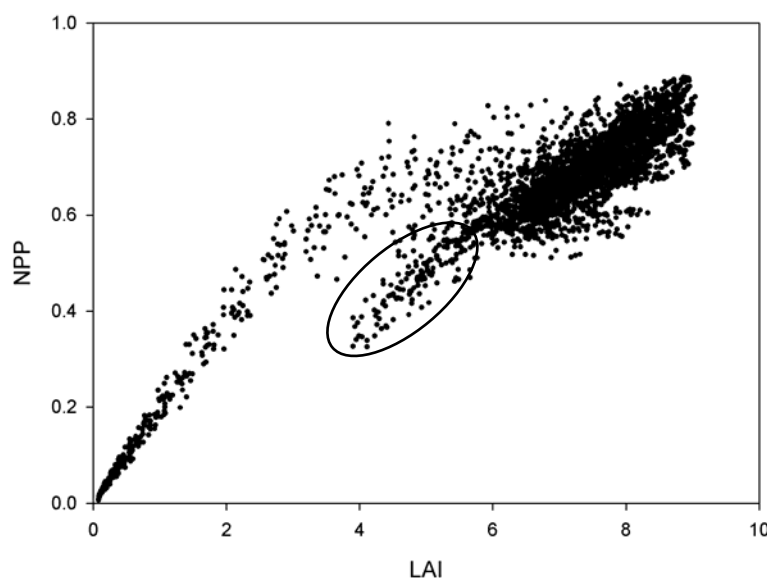


Figure 19. Net Primary Production ($\text{kg C.m}^{-2}.\text{yr}^{-1}$) vs. Leaf Area Index for all 78 plots showing all data of the years 1960-2005. Young developing stands (up to around 30 years) on the left side can be distinguished from the premature and mature stands on the right (densely spotted area) and from old growth stands (circled area; mainly stands older than 140 years, but also thinned stands older than 80 years).

A very wide range of values for these parameters in the years 1960 to 2005 is covered (compare Table 11). Age classes from 1 to 7+ (max. stand age is 230 years) are represented and those are spread over the elevation and the aspect. In addition, stand regeneration exists across the area - in low and high, as well as on North to Southeast slopes. Taking these points into consideration, there should not be a systematic mistake upon incorporation of the data for all 78 plots across these 46 years.

Table 11. Minimum, maximum, mean and median of the Net Primary Production and the Leaf Area Index for all 78 plots in the years 1960-2005.

	Minimum	Maximum	Mean	Median
Net Primary Production (kg C.m⁻².yr⁻¹)	0.01	0.89	0.64	0.68
Leaf Area Index	0.08	9.04	6.72	7.25

Figure 19 (NPP versus LAI) shows that the stands can be analysed in three groups. Firstly, we see the juvenile stands starting with a very low LAI (0.08) and a NPP almost zero (low as 0.006 kg C.m⁻².yr⁻¹) in the first year after planting. These values increase more and more quickly with age and LAI and NPP seem linearly dependent. Only with the age of 10 do single plots reach a LAI of 1, but 20 years old stands already have a LAI between 4 and 7 with a NPP of largely above 0.6 kg C.m⁻².yr⁻¹. These stands come already close to the second group of plots - the densely spotted dark area in Figure 19 - where the majority of the plots in the young (older than 20 years) to mature development phase can be found. LAI mainly lies between 6 and 9 and NPP between 0.5 and 0.9 kg C.m⁻².yr⁻¹. A positive linear trend for NPP over LAI is again visible, like for the juvenile stands, but the slope of a trend line would be less steep here. This trend has already been detected for the data of the year 2005 (again see Figure 21, A). Actually, the same linear trend is still observable when we go to the third group of stands that have been circled in Figure 19. This group consists of old growth stands, which are mainly older than 140 years and partly thinned and slightly younger stands (down to 80 years of age) only if they are thinned. Their LAI lies roughly below 6 and the NPP < 0.6 kg C.m⁻².yr⁻¹. This means that LAI can be as low as the LAI for 15 - 25 year old stands but NPP is comparably and clearly lower. Roughly, for the young stands NPP lies between 0.6 and 0.8 kg C.m⁻².yr⁻¹ but for the old stands NPP varies between approximately 0.3 and 0.6 kg C.m⁻².yr⁻¹ in the same LAI range.

For an easier understanding it is helpful to investigate the relation of NPP and LAI for two single plots: one young and one old stand during the same 46 years time period (Figure 20).

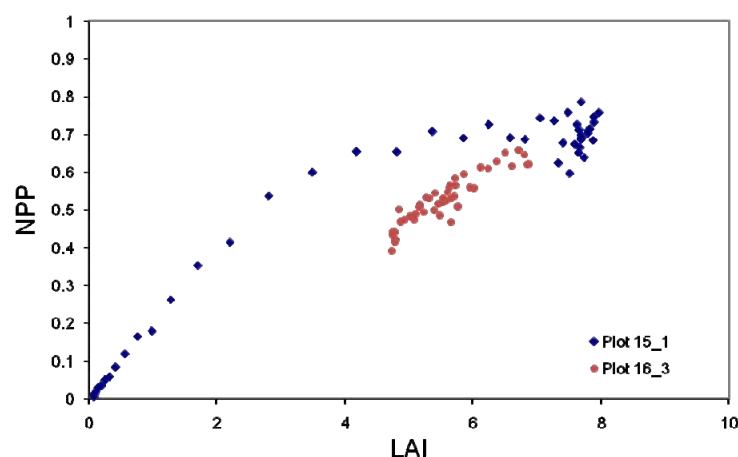


Figure 20. Net Primary Production (kg C.m⁻².yr⁻¹) vs. Leaf Area Index for two different plots showing all data of the years 1960-2005. Plot 15_1 was clear-cut with 100 years in 1974 with subsequent planting. Plot 16_3 is an old growth stand with 145 years of age in 1960 (thinning of 30% simulated twice during the observation time).

At plot 15_1, a 100 years old stand with a LAI of 7.3 was clear cut in 1974 and a new stand planted. For the development of the LAI over time please see Figure 34, A. The second stand at plot 16_3 was 145 years old and had a LAI of 5.5 in 1960. Thinning of 30% of volume had been simulated in 1965 and 1985. Consequently, the LAI each time dropped but did not go below 4.5 and increased afterwards again (also see Figure 34, B).

For the old stand at plot 15_1 the LAI ranges between 7 and 8 and NPP fluctuates around $0.7 \text{ kg C.m}^{-2}.\text{yr}^{-1}$ between 1960 and the year of its harvest, 1974. At 100 years old the stand had a LAI of 7.3 and a NPP of $0.62 \text{ kg C.m}^{-2}.\text{yr}^{-1}$. For the subsequent regeneration the NPP and LAI only slowly increase in a linear relation during the first ten years. Thereafter, the rate of increase accelerates – more for LAI than for NPP – for approximately ten more years, until LAI stays within a narrow range between 7 and 8 and NPP fluctuates around $0.7 \text{ kg C.m}^{-2}.\text{yr}^{-1}$ again.

The old stand at plot 16_3 lies within a separate area on the graph. Due to some thinning activities LAI varies relatively strongly in comparison to a non-thinned stand of the same age (see Figure 34, B). A relatively strong positive linear relation can be observed between LAI and NPP. NPP values are always lower than for plot 15_1 at the same LAI. The lower the LAI of the old stand, the higher this NPP difference between the old and the young stand.

The analysis of NPP versus other stand and site parameters other than LAI and stand age for the final simulation year 2005 are continued below:

Although no trend for the NPP can be detected over a wide range of predicted volume (Figure 21, C), increasing volume goes hand in hand with rising NPP from the lowest volumes up to approximately $300 \text{ m}^3.\text{ha}^{-1}$. Based on this, one can estimate that stands with lowest stock are beyond their maximum productivity. Low growing stock is normally true for young stands as well as for understocked mature stands where already intensive harvesting activities have taken place.

NPP versus site index shows a positive trend. This is an expected result given that site index is a measure describing productivity and similarly, NPP is also a value of productivity and as such, a correlation is crucial. The coefficient of determination in this case is 0.2.

The graphical analysis of NPP versus the aspect gives an interesting picture (Figure 21, E). NPP rises from Northeast to South exposition in a curved manner and seems to decrease in a similar pattern towards North-West exposition again, but measurements on West-slopes are missing. This effect can be explained by changing radiation intensity with the aspect. Clearly, the largest quantity of sunrays for photosynthesis is available on South-slopes and the least on North-slopes. Correlation of NPP with the elevation is considerably lower; however, a slight curved distribution pattern can be recognised (Figure 21, F). Lower incoming solar radiation towards the bottom of the valley and shorter vegetation period in higher elevations, resulting in a lower NPP, can serve as explanations.

No clear tendency of NPP versus Stand Density Index (SDI) according to Reinecke (1933) can be detected (Figure 21, F). Only a very low SDI corresponds to low NPP. This can be seen as a correlation to low NPP at low standing volume, as was described earlier for NPP versus predicted volume. Again, with a very low SDI, a low volume is expected. In any case, volume residuals of all plots have a very highly significant negative trend over the SDI. However, this is not true for the stand means (compare chapter 3.2.1.1., Figure 17) and therefore, NPP over SDI should be analysed on stand level (mean of the plots per stand). In this case, a positive relation between the two parameters is revealed.

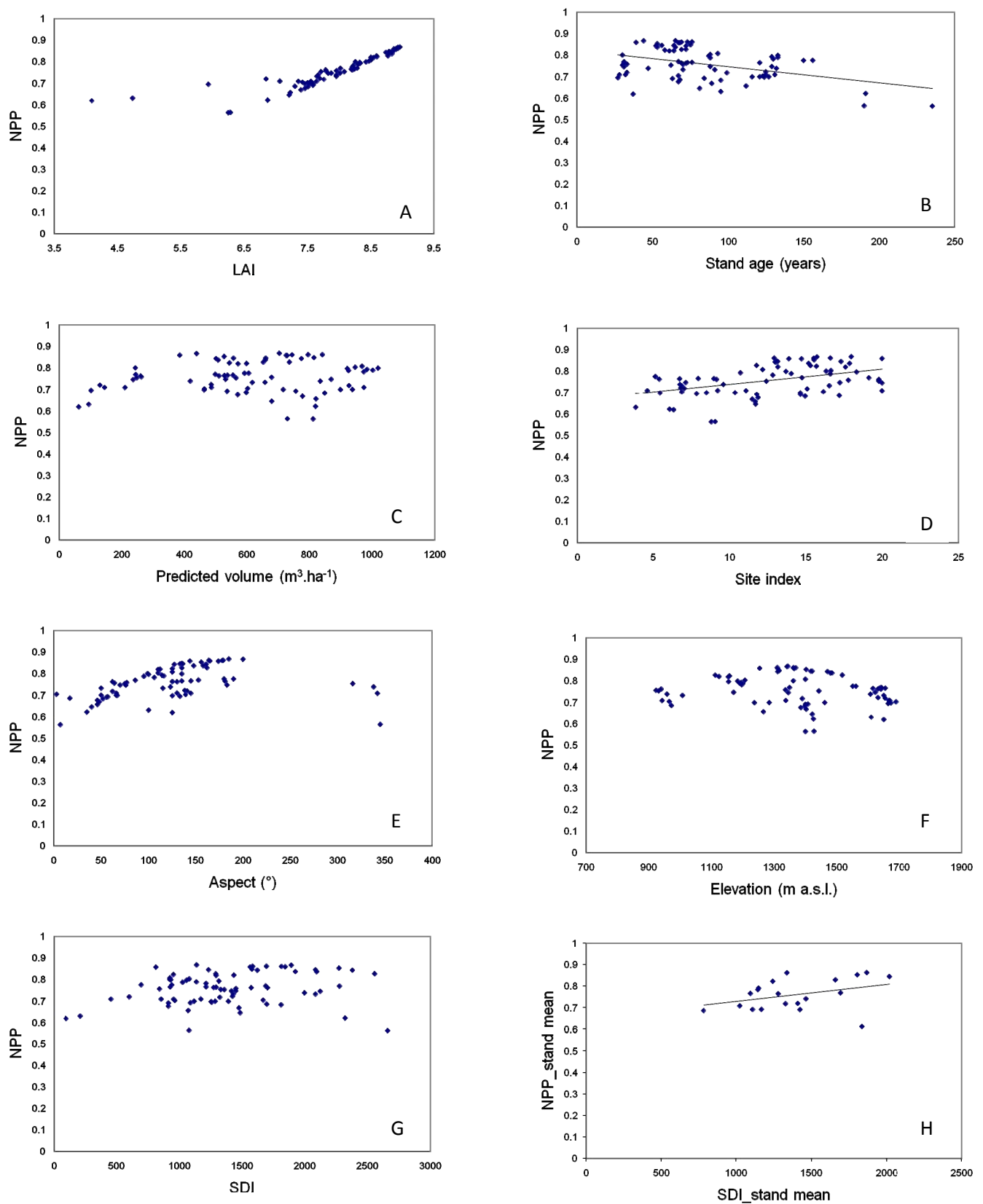


Figure 21. Net Primary Production (NPP) ($\text{kg C.m}^{-2}.\text{yr}^{-1}$) vs. site and stand parameters, i.e. Leaf Area Index (A), stand age (B), predicted volume (C), site index (D), aspect (E), elevation (F) and Stand Density Index (G) for all plots and the stand means (only for SDI) (H) in 2005.

3.2.3 Water use efficiency

Water use efficiency (WUE) is a plant characteristic that describes how much water is transpired to achieve a certain amount of Net Primary Production (NPP). The WUE is given in $\text{g C m}^{-2} \cdot \text{yr}^{-1} \cdot \text{mm}^{-1}$. A lower NPP/water transpiration ratio can be seen as negative for the plant because it needs more water for performing the same amount of NPP. This has the negative implication that the danger of water stress is higher and so water can become a limiting factor earlier.

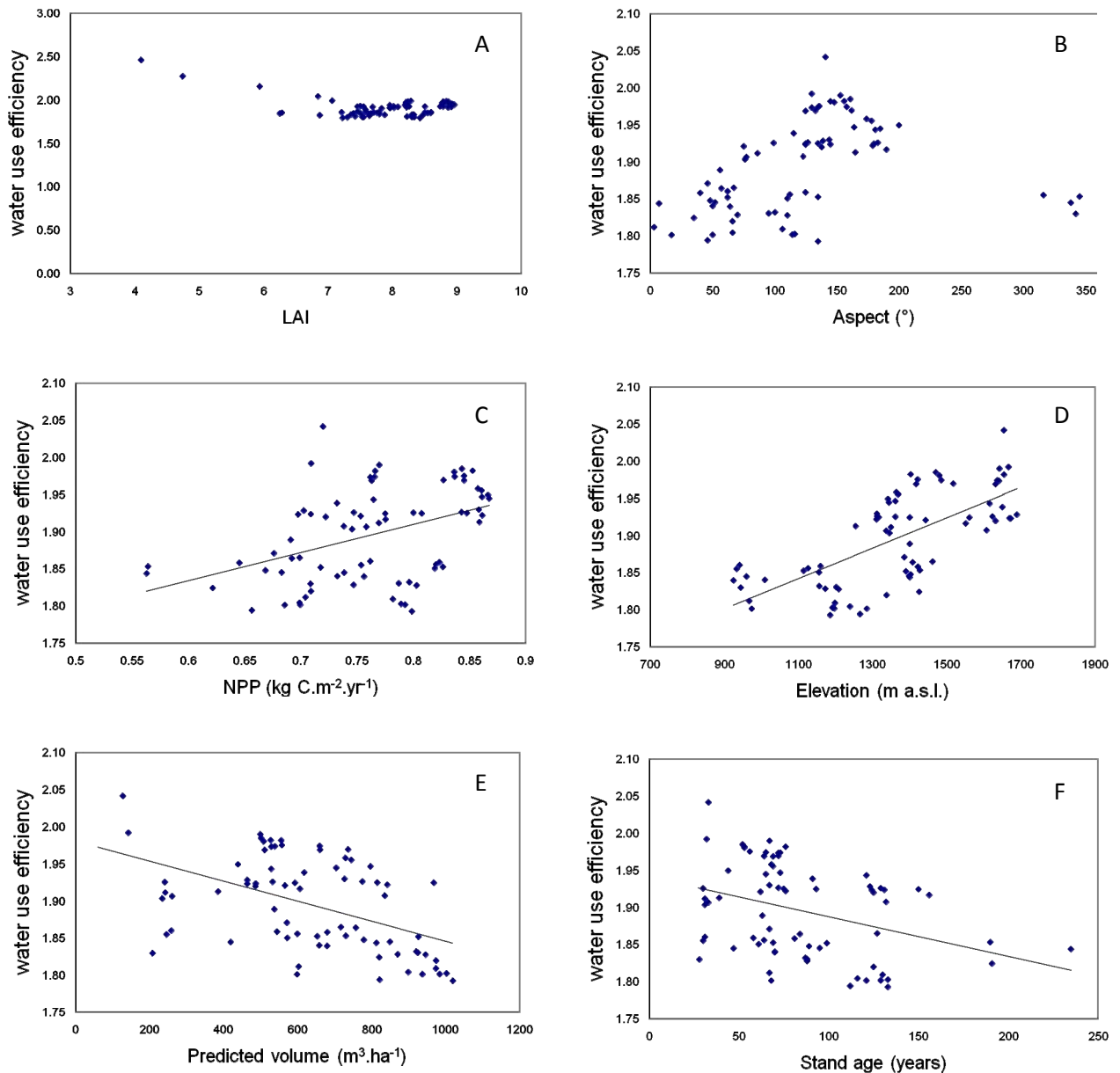


Figure 22. Water use efficiency ($\text{g C m}^{-2} \cdot \text{yr}^{-1} \cdot \text{mm}^{-1}$) vs. Leaf Area Index (A), aspect (B), Net Primary Production (C), elevation (D), predicted volume (E) and stand age (F) for all plots in 2005.

The observed WUE values lie in the range of 1.8 - 2.0 $\text{g C m}^{-2} \cdot \text{yr}^{-1} \cdot \text{mm}^{-1}$ in 95 percent of all cases/plots in 2005. However, there are a few extreme values going up to a WUE of 2.5 $\text{g C m}^{-2} \cdot \text{yr}^{-1} \cdot \text{mm}^{-1}$. These higher WUE values clearly correlate with a Leaf Area Index < 6. For a LAI < 6 WUE is higher the lower the LAI is, whereas at a LAI > 6 WUE is independent of LAI.

No other stand or site parameter served as an explanation for the highest WUE values (bigger than $2 \text{ g C m}^{-2} \cdot \text{yr}^{-1} \cdot \text{mm}^{-1}$). To make interpretation of water use efficiency with respect to other site and stand parameters simpler, those few stands with a $\text{LAI} < 6$ were not considered in the other graphs or corresponding interpretations since low LAI is the obvious explanation for the high WUE.

Firstly, we found a distinct positive correlation between elevation and WUE (Figure 22, D). This can be seen as an ecological adaptation to less favourable growing conditions in higher elevations, e.g. due to shorter vegetation period and lower mean temperature. Transpiration shows a clear decreasing tendency for elevations $> 1300 \text{ m a.s.l.}$ (see chapter 3.2.4.2, Figure 28, E), whereas NPP shows only a moderate decrease with height above sea level (mentioned in chapter 3.2.2, Figure 21, F). Thus, increasing WUE over the elevation is the result of relatively strong reduction of transpiration and a less pronounced decrease of NPP with increasing elevation.

Considering aspect, WUE turns out to be lower on North-West- to North-East-facing slopes and the highest values are confined to South-exposition (Figure 22, B). Both transpiration and NPP show a curved distribution pattern over the aspect (see chapter 3.2.4.2, Figure 28, G; for NPP compare chapter 3.2.2). However, NPP is obviously relatively higher in Southern-exposition. In other words, the relative difference between South and North slope is relatively higher for NPP than for the transpiration. Higher WUE on Southern exposition is an ecologically necessary feature to cope with more probable water stress due to stronger irradiation, and therefore, higher vapour pressure deficit and consequently higher water loss through open stomata.

As one would expect, there is a tendency for higher WUE at higher NPP values (Figure 22, C). This indicates that well developed water use efficiency is a positive physiological plant characteristic that is supportive for photosynthetic production.

WUE gets lower with increasing stand age (Figure 22, E) and with increasing growing stock (Figure 22, F).

A more comprehensive analysis is possible when considering data from the whole time span of the detailed weather record, i.e. the 46 years from 1960 to 2005 (Table 12, Figure 23-25).

Table 12. Minimum, maximum, mean and median of the water use efficiency for all 78 plots in the years 1960-2005.

	Minimum	Maximum	Mean	Median
Water use efficiency ($\text{g C m}^{-2} \cdot \text{yr}^{-1} \cdot \text{mm}^{-1}$)	0.80	2.92	1.85	1.82

In a first step, the left side of the graph with WUE versus LAI shall be considered (Figure 23, A). The distribution of the water use efficiency over the LAI from 0 to 4 and partly to 6 (only the upper group of dots) can be seen as the development of the WUE of growing juvenile stands. The WUE rises rapidly for newly established stands. Already with a LAI of 0.1 a WUE of over $2 \text{ g C m}^{-2} \cdot \text{yr}^{-1} \cdot \text{mm}^{-1}$ is reached. Depending on site quality and the climate, the stands will be in 2nd age class when they reach a LAI of 4-5. Only then does WUE largely drop below $2 \text{ g C m}^{-2} \cdot \text{yr}^{-1} \cdot \text{mm}^{-1}$. For LAI higher than approximately 6, no trend of the WUE is visible (compare also Figure 22, A). However, from a LAI of roughly 7 upwards, the WUE variation gets lower and values below $1.5 \text{ g C m}^{-2} \cdot \text{yr}^{-1} \cdot \text{mm}^{-1}$ do not appear any more. Between a LAI of 4 to around 5.5, a group of plots with a low WUE of around $1.6 \text{ g C m}^{-2} \cdot \text{yr}^{-1} \cdot \text{mm}^{-1}$ is visible.

$\text{C m}^{-2}.\text{yr}^{-1}.\text{mm}^{-1}$ is detectable (circled area, Figure 23, A). These dots are associated with one stand (four plots) with an age of 140 - 240 years. In addition, a few younger stands (> 80 years) can fall into this group if thinning practices have been done. They have a significantly lower WUE in contrast to young growing stands with similar LAI.

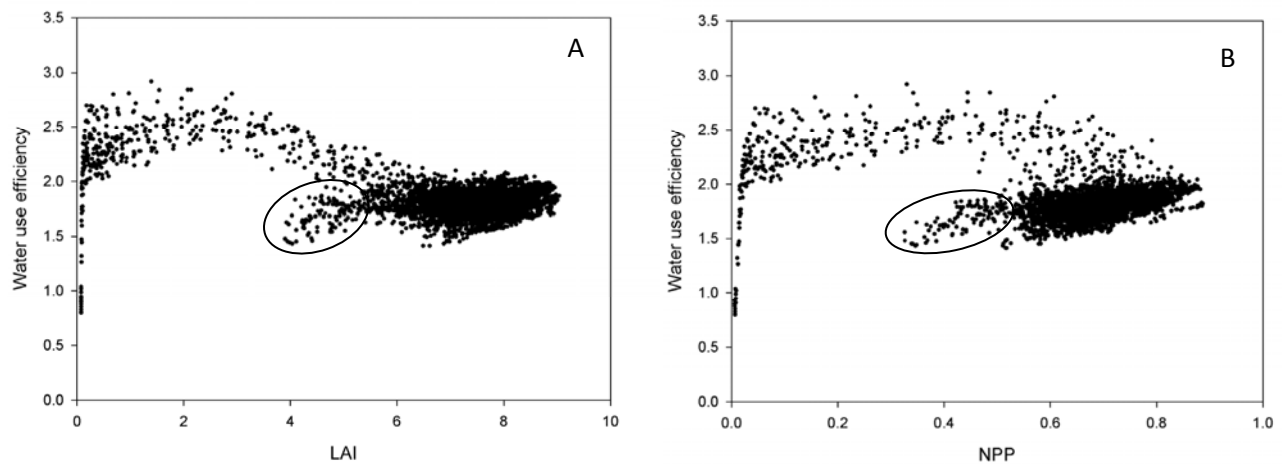


Figure 23. Water use efficiency ($\text{g C m}^{-2}.\text{yr}^{-1}.\text{mm}^{-1}$), the ratio of annual NPP and transpiration, vs. Leaf Area Index (A) and vs. Net Primary Production ($\text{kg C.m}^{-2}.\text{yr}^{-1}$) (B), for all 78 plots in the years 1960-2005. Young developing stands (up to 2nd age class) with a WUE mainly $> 2 \text{ g C m}^{-2}.\text{yr}^{-1}.\text{mm}^{-1}$ (on the left side of the graphs) can be distinguished from the premature and mature stands (on the right side of the graphs, densely spotted area) and from old growth stands (mainly older than 140 years, but also thinned stands older than 80 years) with a WUE clearly $< 2 \text{ g C m}^{-2}.\text{yr}^{-1}.\text{mm}^{-1}$ (circled areas).

To illustrate the differentiation between young and old stands more clearly, the two exemplary stands 15_1 and 16_3 are presented (Figure 24). At plot 15_1 a one hundred years old stand was clear cut in 1974 and a new stand planted. The second stand at plot 16_3 was 145 years old in 1960 and thinned twice (compare chapter 3.2.2, Figure 20 and chapter 3.2.4.3, Figure 34).

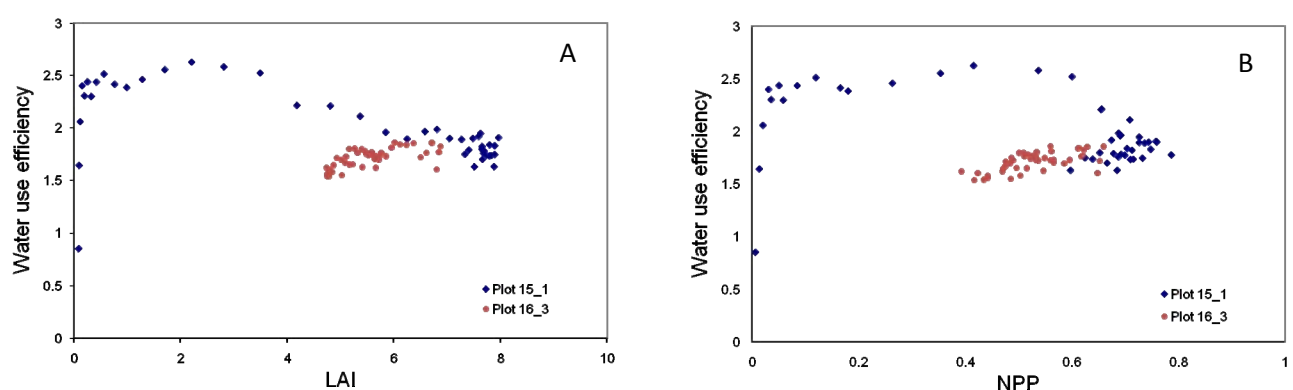


Figure 24. Water use efficiency ($\text{g C m}^{-2}.\text{yr}^{-1}.\text{mm}^{-1}$), the ratio of annual NPP and transpiration, vs. Leaf Area Index (A) and vs. Net Primary Production ($\text{kg C.m}^{-2}.\text{yr}^{-1}$) (B), for two different plots showing all data of the years 1960-2005. Plot 15_1 was clear-cut with 100 years in 1974 with subsequent planting. Plot 16_3 is an old growth stand with 145 years of age in 1960 (thinning of 30% was simulated twice during the observation time).

The relation between water use efficiency and LAI is very different for the two exemplary plots (Figure 24). At plot 15_1 the LAI stayed < 1 for the first ten years after regeneration; Nevertheless, WUE exceeded the $2 \text{ g C m}^{-2} \cdot \text{yr}^{-1} \cdot \text{mm}^{-1}$ already by the 3rd year. LAI increased very quickly between ten and twenty years. The maximum WUE of more than $2.5 \text{ g C m}^{-2} \cdot \text{yr}^{-1} \cdot \text{mm}^{-1}$ was reached at an age of 14 with an LAI of 2.2. 25 years after the establishment of the new stand, LAI again reached the LAI of 7.5, which is approximately the same value as that of the previous stand by the time it was cut. At plot 16_3 WUE varied between 1.5 and $1.9 \text{ g C m}^{-2} \cdot \text{yr}^{-1} \cdot \text{mm}^{-1}$ in the whole period.

Many aspects just described for the relation between WUE and LAI and the development over time are true for WUE and NPP (see Figure 23, B and Figure 24, B). However in juvenile stands NPP increases more quickly and WUE drops quickly to $< 2 \text{ g C m}^{-2} \cdot \text{yr}^{-1} \cdot \text{mm}^{-1}$ when the stands have reached the NPP-range of the pre-mature and mature stands (roughly between NPP of 0.55 and 0.9). This means that young stands lose their high WUE when NPP shows no further significant increases.

After dealing with LAI and NPP, which are more advanced forest ecosystem variables, the question of the simple relation between standing volume and WUE might arise (see Figure 25).

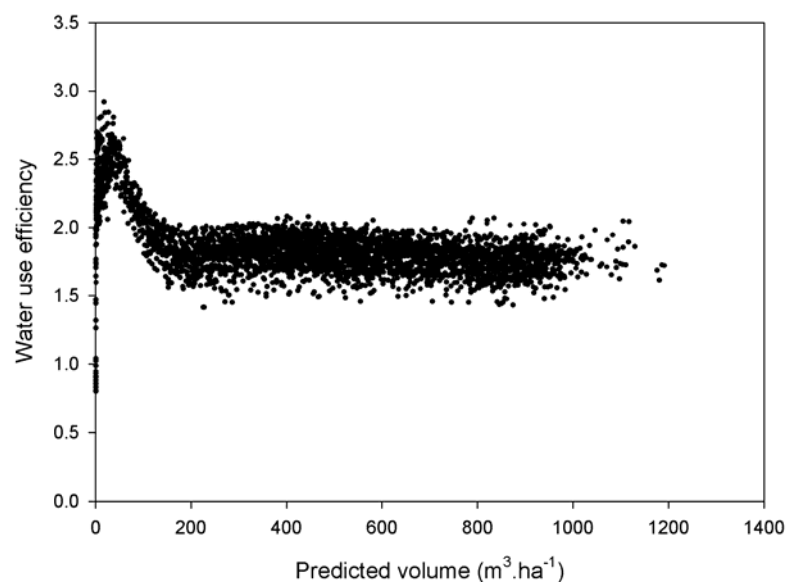


Figure 25. Water use efficiency ($\text{g C} \cdot \text{m}^{-2} \cdot \text{yr}^{-1} \cdot \text{mm}^{-1}$), the ratio of annual NPP and transpiration, vs. predicted volume for all plots in the years 1960-2005.

For WUE vs. predicted volume it can be summarized that under normal growing and management conditions for stands with a standing volume $> 200 \text{ m}^3 \cdot \text{ha}^{-1}$ WUE shows no trend with the volume and varies approximately between 1.5 and $2 \text{ g C m}^{-2} \cdot \text{yr}^{-1} \cdot \text{mm}^{-1}$ (see Figure 25). Juvenile stands show the maximum WUE (as large as $2.9 \text{ g C m}^{-2} \cdot \text{yr}^{-1} \cdot \text{mm}^{-1}$) for a volume $< 100 \text{ m}^3 \cdot \text{ha}^{-1}$.

3.2.4 Water regime

To understand outflow formation in more detail – the final goal of this work – it is helpful to start with a discussion on the water cycle as implemented in the BGC model. Evapotranspiration, in the BGC model calculated as the sum of evaporation, transpiration and snow-sublimation, is the main factor that determines how much water is potentially left for outflow from the full amount of available water. The free, available water comes primarily from precipitation, but also from snowmelt in spring or soil water that is already present at the stand. In this model, precipitation is either intercepted by the canopy or travels into the soil. Rainfall interception by the canopy is a function of the LAI. When temperatures are below zero precipitation comes down as snow stored in a snowpack over winter. Water can sublimate from the snow but mainly evaporates from the soil and from the canopy. Water that does not evaporate from the canopy until the evening is added to the soil water pool as well. Outflow is calculated as the difference between water that gets into the soil and the amount of water that can be kept when the soil is fully saturated. In addition, there is slow leakage that consists of the difference between the amount of soil water at full saturation and the water that can be held at field capacity. The water regime, therefore, is a very dynamic system influenced by several stand and site characteristics.

For the major parts of the water regime the main statistical parameters (minimum, maximum, mean, median) are summarised (Table 13). The values are derived from data of all plots for the years 1960 to 2005, the time for which the full weather data from the DAYMET climate model was available.

Table 13. Important water regime parameters for all plots in the years 1960 – 2005 (the time of full weather data from the DAYMET climate model).

	Minimum	Maximum	Mean	Median
Annual precipitation (mm.yr⁻¹)	705	1763	1286	1312
Annual transpiration (mm.yr⁻¹)	7	491	353	378
Annual snow sublimation (mm.yr⁻¹)	1	243	12	4
Annual evapotranspiration (mm.yr⁻¹)	196	1431	911	949
Annual outflow (mm.yr⁻¹)	0	1268	374	328

3.2.4.1 Precipitation

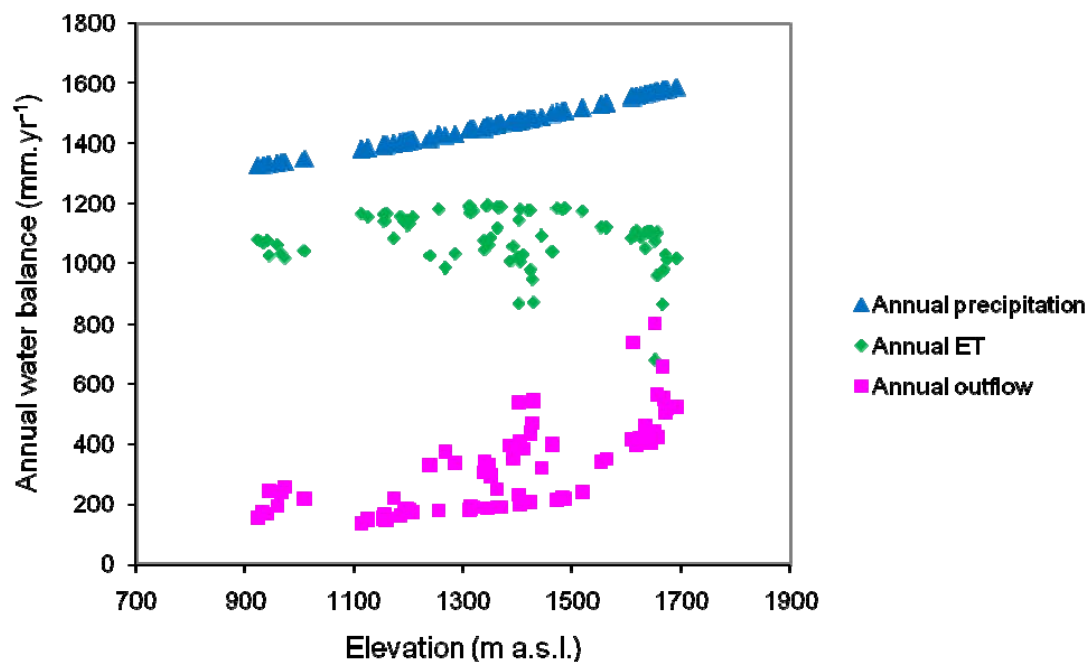


Figure 26. Annual water balance: Precipitation, evapotranspiration and outflow vs. elevation shown for all 78 plots in the year 2005.

In forest ecosystems, precipitation is one of the key drivers for autotrophic biomass production. Therefore, it is also interesting to look at the distribution over the topography, for example, annual precipitation shows an almost linear increase with the elevation on a mountain slope (Figure 26). Since precipitation increases with elevation, it does not seem surprising that outflow increases with elevation as well, especially because evapotranspiration decreases with the elevation (also Figure 26). This evaluation should only give a first picture of the annual water balance in the watershed. The looseness with which annual outflow and evapotranspiration follow their distribution curves over the elevation in contrast to the precipitation indicates that evaluations must include many factors in addition to elevation.

Annual precipitation for all 78 plots used for the simulations varies between 1328 mm.yr^{-1} (at 924 m a.s.l.) and 1587 mm.yr^{-1} (at 1690 m a.s.l.) in 2005 (Figure 27). For the years 1960-2005 mean annual precipitation over all plots was 1286 mm.yr^{-1} (Table 13). Nevertheless, annual precipitation fluctuates significantly over the years (compare Table 13). The year 1970 was the year with the highest annual precipitation and the subsequent year brought the least rain in the region (compare Figure 27). Annual precipitation curves for the different plots are seemingly parallel. However, the difference in annual precipitation between the plot at 1690 m a.s.l. and the plot at 924 m a.s.l. was the lowest with 89 mm.yr^{-1} in the year 1974 and in 1981 the difference was the highest with 367 mm.yr^{-1} . The mean precipitation difference for the two plots (situated at highest and lowest elevation of all plots) is 198 mm.yr^{-1} .

Variations in annual precipitation lead to variations in annual outflow (see Figure 27). It can be estimated that the outflow-curve more or less follows the precipitation curve. However, this precipitation-outflow relation does not solely determine the amount of annual outflow. Especially in a forested area, several more dependencies are expected. In the field, factors such as slope, soil

depth, stand age, stand density and basal area might be considered for the evaluation of outflow formation. In BGC modelling, parameters such as Leaf Area Index and stand productivity (i.e. NPP) or volume are of interest with regard to outflow assessment. Hence, it should not be surprising that outflow values between the two exemplary plots in Figure 27 varies more than it does for precipitation values between the plots. Mean difference between the two plots in annual outflow (384 mm.yr^{-1}) is much higher than in annual precipitation (198 mm.yr^{-1}). Again, this gives reason to presume that the plots differ in more site and stand parameters than only elevation.

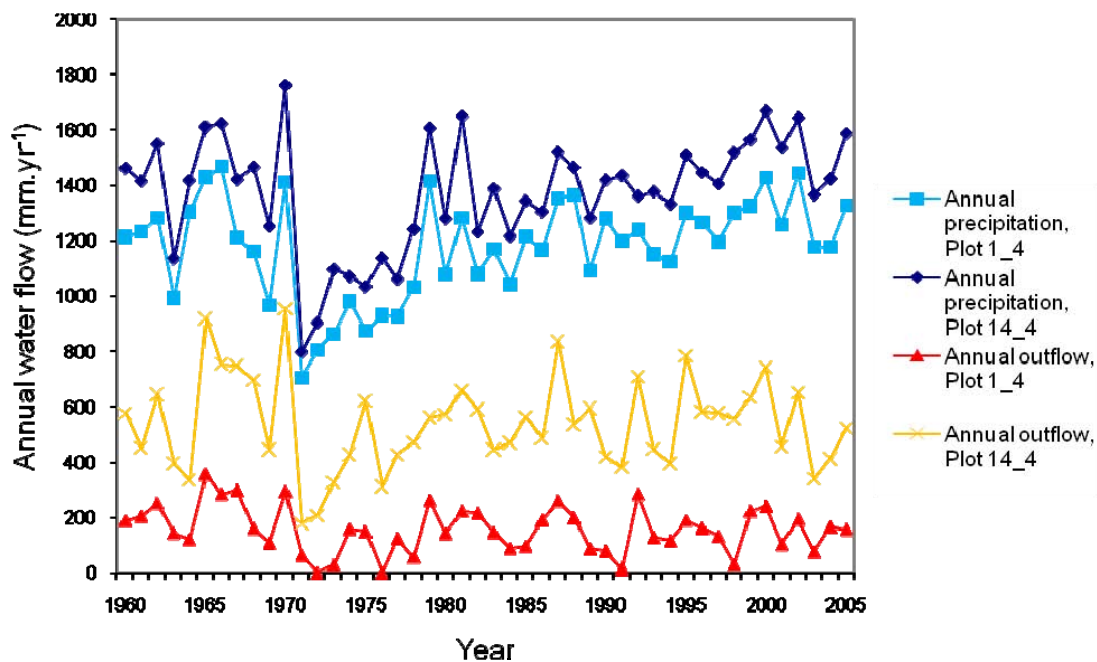


Figure 27. Annual precipitation and annual outflow at two separate plots in the years 1960-2005. Plot 1_4 is the plot at lowest elevation (924 m a.s.l.) and plot 14_4 lies at the highest elevation of all plots (1690 m a.s.l.).

Plot 1_4 is situated on a Northeast slope, the stand in 2005 is 69 years old and can be assigned to the very high yield class 20, whereas the stand of plot 14_4 lies on a Southeast slope, has an age of 122 years and belongs to yield class 7. The predicted volume is 679 and $464 \text{ m}^3 \cdot \text{ha}^{-1}$ in 2005, respectively (at plot 14_4 thinning has been simulated in 1965, 1985 and 1995). The two plots should only give a glimpse on possible stand and site variations and resulting impact on the water-regime.

3.2.4.2 Transpiration & evapotranspiration

Transpiration is the water, which plants lose through their leaves into the ambient atmosphere. It is driven by the plant water potential, the stomatal conductance and the vapour pressure deficit. The plants can control the transpiration by regulating the stomata opening, which is a function of the soil water potential, daily minimum temperature, vapour pressure deficit and short wave solar radiation. Evapotranspiration (ET) is the sum of plant transpiration and evaporation from the canopy and the ground. In the BGC model, the snow-sublimation is also a part of the ET pool. After annual precipitation, annual evapotranspiration resembles the second biggest part in the whole water balance (compare Figure 26) and largely regulates the outflow formation. Therefore, it is important to consider how different stand and site characteristics influence or correlate with annual transpiration and ET (see Figure 28).

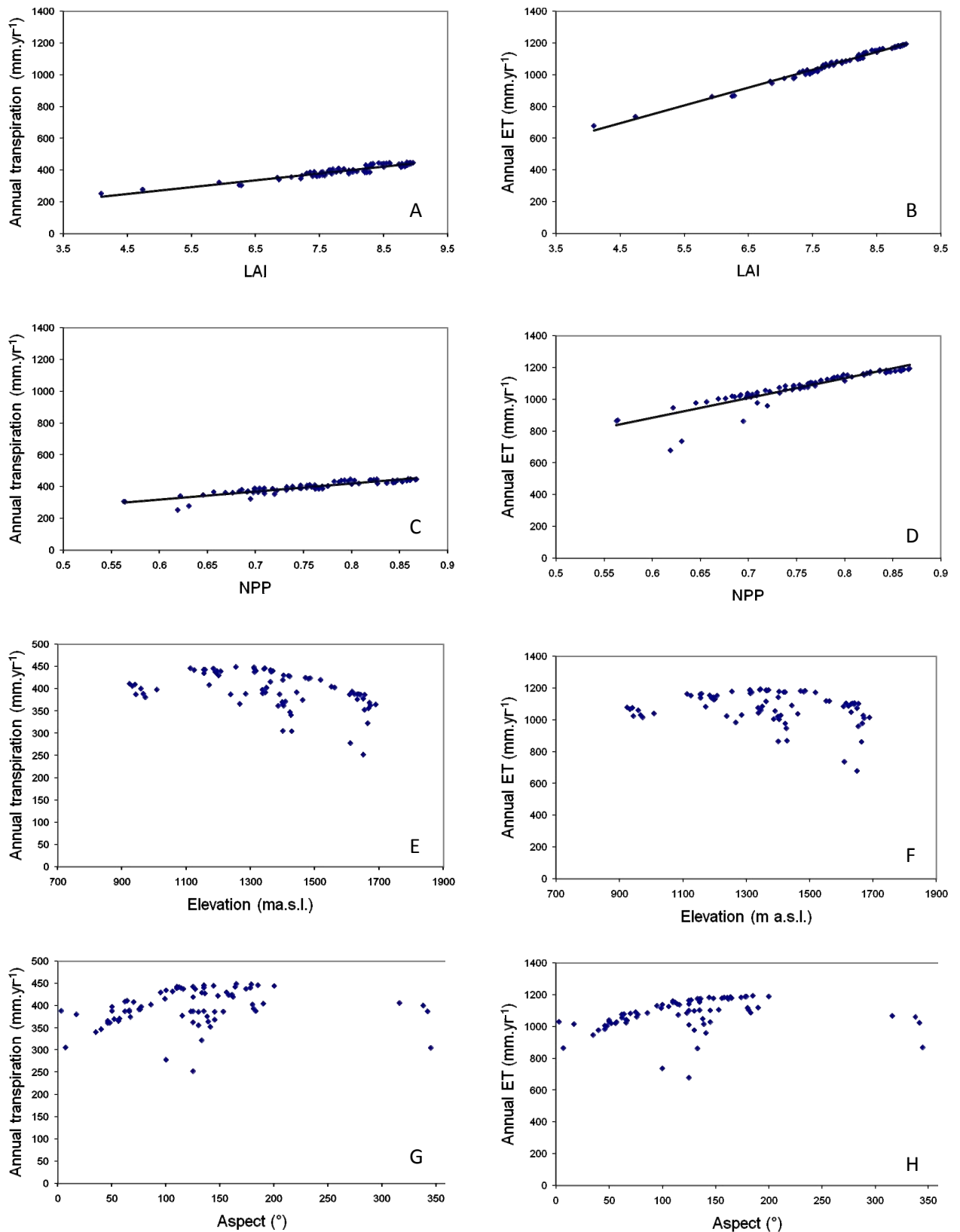


Figure 28. Annual transpiration (left graphs) and annual evapotranspiration (ET) (right graphs) vs. Leaf Area Index (A, B), Net Primary Production ($\text{kg C.m}^{-2}.\text{yr}^{-1}$) (C, D), elevation (E, F) and aspect (G, H) for all plots in 2005.

Annual transpiration and annual ET have a very strong linear dependency on the LAI (Figure 28, A and B). This behaviour is implicit in the model structure, since transpiration takes place at the leaves. Dependency of annual transpiration and ET is also strong (Figure 28, C and D). The points strongly deviating from the regression line between annual ET and NPP (Figure 28, D) are plots in high elevation, above 1600 m a.s.l. with a growing stock below $150 \text{ m}^3 \cdot \text{ha}^{-1}$ (heavy thinning have been simulated).

The four next distributions, the distribution of annual transpiration and annual ET over elevation (Figure 28, E and F) as well as over the aspect (Figure 28, G and H) show roughly curved shapes. This pattern is less pronounced for the distributions of annual transpiration and annual ET over the elevation. The plots at an elevation between 1200 and 1500 m a.s.l., which lie below the 'curve', are situated on North-East slopes. In the next two graphs concerning the aspect, it can be recognised that annual transpiration and ET generally are lower on Northwest to Northeast slopes. The plots that lie well below the curve here are the same plots that lie below the linear regression line between annual transpiration and ET, respectively, and NPP (Figure 28, E and D) as mentioned above. These are stands in high elevation with very low volume per hectare. The two determining factors that lie behind the distribution pattern of annual transpiration and ET over elevation and aspect are incident radiation and temperature. In a valley, short wave solar radiation is less in lower elevations because the surrounding hills obstruct the early and late day sun. On the other hand, temperature naturally decreases with elevation. A combination of both effects results in the tendency of finding the highest transpiration and ET rates in mid-high elevations (at around 1300 m a.s.l.). Determining factor for the annual transpiration and ET distribution over the aspect is the amount of incoming radiation. On the Northern hemisphere, the amount of radiation is highest in southern and lowest in northern exposition. Only shading effects of other hills can change this general pattern.

Annual transpiration and evapotranspiration versus LAI and versus NPP for all plots during the years 1960 to 2005 (Figure 29) can give us some additional information to what we just obtained from the graphs for the year 2005 (Figure 28). Annual transpiration varies between approximately zero and $500 \text{ mm} \cdot \text{yr}^{-1}$, whereas the range for annual evapotranspiration is between 200 and $1400 \text{ mm} \cdot \text{yr}^{-1}$ (see Table 13).

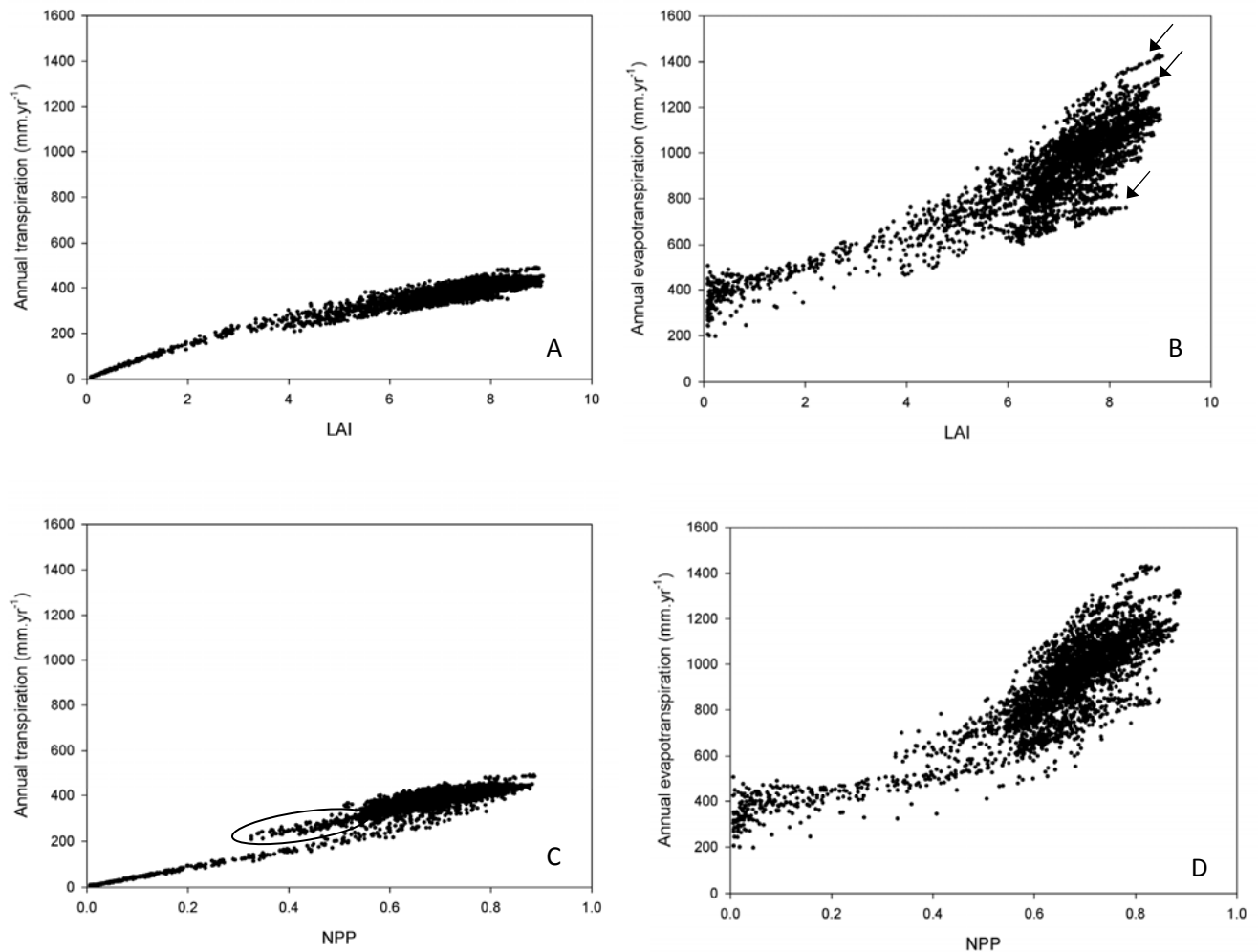


Figure 29. Annual transpiration (left graphs) and annual evapotranspiration (right graphs) vs. Leaf Area Index (A, B) and vs. Net Primary Production ($\text{kg C.m}^{-2}.\text{yr}^{-1}$) (C, D) for all plots in the years 1960-2005. Arrows in graph B indicate distinguishable 'fine lines', which are formed by different plots in the same year. The circled area in graph C confines old growth stands (mainly older than 140 years, but also thinned stands older than 80 years).

The increase of annual transpiration with the LAI gets lower with increasing LAI (see Figure 29, A), whereas annual ET seems to increase consistently over the whole range of LAI (see Figure 29, B). The variation of annual transpiration is caused by differences in stand productivity and stand age and climatic conditions.

The graph of annual transpiration vs. NPP (Figure 29, C) distinguishes three groups of stands which were similarly delineated previously (compare chapter 3.2.2, Figure 19 and chapter 3.2.3, Figure 23). Firstly, we see the newly established stands (starting from a NPP close to zero), which show a strong increase in NPP during their early development and thus a more moderate increase in transpiration with NPP than for LAI. Increase in NPP slows down and finally varies for most of the stands between 0.55 and 0.9 $\text{kg C.m}^{-2}.\text{yr}^{-1}$. Annual transpiration varies between 300 and 450-500 mm.yr^{-1} . This may be regarded as the group of the young to mature stands. Old growth stands (140-240 years old) and some younger (at least 80 years old) recently thinned stands form the third group of plots. The stands of this group have a NPP lower than approximately 0.55 $\text{kg C.m}^{-2}.\text{yr}^{-1}$ but their annual transpiration clearly lies above the annual transpiration of the young stands of the first group which have a similar NPP (for this group also compare chapter 3.2.2, Figure 19).

The relations between annual evapotranspiration and both LAI and NPP are less clear than for the annual transpiration. This is the case especially for the regeneration (with a LAI of < 1 and a NPP of clearly $< 0.1 \text{ kg C.m}^{-2}.\text{yr}^{-1}$) and the highest LAI and NPP values (Figure 29, B and D). The reason for the high ET fluctuations on the very left side of the annual ET-LAI-distribution (Figure 29, B) is that annual transpiration is very little because LAI is also very small and therefore, evaporation is the much larger component of annual ET. Variations of annual ET are based on inter-annual evaporation variations due to climatic fluctuations.

For annual ET over LAI fine lines (indicated with arrows) can be distinguished especially on the right side of the distribution (Figure 29, D). We can understand that one of these fine lines resembles different plots in one specific year, since we realised earlier that for the year 2005 a linear relation exists between ET and LAI (compare Figure 28, first graph). The displacement of the lines then would result from inter-annual changes of the weather conditions.

The next step is an investigation of the relationship between annual evapotranspiration and predicted volume (Figure 30, B). Variation of ET over predicted volume is large. Only for the juvenile stands with a growing stock $< 100 \text{ m}^3.\text{ha}^{-1}$ a dependency of annual ET on the predicted volume exists. For these stands the increase of ET with the volume seems to be linear; nevertheless, considerable variation is evident. With growing stock $> 100 \text{ m}^3.\text{ha}^{-1}$ no dependency is observable on this temporal (46 years) and spatial (78 plots) resolution level.

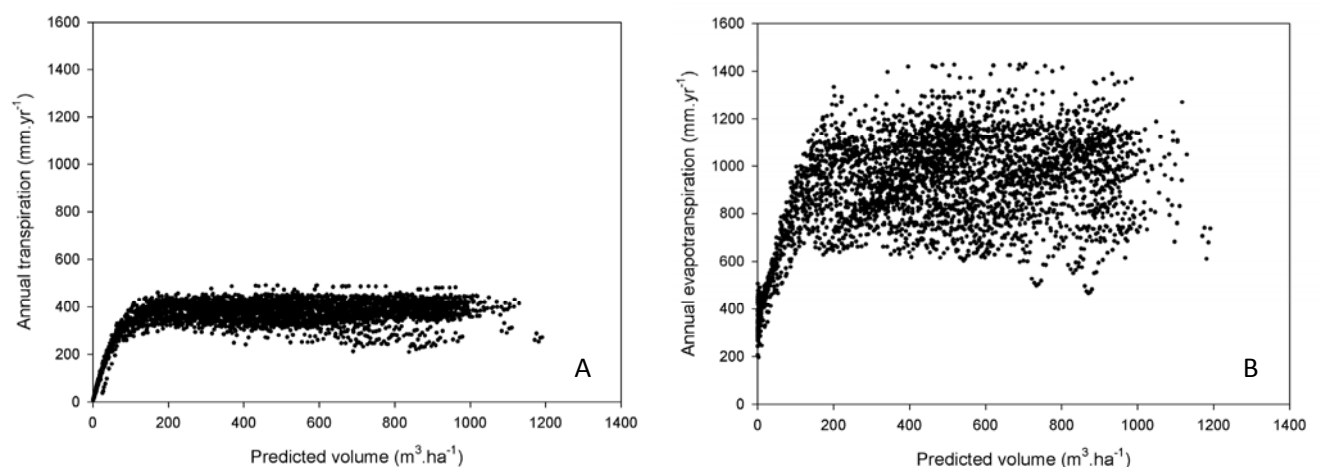


Figure 30. Annual transpiration (A) and annual evapotranspiration (B) vs. predicted volume for all plots in the years 1960-2005.

The graph of annual transpiration vs. predicted volume (Figure 30, A) shows that the strong variation of the ET over the volume (Figure 30, B) must mainly be based on the annual evaporation because annual transpiration vs. predicted volume has considerably less variation. Annual transpiration appears to be virtually independent from the predicted volume $> 100 \text{ m}^3.\text{ha}^{-1}$. The majority of the plots show an annual transpiration rate between 300 and 450 mm.yr^{-1} , but variation increases with higher standing volume. More plots diverge to lower transpiration rates. Easy to realise, these plots with an annual transpiration below 300 mm.yr^{-1} and a standing volume of clearly more than 200 $\text{m}^3.\text{ha}^{-1}$ are the old growth stands (older than 140 years) and a few of somewhat younger stands (at minimum 80 years old) just after thinning has been simulated. This group of plots has been already mentioned several times before (compare chapters 3.2.2 and 3.2.3 and Figure 29, C). The kind of

single 'row' visible above the majority of the plots consists solely of points from the year 2000. The points belong to plots in mid high elevations mainly in Southeast to South exposition. Annual precipitation for these plots is between 1500 and 1600 mm.yr⁻¹ and therefore is considerably higher than the mean annual precipitation of 1286 mm.yr⁻¹ (compare Table 13, chapter 3.2.4.1 on Precipitation). The combination of high precipitation, location in mid-high elevations and Southeast to South exposition can result in high annual transpiration.

Knowledge gained about transpiration and ET behaviour shall support the evaluation of observed outflow behaviour and characteristics.

3.2.4.3 Outflow

Outflow is excessive free water from precipitation, snowmelt and soil water, which is not used up by evaporation and transpiration and is not stored as a snowpack and also cannot be held by the soil.

Outflow behaviour in relation to various important stand and site characteristics in the year 2005 - the final year of the simulation run - shall now be investigated. Annual outflow is plotted over observed stand and site characteristics for all plots (Figure 31).

Firstly, the distributions of annual outflow over the predicted volume, the basal area and the Stand Density Index will be discussed, as they show a similar pattern (Figure 31, A, B, C). Annual outflow turns out to be independent from a predicted volume > 150 m³.ha⁻¹. In this area outflow strongly varies between 140 and 730 mm.yr⁻¹ with a total precipitation in the range of 1328 to 1690 mm.yr⁻¹ for all plots in the year 2005. Nevertheless, for very low standing volume, annual outflow can be high. The maximum outflow value of 800 mm.yr⁻¹ appears at a stand of only 62 m³.ha⁻¹. For annual outflow over the basal area the picture looks similar, however, the high outflow values are less confined to the lowest basal area values (Figure 31, B). Again, a similar picture is seen when plotting annual outflow over the Stand Density Index (SDI) according to Reinecke (1933) (Figure 31, C). For the range of the most common SDI values between 800 and 1500, outflow varies between approximately 150 and 600 mm.yr⁻¹. To summarise, the interpretation of outflow versus predicted volume, basal area and SDI, it can be claimed that high outflow is expected only for the lowest values of these three parameters and hence for juvenile stands. Medium to high predicted volume, basal area and SDI have no predictive capacity for annual outflow.

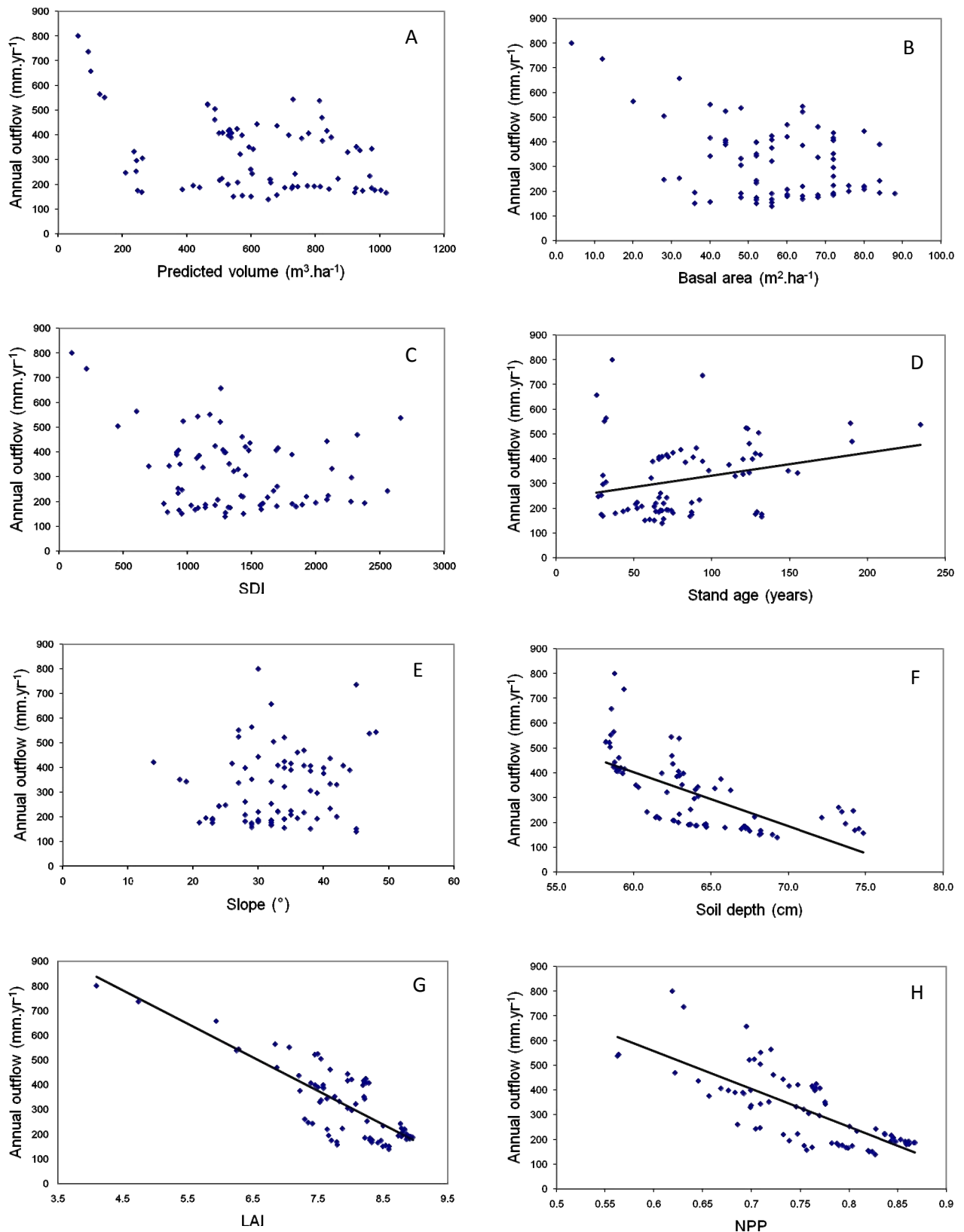


Figure 31. Annual outflow vs. various stand and site characteristics, i.e. predicted volume (A), basal area (B), Stand Density Index (C), stand age (D), slope (E), soil depth (as interpolated from the Austrian Federal Soil Survey; F), Leaf Area Index (G) and Net Primary Production (kg C.m⁻².yr⁻¹) (H) for all plots in the year 2005.

Stand age, at the first glimpse, has a rather weak interpretation power for annual outflow (Figure 31, D). However, a tendency towards higher outflow with increasing stand age from 26 years (the age of the youngest stands in 2005) upwards can be observed. Five stands, four with an age between 26 and 36 and one of 94 years, deviate considerably from the area along the linear regression line where all of the other plots can be found (this range is ± 200 mm of annual outflow about the regression line). For these five stands, heavy thinning was simulated and volume per hectare was smaller than 150 cubic metres. We know that very low standing volume results in high outflow (see Figure 31, A), therefore, it is a justifiable claim that a positive correlation exists between stand age and outflow. Including those five plots, the coefficient of determination for the linear regression line is 0.07, but without those plots it increases to 0.30.

No trend is detectable for outflow versus slope (Figure 31, E). This result contrasts to common hydrological knowledge. The reason is that slope is not yet considered in the process of outflow formation in the current version of the BGC model.

On the contrary, for soil depth a negative correlation to the annual outflow exists (Figure 31, F). Coefficient of determination for the linear trend line is 0.42 without the five poorly stocked stands mentioned above. Including those five plots, the coefficient of determination is 0.44. Naturally, in deeper soils more water can be stored. This is also reflected by the trend line given, when an increase in soil depth by 10 mm decreases average outflow by 22 mm.

The strongest, negative correlation for annual outflow exists with the Leaf Area Index (Figure 31, G). The coefficient of determination for the linear regression line is 0.67. In comparison to the relation between ET and LAI, where the correlation had almost been perfect (with a coefficient of determination of 0.9876 (see Figure 28, A)), here the correlation is lower, although we consider ET to be the strongest determining factor for outflow (second to precipitation). Additional variation for the outflow over LAI comes from the fact that outflow is not formed by the whole amount of available water that has not been evaporated or transpired since water is also kept in the soil or can be stored as a snowpack.

For the relation of annual outflow to the NPP a similar tendency as for the relation of outflow to LAI can be observed (Figure 31, H), but the coefficient of determination of 0.57 is already considerably less than for distribution of annual outflow over LAI (which is 0.67). In the NPP range where most of the plots are found, approximately between 0.65 and 0.85 kg C.m⁻².yr⁻¹, annual outflow ranges roughly ± 150 mm about the regression line. Anyway, if we consider (i) ET as very much depending on LAI and (ii) outflow in turn as depending on LAI, we cannot expect that the similar is true for ET and NPP and in the following outflow and NPP because we have already realised that NPP and LAI are not linearly depending on each other (compare Figure 19).

To get an idea of the relation between annual outflow and both LAI and NPP, the data for all plots in the years 1960 - 2005 are shown in the following graphs (Figure 32, A and B, Figure 33, A and B).

Mind that outflow is given in absolute values in the first two graphs (Figure 32) and as proportion of annual precipitation in the next two graphs (Figure 33). In the graphs, where annual outflow is given versus LAI and NPP, variation is enormously high because outflow variation due to precipitation fluctuations are implicit, whereas in the two graphs showing the share of annual outflow of annual precipitation this is not the case. Especially for annual outflow per annual precipitation versus LAI the distribution is less scattered.

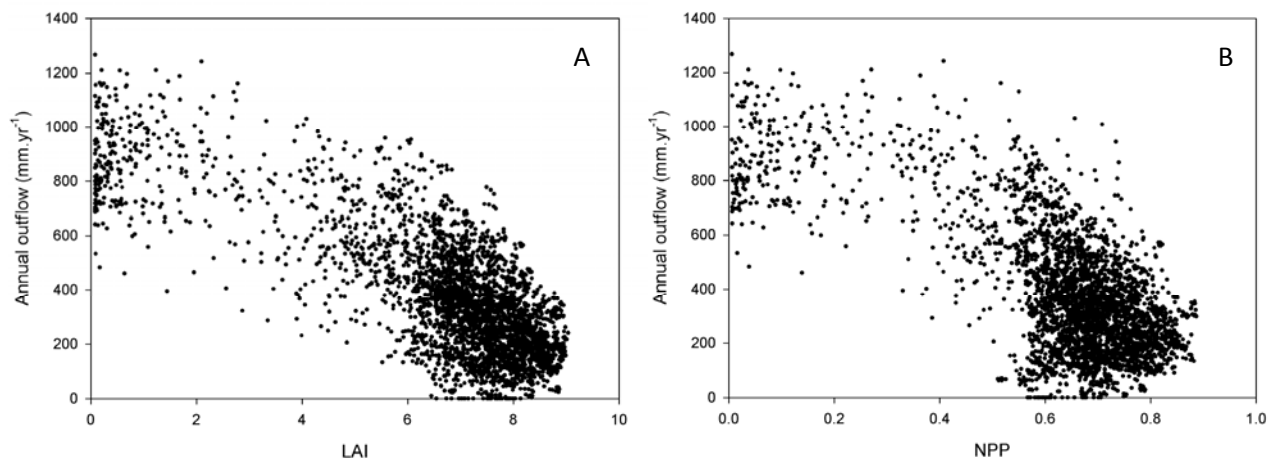


Figure 32. Annual outflow vs. Leaf Area Index (A) and vs. Net Primary Production (B) for all plots in the years 1960-2005.

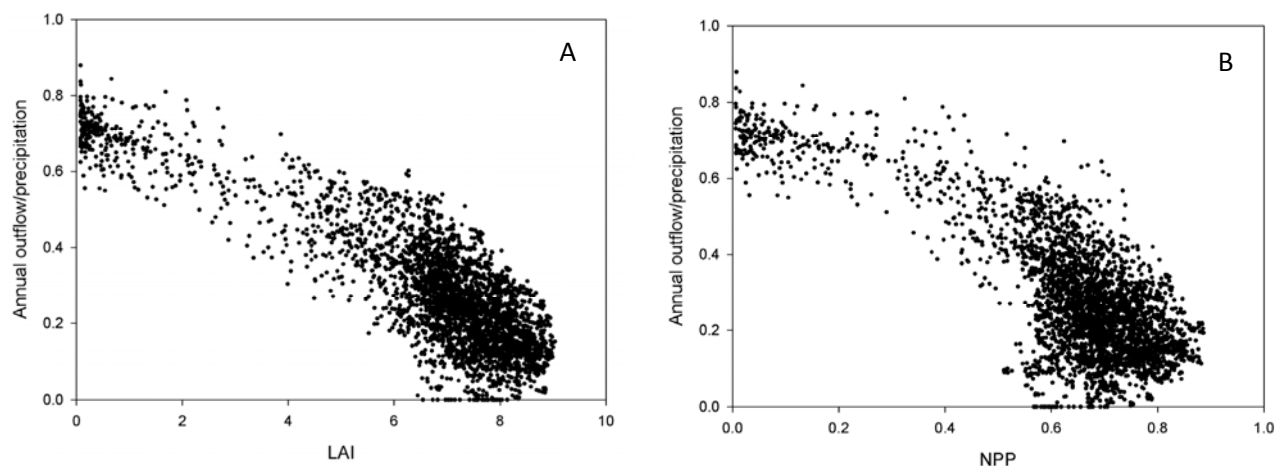


Figure 33. Ratio of annual outflow and annual precipitation vs. Leaf Area Index (A) and vs. Net Primary Production (B) for all plots in the years 1960-2005.

In all four graphs above, the distributions have curved shapes and overall the negative relations are visible. Annual outflow at newly established stands mainly ranges from 600 to 1200 mm.yr⁻¹ or between 60 to 80% of annual precipitation (Figure 32 and Figure 33, A each). Premature and mature stands with a LAI of roughly 6 – 9 show an outflow between zero and approximately 800 mm.yr⁻¹ or between zero and 60% of annual precipitation. The general distribution pattern of the annual outflow and of the annual outflow share in annual precipitation over the NPP is similar (Figure 32 and Figure 33, B each). However, the distributions are less clear than for the distributions over LAI. This fits to the earlier observation that coefficient of determination is higher for annual outflow over LAI than for annual outflow over NPP (compare Figure 31, G and H).

For the purpose of increasing comprehensibility, the two exemplary plots 15_1 and 16_3, already mentioned earlier (compare chapter 3.2.2, Figure 20 and chapter 3.2.3, Figure 24) will be dealt with now again (Figure 34 and Figure 35).

The development of the LAI of the two stands during the years 1960 to 2005 is shown at the beginning (Figure 34, A). At plot 15_1 a 100 years old mature stand with a LAI of 7.3 was clear cut in 1974 and a new stand planted. Consequently LAI is almost zero in the following year. In the next ten years the increase of LAI is rather moderate, but in the following ten years LAI quickly approaches the LAI value of the old stand. In 1999, with 25 years, the new stand already exceeds the LAI of the former stand. The second stand at plot 16_3 was 145 years old having a LAI of 5.5 in 1960. Thinning of 30% had been simulated in 1965 and 1985. Consequently, the LAI dropped twice but did not fall below 4.5 and increased afterwards again. By the year 2005, with an age of 190 the LAI was even clearly higher than in 1960 (also see Figure 34, A).

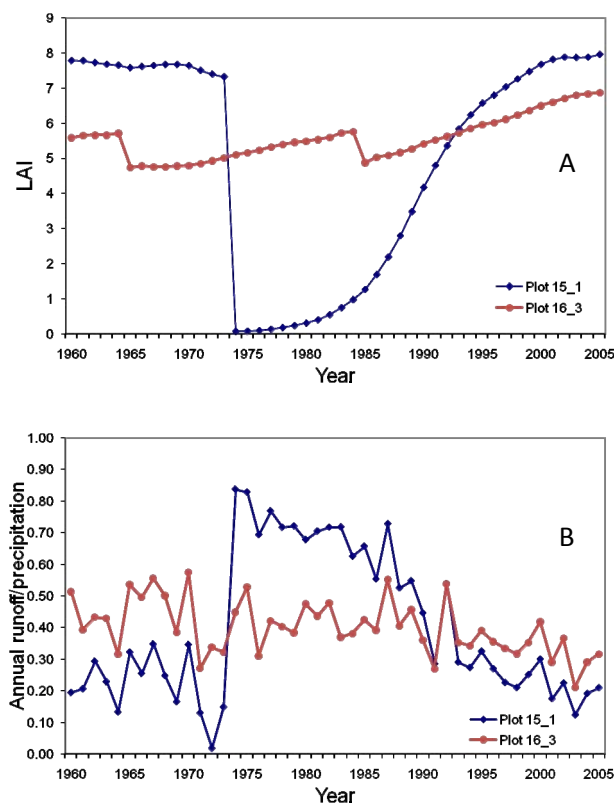


Figure 34. Development of the Leaf Area Index (A) and the annual outflow/precipitation ratio (B) in the years 1960 to 2005 for two different plots showing all data of the years 1960-2005. Plot 15_1 was clear-cut with 100 years in 1974 with subsequent planting. Plot 16_3 is an old growth stand with 145 years of age in 1960 (thinning of 30% was simulated twice during the observation time).

A dependency of the annual outflow/precipitation ratio to the LAI can be easily estimated. The harvest (drop of LAI to almost zero) at plot 15_1 made that annual outflow/precipitation ratio jump to 0.85 (Figure 34, B). The subsequent decrease of this ratio comes along with the increase of LAI following the harvest/planting activity. The moderate thinning activities at plot 16_3 did not result in an obvious change of the annual outflow/precipitation ratio. Inter-annual variations of this ratio are so strong that the small changes of LAI at plot 16_3 in comparison to plot 15_1 have no visible impact. When plotting the annual outflow/precipitation ratio over the LAI a comparably much lower dependency between those two parameters for plot 16_3 than for plot 15_1 is revealed (Figure 35). Coefficient of determination is 0.9 for plot 15_1 and only 0.3 for the other plot. However, variations of the ratio around the linear regression line are not very much different for the two plots, but plot 16_3 is confined to a smaller LAI range. Consequently, the annual climate variations resulting in the fluctuations of the annual outflow/precipitation ratio over the LAI can reduce the coefficient of

determination for plot 16_3 easily. The slope of the two linear regression curves, however, is practically the same for both plots. Only the regression line of plot 16_3 is shifted upwards. This is an indicator that higher outflow takes place at older stands under similar conditions.

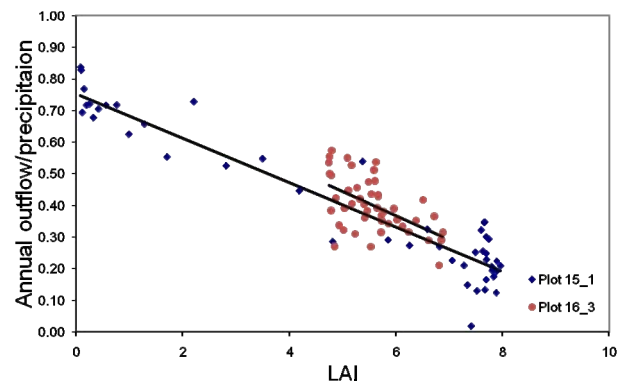


Figure 35. Relation between the annual outflow/precipitation ratio and the Leaf Area Index for two plots during 1960-2005. Plot 15_1 was clear-cut with 100 years in 1974 with subsequent planting. Plot 16_3 is an old growth stand with 145 years of age in 1960 (thinning of 30% simulated twice during the observation time).

Final analysis of annual outflow data from all plots for the years 1960 to 2005 is done on their relation to the predicted volume. Since standing volume is a key parameter in forestry possible dependencies of volume per hectare to annual outflow and the annual outflow/precipitation ratio are crucial (Figure 36, A and B).

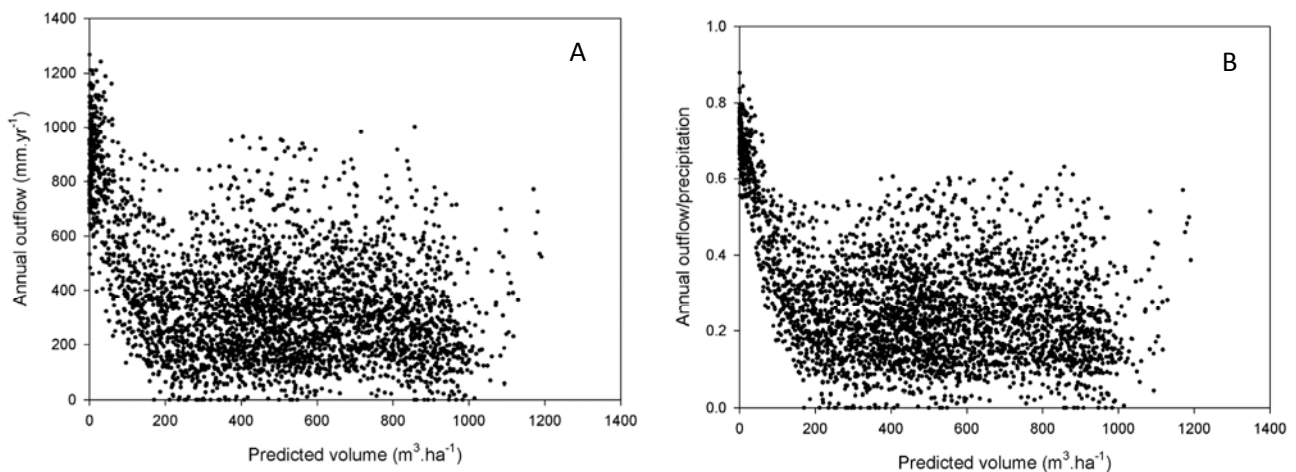


Figure 36. Annual outflow vs. predicted volume (A) and the ratio of annual outflow and annual precipitation vs. predicted volume (B) for all plots in the years 1960-2005.

Both distributions, annual outflow vs. predicted volume and share of annual outflow in annual rainfall vs. predicted volume, exhibit a similar shape. Highest values are clearly confined to the barely stocked stands up to growing stock of $100 \text{ m}^3 \cdot \text{ha}^{-1}$. In that range, it becomes obvious that the distribution in the second graph is less scattered. However, at a growing stock $> 200 \text{ m}^3 \cdot \text{ha}^{-1}$, absolutely no dependency of annual outflow and the annual outflow/precipitation ratio on the predicted volume is detectable. Zero outflow appears at growing stock values from roughly $200 - 1000 \text{ m}^3 \cdot \text{ha}^{-1}$. This range is relatively much bigger than for zero outflow over LAI or NPP (compare Figure 32). Overall, the range with low to no prediction power for annual outflow is bigger for the predicted volume than for NPP and especially for LAI.

3.2.5 Soil analysis

Predicted soil carbon and soil nitrogen are the sum of the four soil carbon and soil nitrogen fractions (differing in their resilience to microbial degradation). They were compared with the soil carbon and soil nitrogen contents measured in the lab from the soil samples collected during the field campaign in 2007 (Figure 37).

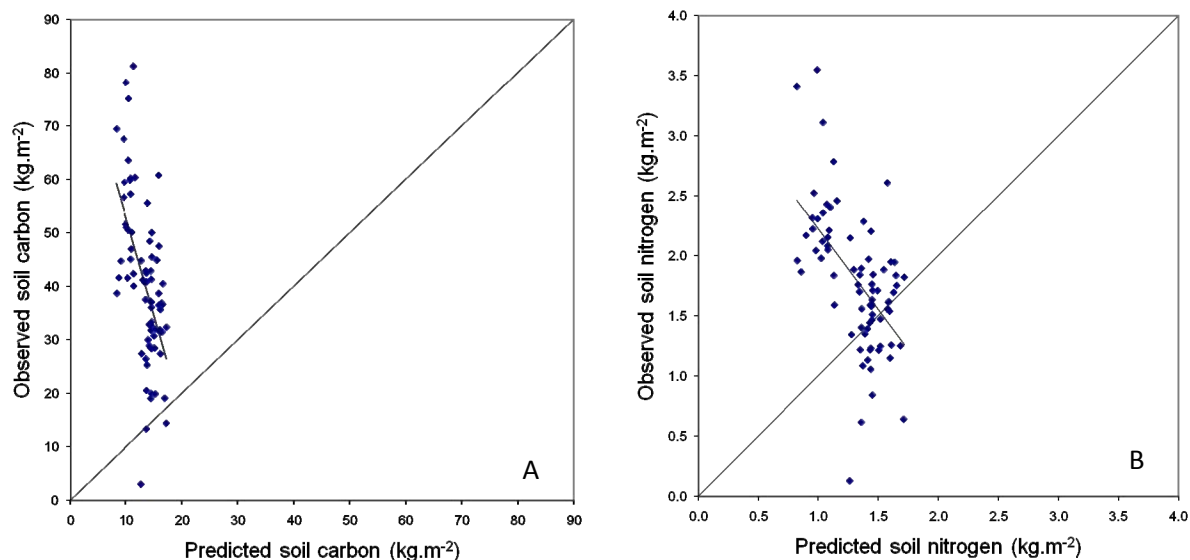


Figure 37. Observed vs. predicted soil carbon (A) and soil nitrogen (B) for all plots in 2005.

The model simulation clearly underestimates the soil carbon and nitrogen. The mean difference between predictions and observations is -207% for soil carbon and -35% for soil nitrogen. The confidence intervals for soil carbon and soil nitrogen also reveal a negative bias, since both confidence intervals include only negative values (see Table 14). Only the prediction interval for soil carbon and nitrogen includes zeros.

Table 14. Results of the error analysis for soil carbon and soil nitrogen for all plots in the year 2005.

Species parameters	\overline{obs}	\overline{Di}	SD	t	CI	PI
Soil carbon (kg.m ⁻²)	13.37	-27.68 (-207%)	16.06 (120%)	11.3340	-31.84 – -23.52 (-238 – -176%)	-64.62 – 9.26 (-483 – 69%)
Soil nitrogen (kg.m ⁻²)	1.33	-0.46 (-35%)	0.72 (54%)	11.5868	-0.65 – -0.28 (-49 – -21%)	-2.26 – 1.16 (-159 – 89%)

Where \overline{obs} is the mean of observations, \overline{Di} the mean of the differences between predicted and observed values, SD the standard deviation of the differences and t the value from paired t-statistics. CI and PI are the confidence and prediction intervals of the error ($\alpha = 0.05$) (Reynolds, 1984, in Pietsch et al., 2005).

An analysis of the standardised residuals (predicted minus observed soil carbon divided by the standard deviation of the soil carbon observations; similar for soil nitrogen) was conducted as well (Table 15). Mean soil carbon residual for all plots is -1.85 and mean soil nitrogen residual for all plots is -0.81. The range of soil carbon residuals for all plots is -4.67 – 0.18 and soil nitrogen the range is

wider with residuals between -4.51 and 1.08 (Table 15). The mean stand carbon and nitrogen residuals are even more negative.

Table 15. Minimum, maximum and mean soil carbon and soil nitrogen - residuals (predicted minus observed soil carbon or soil nitrogen divided by the standard deviation of the observations) for all plots (78) and for the stand-means soil carbon and soil nitrogen - residuals (20) in the year 2005.

		Minimum	Maximum	Mean
Soil carbon - residuals	all plots	-4.67	0.18	-1.85
	stand means	-4.56	-0.50	-2.14
Soil nitrogen - residuals	all plots	-4.51	1.86	-0.81
	stand means	-3.65	1.08	-0.93

Standardised residuals can be plotted against stand and site characteristics. In this case, the trend analysis is done for the stand age, the soil depth determined by the soil samplings during the field campaign in 2007 (for the method see chapter 2.1.4), the aspect and the elevation (Figure 38).

The residual analysis shows a negative trend for the stand age (Figure 38, A and B). The coefficient of determination is quite low for both soil carbon and nitrogen (0.090).

A stronger negative trend is revealed for the analysis on soil sampling soil depth (Figure 38, C and D). For the soil carbon trend line, the coefficient of determination is 0.606, for soil nitrogen it is slightly lower at 0.549. The reason is obvious - the higher the soil depth we determined in the field the higher are the soil carbon and soil nitrogen results and the less the model is able to predict these high values. For soil carbon, the trend line cuts the X-axis at approximately 12 cm. This means that predicted soil carbon fits the best to field measurements of around 12 cm soil depth. On the other hand, for soil nitrogen the model predictions fit best for an observed soil depth of around 28 cm. Generally, the residual analysis shows more positive values for soil nitrogen. The different behaviour of soil carbon and soil nitrogen is also reflected by the different soil carbon/nitrogen ratio. Field observations give a mean C/N of 23, whereas the model output gives a constant ratio of only 10 (Table 16, compare also Appendix, Table 20). This explains why the underestimation of the BGC model for soil nitrogen is less (compare Table 15).

Table 16. Mean, minimum and maximum soil carbon/nitrogen ratio for all plots of the soil sampling in the Schmittenbach watershed in 2007 and of the model predictions for all plots in 2005.

		Minimum	Maximum	Mean
C/N	soil sampling	15	19	23
	model predictions	10.01	10.02	10.03

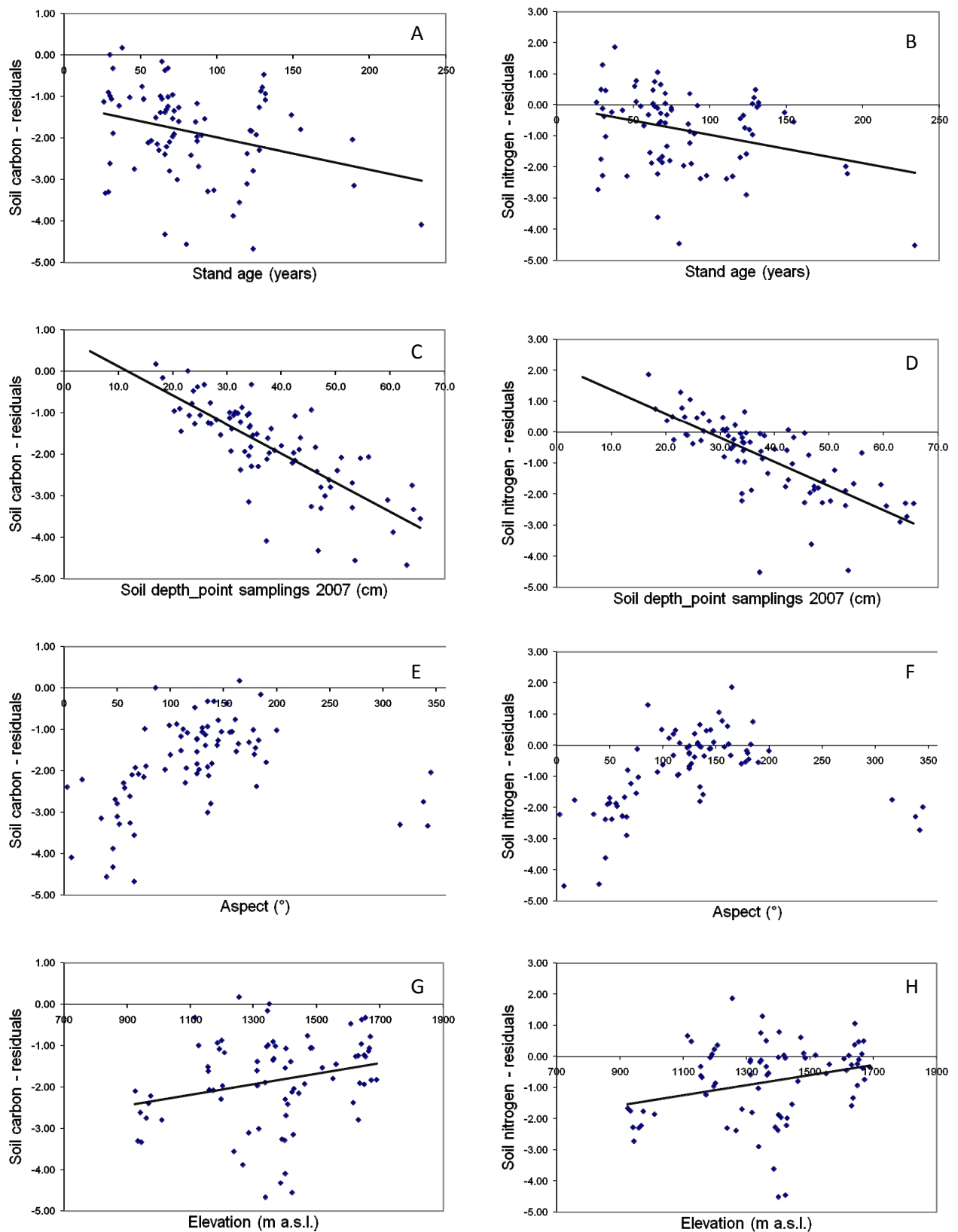


Figure 38. Trend analysis of standardised soil carbon residuals (left graphs) and soil nitrogen residuals (right graphs) (i.e. predicted minus observed soil carbon or nitrogen divided by the standard deviation of the observations) vs. stand age (A, B), soil depth from field measurements (C, D), aspect (E, F) and elevation (G, H) for all plots in 2005.

Further soil carbon and soil nitrogen residual analysis is done on the aspect (Figure 38, E and F). The distribution of the residuals over the aspect obviously has a curved shape. A similar but less strong curved shape has already been detected for the distributions of Net Primary Production, annual transpiration and annual evapotranspiration over the aspect (compare Figure 21, D and Figure 28, G and H). Underestimation of soil carbon and soil nitrogen is the strongest in Northwest to Northeast exposition and is the lowest on South facing slopes.

Finally, the soil carbon and soil nitrogen residuals distribution over the elevation shall be discussed (Figure 38, G and H). A weak positive trend is detectable. With higher elevation, the model predictions come closer to the field observations of soil carbon and nitrogen. However, coefficient of determination is low with a value of 0.063 for soil carbon and a value of 0.076 for soil nitrogen.

As a result of the standardised residual analysis for soil carbon and soil nitrogen, it can be claimed that the model is able to describe the actual soil carbon and soil nitrogen state the best in higher elevations in Southern exposition where soil is shallower.

4 Summary and conclusion

This study was initiated by a project trying to assess the protection function of forests (against floods events etc.) in the alpine area by investigating the flux dynamics within a watershed, which may depend on vegetation patterns in the area and the forest management practices. Analysis can be done using the mechanistic ecosystem model BIOME-BGC but interactions among the simulation points are not yet implicit in the BIOME-BGC model. This study provides preparatory analysis work for the model revisions.

The study consists of three main working and analysis steps:

1. Field study in the test region Schmittenbach watershed to gain information about site and stand conditions and characteristics (stand age, dominant height, standing volume, site index; humus and topsoil depth, soil carbon and soil nitrogen content) and about the current vegetation distribution
2. Comparison of results of the point samplings in the catchment with data from the current forest management plan of the local forest company 'Zeller Waldgemeinschaft' - consistency test on stand age, dominant height, standing volume and site index
3. Application of the BIOME-BGC model - simulation of forest at the point sampling plots and analysis of flux dynamics (water, nutrients, carbon) within the simulation points

The Schmittenbach watershed has been selected as a test case since it is one of the most thoroughly investigated watersheds in Austria with very good historical data on both vegetation dynamics and hydrology. Preparatory work for the field study was a literature research on topographic, geological, hydrological conditions of the test region Schmittenbach watershed, as well as on history of catastrophic flood events, which repeatedly took place as a result of massive deforestation during the last centuries, and on historical changes in land use practices and the vegetation distribution.

During the field campaign an investigation on the current land cover types was done. In a coarse vegetation mapping the main vegetation categories: evergreen needle forest, good pastures, planed pastures (ski slopes with poor grass cover) and dwarf shrub/curved wood area with alpine pastures were distinguished and drawn onto a orthophoto. This should serve as information for BIOME-BGC modelling where seven different biome types can be modelled.

Stem analysis have been conducted in order to determine whether or not the regionally applied yield table gives information comparable to our own data and therefore to get an idea if future analysis can be built on existing data provided by the management plan of a local forest company. For this purpose nine different stands with 27 trees were selected in such a way that the three main age classes: (i) young, (ii) middle aged and (iii) mature forests in combination with the three different site quality categories: (i) poor, (ii) medium and (iii) very good sites were covered. The gained tree growth curves were compared with the dominant height growth curves of Mitscherlich/Richard (1919) of 'Fichte Bayern' and 'Fichte Hochgebirge'. The determined growth curves of trees in the Schmittenbach watershed fit better to dominant height growth curves for 'Fichte Hochgebirge', which is the recommended site index system for the area of Zell am See. However, especially for older stands height increment of the measured trees exceeds height increment given by the dominant height growth functions. This might be explained by better growing conditions in the recent decades due to higher atmospheric CO₂ content, higher mean temperature and therefore longer growing season.

In addition, this study contains the calculation and analysis work comparing the management plan 2003 of the 'Zeller Waldgemeinschaft' for the Schmittenbach watershed with the stand data obtained during the field campaign. To get the information about stand and site conditions, i.e. stand age, dominant height, standing volume and site index, 20 stands with 78 point samplings have been measured.

- The stand age was obtained from coring a typical tree at each point sampling location.
- The Mean dominant height of a stand was derived from the dominant heights for each plot of one stand, which had been calculated as the mean height of the three biggest trees from the point sampling.
- Site index was interpolated from the yield table 'Fichte Hochgebirge' applying measured information on stand age and dominant height.
- The standing volume was calculated from point sampling data (dbh, tree height) using the form factor function of Pollandschütz (1974).

Afterwards these data were compared with the information given in the management plan of the local forest company. Stand age, volume and site index could be directly taken from the management plan, whereas the dominant height was calculated from stand age and site index using dominant height growth functions of Mitscherlich/Richard (1919) for 'Fichte Hochgebirge'.

Highest accordance between field data and information from the management plan exist for the stand age. Only for young stands a slight underestimation of age in the management plan can be detected. Measured dominant height generally is higher than dominant height calculated from stand age and site index information from the management plan using the dominant height growth functions of Mitscherlich/Richards (1919). For the site index, the strongest deviation of management data from our results can be observed. An underestimation of the site index in the management plan has to result also in an underestimation of the dominant height due to the described calculation approach of dominant height. Site index given in the management plan does not exceed the value of 9, whereas very high values (approaching 20) could be derived from the stand age and dominant height field measurements. Finally, standing volume as the last stand parameter compared between field measurements and the values given in the management plan turns out to be more and more underestimated with increasing measured standing volume, however, variation is quite high.

The next working step was the in-depth analysis using modelling theories. With the mechanistic ecosystem model BIOME-BGC energy and matter cycles (short wave solar radiation, water, carbon, nutrients) were simulated for the 78 point sampling plots and state and flux output variables were analysed with accordance to stand and site characteristics. For the model simulations, 46 years of detailed weather records obtained from the DAYMET climate model (1960 – 2005) were used. Soil depth and texture (soil sand, silt and clay content) as two important input parameters were interpolated from data from the Austrian Federal Soil Survey. Thinning operations have been included in the simulations. Thinning interventions were planned and conducted homogenously for the whole stand (which consisted of four plots in most cases).

First step is to investigate whether the model volume predictions match the volume observations, which have been obtained during the field campaign. Average model predictions turned out to correlate very well with mean observations. Average growing stock for all plots determined in the field was 640 m³, whereas mean volume predictions were 614 m³, which means a slight underestimation of 4%. However, between end of simulation (2005) and observations (July 2007) a small time gap exists. Including this knowledge into the volume analysis it can be estimated that the volume difference would be around 2%. Residual analysis has been conducted on plot level (for all 78

plots) and on stand level (for the stand means – mostly four plots belong to one stand). Mean standardised volume residual for all plots is -0.09 and from the stand means it is -0.11. Trend analysis of standardised volume residuals on different stand and site characteristics (i.e. stand age, dominant height, basal area, SDI...Stand Density index according to Reinecke (1933), site index, elevation, slope and aspect) for all plots revealed a significant trend for the basal area, the SDI, the stand age and the dominant height. However, on stand level – the level on which thinning operations have been planned and conducted – residual analysis on basal area and SDI showed no significant trend.

Net Primary Production NPP was also investigated. Since the Leaf Area Index (LAI) controls photosynthesis, it is not surprising that a strong correlation between NPP and LAI could be observed and fluctuations of the NPP are due to climatic variations over the years. However, in young development phases and in old growth stands NPP can differ considerably despite same LAI values. These significant differences were observed in a LAI range of roughly 4 to 6. Besides, NPP turns out to be dependent on aspect and elevation with highest values on South-facing slopes in mid high elevations around 1300 m a.s.l..

Analysis on water use efficiency (WUE), the ratio between NPP and annual transpiration, shows similar dependence on the aspect as the NPP but WUE clearly increases with elevation. Again, differences in WUE between juvenile stands and old growth stands despite similar LAI were detected. This holds true also for the NPP and the effect is even more pronounced.

An in-depth analysis of the water regime at a site increases understanding of the mechanisms of outflow formation. The annual water balance consists of annual precipitation, snowpack formation and storage over the winter, snow melt in spring, soil water storage, transpiration and evaporation – combined as evapotranspiration (ET) – and finally outflow of excess water.

Annual transpiration and evapotranspiration are very strongly positively dependent on LAI and also strongly on NPP. A slight dependency on elevation is observable and a more pronounced correlation with the aspect. Highest values, similar to the NPP, exist for mid high elevations and in Southern exposition. The analysis of annual transpiration and evapotranspiration on the growing stock reveals that from approximately $100 \text{ m}^3 \cdot \text{ha}^{-1}$ upwards no trend for annual transpiration and evapotranspiration exists over the volume for all plots observed during the years 1960-2005. However, for juvenile stands with a volume $< 100 \text{ m}^3 \cdot \text{ha}^{-1}$ a nearly linear relationship is evident.

A final issue with regard to water balance analysis is the annual outflow. Investigating annual outflow of all plots in 2005, the final year of the simulations, it was highest for plots with smallest standing volume ($< 200 \text{ m}^3 \cdot \text{ha}^{-1}$) but was independent from a standing volume $> 200 \text{ m}^3 \cdot \text{ha}^{-1}$. Three clearly negative trends for annual outflow over certain stand and site parameters were observed - annual outflow decreases with the soil depth (as interpolated from the Austrian Federal Soil Survey), with the LAI (observed LAI range was 4-9) and the NPP (observed NPP range was $0.56\text{-}0.88 \text{ kg C} \cdot \text{m}^{-2} \cdot \text{yr}^{-1}$). Total values of annual outflow were difficult to interpret for all of the plot over the longer period (years 1960 to 2005). Climatic fluctuations caused very high variation and therefore, it was decided to calculate the annual outflow/annual precipitation ratio in order to reduce variability caused by inter-annual precipitation variations. For this new parameter, a negative relation to LAI and NPP - from zero to maximum LAI and NPP values (9 and $0.9 \text{ kg C} \cdot \text{m}^{-2} \cdot \text{yr}^{-1}$, respectively) - could be observed. Finally, this new outflow/precipitation ratio was analysed on dependency to the growing stock. The graphical analysis reveals an opposite behaviour of this ratio over the volume as it was observed for annual evapotranspiration over the volume. Highest values are found at the juvenile stands and at a volume $> 200 \text{ m}^3 \cdot \text{ha}^{-1}$ no trend is evident. Overall, growing stock has a lower predictive power for annual outflow than NPP and especially LAI.

The last major topic of investigations were the correlation between soil carbon and soil nitrogen content measured in the field and predicted by the BGC model. For the soil carbon and nitrogen content, four soil samples were taken at each plot and humus and topsoil depth was measured. All soil samples were analysed in the lab, and the soil carbon and nitrogen content were determined. Analysis of soil carbon and soil nitrogen simulation results revealed a significant underestimation of observed values. Mean underestimation is slightly more than 200% for soil carbon and 35% for soil nitrogen. For all plots, the mean standardised residual for soil carbon is -1.85 and for soil nitrogen it is -0.81. A less severe underestimation of soil nitrogen is also reflected by the higher mean C/N ratio of the model outputs than for the field observations (10 for the BGC model and 23 for the field observations). Distribution analysis of soil carbon and soil nitrogen residuals over site and stand parameters revealed that underestimation by the model is more severe for deeper soils in lower elevations, in Northwest to Northeast expositions and for higher stand age. Simulation results showed highest accordance with field measurements for shallow soils on South-facing slopes in higher elevations.

Summing up, analysis on correlation between field data obtained in the Schmittenbach watershed and data from the management plan of the local forest company 'Zeller Waldgemeinschaft' showed, that consistency for the stand age is very good, but in the management plan site productivity is much underestimated. Simulations of the point sampling plots with the mechanistic ecosystem model BIOME-BGC delivered no bias between observed and predicted volume data and provided a good insight into flux dynamics (water, carbon, nutrients) within the region. Further study work on assessing the protection function of forests in mountainous areas by analysing vegetation patterns in a watershed and vegetation dynamics along the topographic gradient applying mechanistic ecosystem models may follow.

5 References

- Aulitzky, H. 1963. Ökologische Untersuchungen in der subalpinen Stufe zum Zwecke der Hochlagenaufforstung, Mitteilungen der Forstlichen Bundes-Versuchsanstalt Mariabrunn, 59, 491 p.
- Forsttechnischer Dienst für Wildbach und Lawinenverbauung, Gebietsbauleitung Pinzgau. 1996. Technischer Bericht des Flächenwirtschaftlichen Projektes Schmittbach, unpublished
- Forsttechnischer Dienst für Wildbach und Lawinenverbauung, Gebietsbauleitung Pinzgau. 2002. Entwicklung 'Projekt Schmidten-Wildbach 1889', unpublished
- Fosberg, M. 1977. Heat and water transport properties in conifer duff and humus. USDA Forest Service. Res. Pap. RM-195. USDA Forest Service, Fort Collins, CO.
- Gayl, A. 1958. Pflanzensoziologisches Gutachten zum Aufforstungsgebiet Schmittenhöhe, Klagenfurt.
- Hagen, K. 2003. Wildbacheinzugsgebiet Schmittbach (Salzburg), Analyse des Niederschlags- und Abflussgeschehens 1977 – 1998, Bundesamt u. Forschungszentrum für Wald, Vienna. BWF Berichte 129, 101 p.
- Haiden, A. 1957. Bauerfahrungen über die Wildbachverbauung im Mittelpinzgau. In: Wasserwirtschaft und Technik, (1935), Issue 1,2,3,4,7.
- Hasenauer, H. Merganicova, K., Petritsch, R.; Pietsch, S., Thornton, P., 2003. Validating daily climate interpolation over complex terrain in Austria. Agricultural and Forest Meteorology 119, 87-107.
- Hinterstoisser, H. 1981. Waldbauliche Auswirkungen der Standard- und Trassschiabfahrt auf der Schmittenhöhe. diploma thesis, University of Applied Life Sciences, Vienna, 146 p.
- Hinterstoisser, H. 1985. Die forstliche Problematik intensiver Wintersporterschließung am Beispiel der Schmittenhöhe, Zell am See, Sonderdruck, aus Mitteilungen der Gesellschaft für Salzburger Landeskunde, Band 124, 497-611.
- IPCC WG I, 1996. Technical summary. In: Houghton, J.T., Meira Filho, L.G., Callander, B.A., Harris, N., Kattenberg, A, Maskell, K. (Eds.), Climate Change 1995-The Science of Climate Change: Contribution of the Working Group I, to the Second Assessment Report of the Intergovernmental Panel on Climate Change, Cambridge University Press, Cambridge, U.K., pp. 9-50.
- Kindermann, G. Hasenauer, H. 2005. Zusammenstellung der Oberhöhenfunktionen für die wichtigsten Baumarten in Österreich – Reassessing site index functions for tree species in Austria. Austrian Journal of Forest Science. 122/4, pp. 163-184.
- Küster, Hansjörg. 2002. Geschichte des Waldes. Von der Urzeit bis zur Gegenwart. C.H.-Beck
- Marshall, J. 1975. Hilfstafeln für die Forsteinrichtung, Wien, Österreichischer Agrarverlag, 199 p.
- Petritsch, R. 2002. Anwendung und Validierung des Klimainterpolationsmodells DAYMET in Österreich Master thesis, University of Natural Resources and Applied Life Sciences, Vienna, pp. 95.
- Petritsch, R., Hasenauer, H., Pietsch, S.A., 2007. Incorporating forest growth response to thinning within biome-BGC. For. Ecol. Manage. 242, 324-336.

Pietsch, S.A., Hasenauer, H., 2002. Using mechanistic modelling within forest ecosystem restoration. *For. Ecol. Manage.* 159, 111-131.

Pietsch, S.A., Hasenauer, H., Kucera, J., Cermak, J., 2003. Modelling effects of hydrological changes on the carbon and nitrogen balance of oak in floodplains. *Tree Physiol.* 23, 735-746.

Pietsch, S.A., Hasenauer, H., Thornton, P.E., 2005. BGC model parameters for tree species growing in central European forests. *For. Ecol. Manage.* 211, 264-295.

Pietsch, S.A., Hasenauer, H., 2006. Evaluating the self-initialization procedure of large scale ecosystem models. *Global Change Biol.* 12, 1658-1669.

Pollanschütz, J. 1974. Formzahlfunktion der Hauptbaumarten Österreichs. *Allgemeine Forstzeitung* 85, 341-343.

Reinecke, L.M., 1933. Perfecting a stand density index for even-aged forests. *Journal of Agricultural Research* 46, 627-638.

Ulrich, E., Williot, B., 1993. Les depots atmosperiques en France de 1850 a 1990, depots en milieu rural et en foret, depots dans les zones industialisees et urbaines. Imprimiere de l'Office National des Forets, 154 pp.

Thoma, R. 1900. [Ed] *Berichte des Forst-Vereines für Oberösterreich und Salzburg*, Verlag des Vereines, Gmunden

Thornton, P.E., Law, B.E., Gholz, H.L., Clark, K.L., Falge, E., Ellsworth, D.S., Goldstein, A.H., Monson, R.K., Hollinger, D., Falk, M., Dhen, J., Sparks, J.P., 2002. Modelling and measuring the effects of disturbance history and climate on carbon and water budgets in evergreen needleleaf forests. *Agric. For. Meteorol.* 113, 185-222.

Internet:

Schmittenhöhebahn-AG, <http://www.schmitten.at>, Download on the 24th of June, 2007

6 Appendix

Table 17. Part 1. Site characteristics measured and calculated for all plots during the field campaign in the Schmittenbach watershed 2007.

Name	Elevation (m)	Stand mean	Aspect (°)	Stand mean	Slope (°)	Stand mean	Soil depth (cm)	Stand mean
1_1	973		17		28		42	
1_2	1009		50		30		47	
1_3	967		3		24		50	
1_4	924	968	64	34	29	28	55	49
2_1	933		316		23		47	
2_2	941		62		29		49	
2_3	959		338		22		64	
2_4	944	944	342	265	25	25	64	56
3_1	1267		46		40		61	
3_2	1238		66		42		66	
3_3	1285		50		27		60	
3_4	1338	1282	66	57	32	35	63	62
4_1	1403		48		38		53	
4_2	1409		57		38		47	
4_3	1399		52		35		53	
4_4	1391	1400	62	55	29	35	46	50
5_1	1418		133		28		31	
5_2	1401		125		41		35	
5_3	1518		162		24		29	
5_4	1486	1456	158	145	33	32	34	32
6_1	1403		156		42		23	
6_2	1422		136		35		37	
6_3	1471		161		37		27	
6_4	1481	1444	148	150	35	37	31	30
7_1	1370		178		34		32	
7_2	1362		164		23		34	
7_3	1365		174		39		34	
7_4	1345	1360	185	175	23	30	18	30
8_1	1562		180		18		22	
8_2	1552		190		19		40	
8_3	1616		181		28		33	
8_4	1624	1588	183	184	14	20	27	30
9_1	1312		144		32		38	
9_2	1311		179		28		44	
9_3	1313		127		36		42	
9_4	1317	1313	135	146	34	33	48	43
10_1	1255		165		30		17	
10_2	1342	1298	200	183	30	30	34	25

Table 18. Part 2. Site characteristics measured and calculated for all plots during the field campaign in the Schmittbach watershed 2007.

Name	Elevation (m)	Stand mean	Aspect (°)	Stand mean	Slope (°)	Stand mean	Soil depth (cm)	Stand mean
11_1	1667		130		27		25	
11_2	1655		141		29		26	
11_3	1665		133		32		31	
11_4	1651	1659	125	132	30	30	33	28
12_1	1655		145		34		24	
12_2	1637		135		37		39	
12_3	1632		125		33		27	
12_4	1642	1641	130	134	35	35	20	27
13_1	1643		153		43		25	
13_2	1651		115		30		33	
13_3	1611		100		45		5	
13_4	1608	1628	123	123	26	36	24	22
14_1	1673		125		34		46	
14_2	1632		138		36		49	
14_3	1670		145		32.33		24	
14_4	1690	1666	139	137	27	32	34	38
15_1	1337		77		38		43	
15_2	1350		86		39		23	
15_3	1346		76		41		32	
15_4	1362	1349	99	85	32	38	21	30
16_1	1401		7		47		37	
16_2	1428		345		48		34	
16_3	1426		35		37		34	
16_4	1462	1429	67	114	34	42	31	34
17_1	1423		40		41		54	
17_2	1386		46		40		47	
17_3	1444		75		34		43	
17_4	1401	1413	56	54	44	40	36	45
18_1	1113		135		45		35	
18_2	1159		125		45		56	
18_3	1125		112		38		31	
18_4	1155	1138	110	121	34	41	36	39
19_1	1196		114		21		35	
19_2	1185		135		32		46	
19_3	1191		116		32		43	
19_4	1198	1192	106	118	32	29	33	39
20_1	1208		110		29		28	
20_2	1201		95		30		38	
20_3	1172		70		33		51	
20_4	1155	1184	100	94	32	31	38	39
Total mean	1369	1368	124	125	33	33	38	37

Table 19. Thickness of soil layers at the different stands in the Schmittenbach watershed in 2007.

Stand:	Average (of average of the single plots)			Average (of the median of the single plots)		
	Humus (cm)	Topsoil (cm)	Total (cm)	Humus (cm)	Topsoil (cm)	Total (cm)
1	14	34	49	14	34	48
2	14	42	56	14	43	57
3	17	45	62	16	47	64
4a	10	40	50	11	39	50
4b	16	33	49	16	29	47
5	8	25	32	7	24	32
6	6	23	30	6	25	30
7	5	25	30	5	24	29
8a	9	22	31	9	21	31
8b	11	19	30	11	21	31
9	11	32	43	10	32	43
10	5	20	25	7	20	28
11	5	23	28	5	23	28
12	8	20	27	8	23	29
13	7	14	22	6	14	23
14	10	28	38	11	28	39
15	8	22	30	9	18	25
16	10	24	34	9	24	34
17	13	32	45	14	30	43
18	12	27	39	13	27	39
19	10	29	39	10	28	37
20	11	28	39	11	22	34
Mean	10	27	38	10	27	37

Table 20. Mean and standard deviation (SD) of soil carbon (t.ha^{-1}) and nitrate (t.ha^{-1}) and the carbon/nitrogen ratio for each stand in the Schmittenbach watershed in 2007. The analyse values include humus and topsoil.

Stand:	Mean carbon (t.ha^{-1})	SD C	Mean nitrogen (t.ha^{-1})	SD N	C/N
1	449.04	40.79	20.14	1.10	22
2	552.37	46.45	23.29	1.63	24
3	674.43	87.94	23.77	2.64	28
4a	488.08	17.93	21.65	0.45	23
4b	601.51	2.28	24.45	0.15	25
5	360.55	26.49	15.44	0.63	23
6	346.63	76.56	13.91	1.92	25
7	307.39	69.70	17.46	2.88	17
8a	387.19	26.10	16.77	0.85	23
8b	415.22	85.89	15.52	1.59	26
9	457.94	91.03	19.85	3.66	23
10	234.39	89.90	12.32	5.89	20
11	288.66	52.04	15.03	1.69	19
12	344.63	52.25	16.31	3.58	21
13	218.63	161.62	9.57	7.24	23
14	406.32	106.99	16.72	4.30	24
15	276.44	98.50	12.66	4.50	22
16	512.41	126.75	22.95	6.81	23
17	608.39	159.02	27.39	6.09	22
18	326.60	97.81	14.17	3.31	23
19	333.54	88.24	15.02	2.85	22
20	386.80	44.71	16.52	2.49	24
Mean	408.05	74.95	17.77	3.01	23

Table 21. Part 1. Stand characteristics measured and calculated for all plots in the Schmittenbach watershed 2007.

Name	Volume (V.ha ⁻¹)	Stand mean	Stand age	Stand mean	Dominant height	Stand mean	Site index ₁	Site index	Stand mean	SDI ₂	Stand mean
1_1	977		68		32.0		17	17		1697	
1_2	868		70		32.2		17	17		1431	
1_3	647		67		30.9		16	16		1669	
1_4	568	765	70	69	34.8	32	20	20	17	843	1410
2_1	345		30		16.5		29	20		1331	
2_2	669		31		23.5		48	20		1573	
2_3	251		47		16.6		10	10		1998	
2_4	179	361	28	34	16.5	18	36	20	20	956	1465
3_1	820		112		35.7		12	12		1072	
3_2	1139		116		39.0		15	15		1392	
3_3	989		121		34.9		10	10		1119	
3_4	771	930	125	119	36.4	37	11	11	12	856	1110
4_1	891		89		31.9		11	11		1476	
4_2	824		84		31.2		12	12		1090	
4_3	1141		95		36.5		15	15		1812	
4_4	986	960	99	92	37.2	34	15	15	13	1324	1425
5_1	665		64		30.7		17	17		1234	
5_2	657		93		33.5		12	12		925	
5_3	918		72		28.2		12	12		2557	
5_4	841	770	65	74	29.4	30	15	15	14	1925	1660
6_1	691		53		25.0		16	16		2273	
6_2	758		56		24.5		13	13		2085	
6_3	686		52		22.8		13	13		1622	
6_4	575	678	53	54	26.5	25	18	18	15	2095	2019
7_1	1172		69		31.1		16	16		1815	
7_2	917		73		33.1		17	17		1586	
7_3	549		68		30.1		15	15		814	
7_4	788	857	65	69	31.5	31	18	18	16	1139	1338
8_1	571		150		27.0		5	5		941	
8_2	465		156		27.6		5	5		697	
8_3	507		121		27.9		7	7		1295	
8_4	669	553	129	139	29.7	28	7	7	6	1450	1096
9_1	775		67		29.1		14	14		1566	
9_2	703		76		30.7		13	13		1695	
9_3	916		72		29.7		13	13		2379	
9_4	640	758	75	73	30.6	30	13	13	13	1579	1805
10_1	454		39		24.3		29	20		1845	
10_2	584	519	44	42	20.7	23	16	16	18	1893	1869

Site index₁ including unrealistic high values (>20), which are set to 20 in the following and thus not used any more!

SDI₂... Stand Density Index according to Reinecke (1933)

Table 22. Part 2. Stand characteristics measured and calculated for all plots in the Schmittenbach watershed 2007.

Name	Volume (V.ha ⁻¹)	Stand mean	Stand age	Stand mean	Dominant height	Stand mean	Site index ₁	Site index	Stand mean	SDI ₂	Stand mean
11_1	179		32		10.0		9	9		1173	
11_2	79		33		8.2		7	7		602	
11_3	108		27		6.7		8	8		1259	
11_4	17	96	37	32	8.9	8	6	6	8	98	783
12_1	481		76		23.0		8	8		1214	
12_2	393		73		24.2		9	9		928	
12_3	459		69		16.4		5	5		1275	
12_4	673	502	72	73	24.3	22	9	9	8	1704	1280
13_1	570		67		29.9		15	15		1690	
13_2	632		91		23.9		7	7		2085	
13_3	82		95		17.7		4	4		212	
13_4	331	404	132	96	29.1	25	7	7	8	5080	1329
14_1	598		124		25.2		5	5		1254	
14_2	700		125		28.5		7	7		1425	
14_3	242		131		23.8		5	5		457	
14_4	429	492	123	126	28.4	26	7	7	6	965	1025
15_1	324		33		15.0		18	18		1452	
15_2	302		31		14.1		19	19		2276	
15_3	289		31		14.8		21	20		2124	
15_4	201	279	30	31	12.6	14	16	16	18	925	1694
16_1	527		235		41.5		9	9		2660	
16_2	874		190		38.5		9	9		1079	
16_3	707		191		32.3		6	6		2321	
16_4	634	686	127	186	32.3	36	8	8	8	1287	1837
17_1	894		81		30.5		12	12		1486	
17_2	472		67		26.9		12	12		914	
17_3	612		62		25.9		12	12		1359	
17_4	505	621	63	68	28.4	28	15	15	13	915	1169
18_1	667		69		30.9		15	15		1292	
18_2	405		58		27.2		16	16		954	
18_3	551		64		27.4		13	13		1435	
18_4	688	578	61	63	29.9	29	18	18	15	1294	1244
19_1	1019		129		36.3		11	11		1316	
19_2	835		133		39.8		14	14		933	
19_3	1058		133		40.0		14	14		1137	
19_4	1082	998	130	131	38.8	39	13	13	13	1214	1150
20_1	746		88		36.6		17	17		1081	
20_2	916		88		36.6		17	17		1027	
20_3	1185		88		37.1		17	17		1416	
20_4	856	926	87	88	37.7	37	18	18	17	1059	1146
Total	640	637	84	83	28	28	14	13	13	1429	1393

Site index₁ including unrealistic high values (>20), which are set to 20 in the following and thus not used any more!

SDI₂... Stand Density Index according to Reinecke (1933)

Table 23. Comparison of stand characteristics between the management plan 2003 of the local forest company 'Zeller Waldgemeinschaft' with the results from the field campaign 2007. For the point sampling data the mean and the median of all (4) plots per stand are calculated.

Stand	Local stand Nr.	Management plan 2003				Point Sampling 2007_Stand mean					Point Sampling 2007_Stand median				
		Site index	Total volume (m ³ .ha ⁻¹)	Stand age (y)	Dominant height (m)	Site index	Total volume (m ³ .ha ⁻¹)	Stand age (y)	Dominant height (m)	Tree number (N.ha ⁻¹)	Site index	Total volume (m ³ .ha ⁻¹)	Stand age (y)	Dominant height (m)	Tree number (N.ha ⁻¹)
1	2 c	9	351	61	21.3	17	765	69	32.5	927	16.4	757	69	32.1	1071
2	1 e 1	9	20	21	6.2	20	361	34	18.3	2870	18.4	298	31	16.6	2908
3	3 i	8	508	126	30.5	12	930	119	36.5	428	12.4	904	119	36.1	435
4a	5 k	7	312	86	24.0	12	857	87	31.6	873	12.2	857	87	31.6	873
4b	4 h	6	263	86	22.3	15	1063	97	36.8	814	15.1	1063	97	36.8	814
5	9 e	7	375	81	23.1	14	770	74	30.5	1001	13.8	753	69	30.1	998
6	9 a	7	107	41	12.3	15	678	54	24.7	1775	13.8	688	53	24.8	1776
7	8 g	8	270	61	19.9	16	857	69	31.4	697	15.7	853	69	31.3	682
8a	9 h	5	431	131	25.5	5	518	153	27.3	492	4.7	518	153	27.3	492
8b	9 i	5	415	151	26.7	7	588	125	28.8	594	7.0	588	125	28.8	594
9	7 i	8	295	56	18.5	13	758	73	30.0	1206	13.4	739	74	30.2	1147
10	7 k 1	7	23	26	6.8	18	519	42	22.5	3038	17.8	519	42	22.5	3038
11	8 k 1	7	7	23	5.7	8	96	32	8.5	3252	6.1	94	33	8.6	2445
12	8 k	5	335	131	25.5	8	502	73	22.0	893	8.3	470	73	23.6	972
13	7 u	6	186	61	17.0	8	404	96	25.2	1244	6.6	450	93	26.5	1560
14	8 o	6	389	161	29.0	6	492	126	26.5	413	5.9	513	125	26.8	449
15	5 g	7	13	21	5.0	18	279	31	14.2	4126	13.7	295	31	14.5	4364
16	6 d	6	375	151	28.6	8	686	186	36.1	693	8.4	670	191	35.4	643
17	5 m	6	122	46	12.7	13	621	68	27.9	889	12.4	558	65	27.6	943
18	5 b	7	222	56	17.1	15	578	63	28.9	1037	15.0	609	63	28.7	1003
19	5 e	8	610	136	31.1	13	998	131	38.7	408	13.8	1038	132	39.3	423
20	5 c	8	389	81	24.7	17	926	88	37.0	513	16.5	886	88	36.8	499

Table 24. Plausibility check: comparison of the data from the field campaign 2007 (stand median) with suitable data from the local yield table 'Fichte Hochgebirge'. For the point sampling data the median of all (mostly 4) plots per stand are calculated.

Stand	Local stand Nr.	Point sampling 2007_stand median					Yield table 'Fichte Hochgebirge'				
		Site index	Total volume (m ³ .ha ⁻¹)	Stand age (y)	Dominant height (m)	Tree number (N.ha ⁻¹)	Site index	Total volume (m ³ .ha ⁻¹)	Stand age (y)	Dominant height (m)	Tree number (N.ha ⁻¹)
1	2 c	16.9	757	69	32.1	1071	15	806	70	31.0	710
2	1 e 1	19.8	298	31	16.6	2908	15	180	30	12.2	1708
3	3 i	11.4	904	119	36.1	435	11	967	120	35.8	507
4a	5 k	11.6	857	87	31.6	873	12	847	90	32.8	635
4b	4 h	15.0	1063	97	36.8	814	15	1143	100	37.3	508
5	9 e	13.7	753	69	30.1	998	14	760	70	30.2	749
6	9 a	14.3	688	53	24.8	1776	14	474	50	22.8	1082
7	8 g	16.1	853	69	31.3	682	15	806	70	31.0	710
8a	9 h	5.1	518	153	27.3	492	5	532	150	26.4	598
8b	9 i	6.9	588	125	28.8	594	7	613	120	28.4	625
9	7 i	13.0	739	74	30.2	1147	13	707	70	29.2	792
10	7 k 1	17.9	519	42	22.5	3038	15	334	40	18.3	1266
11	8 k 1	7.4	94	33	8.6	2445	7	49	30	7.1	4052
12	8 k	8.5	470	73	23.6	972	9	469	70	23.6	1022
13	7 u	6.8	450	93	26.5	1560	7	470	90	24.0	857
14	8 o	6.1	513	125	26.8	449	6	528	120	26.2	669
15	5 g	18.5	295	31	14.5	4364	15	180	30	12.2	1708
16	6 d	8.6	670	191	35.4	643	9	902	150	35.2	495
17	5 m	12.1	558	65	27.6	943	12	651	70	28.0	840
18	5 b	15.5	609	63	28.7	1003	15	659	60	27.6	830
19	5 e	13.3	1038	132	39.3	423	13	1138	120	38.1	471
20	5 c	16.9	886	88	36.8	499	15	1048	90	35.7	557

Table 25. Mean and median of aspect, slope, elevation and coordinates for all stands.

Stand	Local stand Nr.	Stand mean							Stand median						
		Aspect (°)	Slope (°)	Elevation (m)	Coordinates North		Coordinates East		Aspect (°)	Slope (°)	Elevation (m)	Coordinates North		Coordinates East	
					(°)	(')	(°)	(')				(°)	(')	(°)	(')
1	2 c	34	28	968.0	47	19.371	12	46.904	34	29	969.8	47	19.403	12	46.909
2	1 e 1	265	25	943.9	47	19.361	12	47.072	327	24	942.0	47	19.362	12	47.077
3	3 i	57	35	1281.9	47	19.119	12	46.241	58	36	1275.8	47	19.121	12	46.228
4a	5 k	53	38	1405.8	47	19.265	12	45.334	53	38	1405.8	47	19.265	12	45.334
4b	4 h	57	32	1394.8	47	19.262	12	45.400	57	32	1394.8	47	19.262	12	45.400
5	9 e	145	32	1455.5	47	20.265	12	46.159	146	31	1451.8	47	20.263	12	46.166
6	9 a	150	37	1444.1	47	20.227	12	45.981	152	36	1446.5	47	20.222	12	45.981
7	8 g	175	30	1360.1	47	20.127	12	45.691	176	29	1363.3	47	20.126	12	45.690
8a	9 h	185	19	1556.5	47	20.421	12	46.506	185	19	1556.5	47	20.421	12	46.506
8b	9 i	182	21	1619.8	47	20.537	12	46.082	182	21	1619.8	47	20.537	12	46.082
9	7 i	146	33	1313.1	47	20.046	12	45.693	140	33	1312.3	47	20.035	12	45.696
10	7 k 1	183	15	1298.3	47	20.059	12	45.640	183	15	1298.3	47	20.059	12	45.640
11	8 k 1	132	30	1659.1	47	20.359	12	45.291	132	30	1659.5	47	20.360	12	45.289
12	8 k	134	26	1641.3	47	20.283	12	45.240	133	34	1639.0	47	20.274	12	45.240
13	7 u	123	36	1627.9	47	20.264	12	45.203	119	37	1626.5	47	20.264	12	45.205
14	8 o	137	24	1666.1	47	20.564	12	45.807	139	31	1671.5	47	20.570	12	45.802
15	5 g	85	38	1348.8	47	19.586	12	45.447	82	39	1348.0	47	19.563	12	45.446
16	6 d	114	42	1429.1	47	19.580	12	45.282	51	42	1427.0	47	19.582	12	45.285
17	5 m	54	40	1413.1	47	19.239	12	45.302	51	41	1411.5	47	19.239	12	45.309
18	5 b	121	41	1137.8	47	19.469	12	45.743	119	42	1139.8	47	19.474	12	45.751
19	5 e	118	29	1192.2	47	19.487	12	45.660	115	32	1193.3	47	19.491	12	45.666
20	5 c	94	31	1183.8	47	19.565	12	45.700	98	31	1186.3	47	19.564	12	45.695